African Journal of Biotechnology

Volume 14 Number 33, 19 August, 2015
ISSN 1684-5315

Academic Journals

ABOUT AJB

The **African Journal of Biotechnology (AJB)** (ISSN 1684-5315) is published weekly (one volume per year) by Academic Journals.

African Journal of Biotechnology (AJB), a new broad-based journal, is an open access journal that was founded on two key tenets: To publish the most exciting research in all areas of applied biochemistry, industrial microbiology, molecular biology, genomics and proteomics, food and agricultural technologies, and metabolic engineering. Secondly, to provide the most rapid turn-around time possible for reviewing and publishing, and to disseminate the articles freely for teaching and reference purposes. All articles published in AJB are peer-reviewed.

Submission of Manuscript

Please read the **Instructions for Authors** before submitting your manuscript. The manuscript files should be given the last name of the first author

Click here to Submit manuscripts online

If you have any difficulty using the online submission system, kindly submit via this email ajb@academicjournals.org.

With questions or concerns, please contact the Editorial Office at ajb@academicjournals.org.

Editorial Board

Instructions for Author

Electronic submission of manuscripts is strongly encouraged, provided that the text, tables, and figures are included in a single Microsoft Word file (preferably in Arial font).

The **cover letter** should include the corresponding author's full address and telephone/fax numbers and should be in an e-mail message sent to the Editor, with the file, whose name should begin with the first author's surname, as an attachment.

Article Types
Three types of manuscripts may be submitted:

Regular articles: These should describe new and carefully confirmed findings, and experimental procedures should be given in sufficient detail for others to verify the work. The length of a full paper should be the minimum required to describe and interpret the work clearly.
Short Communications: A Short Communication is suitable for recording the results of complete small investigations or giving details of new models or hypotheses, innovative methods, techniques or apparatus. The style of main sections need not conform to that of full-length papers. Short communications are 2 to 4 printed pages (about 6 to 12 manuscript pages) in length.

Reviews: Submissions of reviews and perspectives covering topics of current interest are welcome and encouraged. Reviews should be concise and no longer than 4-6 printed pages (about 12 to 18 manuscript pages). Reviews are also peer-reviewed.

Review Process

All manuscripts are reviewed by an editor and members of the Editorial Board or qualified outside reviewers. Authors cannot nominate reviewers. Only reviewers randomly selected from our database with specialization in the subject area will be contacted to evaluate the manuscripts. The process will be blind review.
Decisions will be made as rapidly as possible, and the journal strives to return reviewers' comments to authors as fast as possible. The editorial board will re-review manuscripts that are accepted pending revision. It is the goal of the AJFS to publish manuscripts within weeks after submission.

Regular articles

All portions of the manuscript must be typed double-spaced and all pages numbered starting from the title page.

The Title should be a brief phrase describing the contents of the paper. The Title Page should include the authors' full names and affiliations, the name of the corresponding author along with phone, fax and E-mail information. Present addresses of authors should appear as a footnote.

The Abstract should be informative and completely self-explanatory, briefly present the topic, state the scope of the experiments, indicate significant data, and point out major findings and conclusions. The Abstract should be 100 to 200 words in length.. Complete sentences, active verbs, and the third person should be used, and the abstract should be written in the past tense. Standard nomenclature should be used and abbreviations should be avoided. No literature should be cited.
Following the abstract, about 3 to 10 key words that will provide indexing references should be listed.

A list of non-standard **Abbreviations** should be added. In general, non-standard abbreviations should be used only when the full term is very long and used often. Each abbreviation should be spelled out and introduced in parentheses the first time it is used in the text. Only recommended SI units should be used. Authors should use the solidus presentation (mg/ml). Standard abbreviations (such as ATP and DNA) need not be defined.

The Introduction should provide a clear statement of the problem, the relevant literature on the subject, and the proposed approach or solution. It should be understandable to colleagues from a broad range of scientific disciplines.

Materials and methods should be complete enough to allow experiments to be reproduced. However, only truly new procedures should be described in detail; previously published procedures should be cited, and important modifications of published procedures should be mentioned briefly. Capitalize trade names and include the manufacturer's name and address. Subheadings should be used. Methods in general use need not be described in detail.

Results should be presented with clarity and precision. The results should be written in the past tense when describing findings in the authors' experiments. Previously published findings should be written in the present tense. Results should be explained, but largely without referring to the literature. Discussion, speculation and detailed interpretation of data should not be included in the Results but should be put into the Discussion section.

The Discussion should interpret the findings in view of the results obtained in this and in past studies on this topic. State the conclusions in a few sentences at the end of the paper. The Results and Discussion sections can include subheadings, and when appropriate, both sections can be combined.

The Acknowledgments of people, grants, funds, etc should be brief.

Tables should be kept to a minimum and be designed to be as simple as possible. Tables are to be typed double-spaced throughout, including headings and footnotes. Each table should be on a separate page, numbered consecutively in Arabic numerals and supplied with a heading and a legend. Tables should be self-explanatory without reference to the text. The details of the methods used in the experiments should preferably be described in the legend instead of in the text. The same data should not be presented in both table and graph form or repeated in the text.

Figure legends should be typed in numerical order on a separate sheet. Graphics should be prepared using applications capable of generating high resolution GIF, TIFF, JPEG or Powerpoint before pasting in the Microsoft Word manuscript file. Tables should be prepared in Microsoft Word. Use Arabic numerals to designate figures and upper case letters for their parts (Figure 1). Begin each legend with a title and include sufficient description so that the figure is understandable without reading the text of the manuscript. Information given in legends should not be repeated in the text.

References: In the text, a reference identified by means of an author‘s name should be followed by the date of the reference in parentheses. When there are more than two authors, only the first author‘s name should be mentioned, followed by ’et al‘. In the event that an author cited has had two or more works published during the same year, the reference, both in the text and in the reference list, should be identified by a lower case letter like ’a‘ and ’b‘ after the date to distinguish the works.

Examples:

Abayomi (2000), Agindotan et al. (2003), (Kelebeni, 1983), (Usman and Smith, 1992), (Chege, 1998; 1987a,b; Tijani, 1993,1995), (Kumasi et al., 2001)
References should be listed at the end of the paper in alphabetical order. Articles in preparation or articles submitted for publication, unpublished observations, personal communications, etc. should not be included in the reference list but should only be mentioned in the article text (e.g., A. Kingori, University of Nairobi, Kenya, personal communication). Journal names are abbreviated according to Chemical Abstracts. Authors are fully responsible for the accuracy of the references.

Examples:

Chikere CB, Omoni VT and Chikere BO (2008). Distribution of potential nosocomial pathogens in a hospital environment. Afr. J. Biotechnol. 7: 3535-3539.

Moran GJ, Amii RN, Abrahamian FM, Talan DA (2005). Methicillinresistant Staphylococcus aureus in community-acquired skin infections. Emerg. Infect. Dis. 11: 928-930.

Pitout JDD, Church DL, Gregson DB, Chow BL, McCracken M, Mulvey M, Laupland KB (2007). Molecular epidemiology of CTXM-producing Escherichia coli in the Calgary Health Region: emergence of CTX-M-15-producing isolates. Antimicrob. Agents Chemother. 51: 1281-1286.

Pelczar JR, Harley JP, Klein DA (1993). Microbiology: Concepts and Applications. McGraw-Hill Inc., New York, pp. 591-603.

Short Communications

Short Communications are limited to a maximum of two figures and one table. They should present a complete study that is more limited in scope than is found in full-length papers. The items of manuscript preparation listed above apply to Short Communications with the following differences: (1) Abstracts are limited to 100 words; (2) instead of a separate Materials and Methods section, experimental procedures may be incorporated into Figure Legends and Table footnotes; (3) Results and Discussion should be combined into a single section.
Proofs and Reprints: Electronic proofs will be sent (e-mail attachment) to the corresponding author as a PDF file. Page proofs are considered to be the final version of the manuscript. With the exception of typographical or minor clerical errors, no changes will be made in the manuscript at the proof stage.

Fees and Charges: Authors are required to pay a $650 handling fee. Publication of an article in the African Journal of Biotechnology is not contingent upon the author's ability to pay the charges. Neither is acceptance to pay the handling fee a guarantee that the paper will be accepted for publication. Authors may still request (in advance) that the editorial office waive some of the handling fee under special circumstances

Submission of a manuscript implies: that the work described has not been published before (except in the form of an abstract or as part of a published lecture, or thesis) that it is not under consideration for publication elsewhere; that if and when the manuscript is accepted for publication, the authors agree to automatic transfer of the copyright to the publisher.

African Journal of Biotechnology

Table of Contents: Volume 14 Number 33, 19 August, 2015

ARTICLES

academicJournals

Vol. 14(33), pp. 2532-2538, 19 August, 2015
DOI: 10.5897/AJB2015.14829
Article Number: 089364054966
ISSN 1684-5315

http://www.academicjournals.org/AJB

African Journal of Biotechnology

Full Length Research Paper

Phylogenetic study on *Microcotyle* sp. (Monogenea) from common dentex (*Dentex dentex*) in the Mediterranean Sea, Greece

Jin Woo Jun

Laboratory of Aquatic Biomedicine, College of Veterinary Medicine and Research Institute for Veterinary Science, Seoul National University, Seoul 151-742, Republic of Korea.

Received 30 June, 2015; Accepted 13 August, 2015

The monogenean *Microcotyle* sp. was isolated from common dentex in the Sea of Crete, the part of the Mediterranean Sea. The 28S rRNA gene of *Microcotyle* sp. was amplified by polymerase chain reaction (PCR). The PCR product was sequenced and compared with other 28S rRNA sequences of Monogenea. Phylogenetic analyses were performed with neighbour-joining (NJ), minimum evolution (ME), maximum likelihood (ML) and maximum parsimony (MP) method. The result of analysis shows that NJ and ME method presented the same topology; ML method led to a similar but slightly different topology from NJ or ME method; MP method resulted in a totally different topology from the other methods. Also, *Microcotyle* sp. isolated in this study was proven to be closest to Microcotylidae gen. sp. MAF-2012 and *Bivagina pagrosomi*.

Key words: *Microcotyle* sp., common dentex, Mediterranean Sea, 28S rRNA gene, phylogenetic analysis.

INTRODUCTION

Mediterranean mariculture production has focused on two species: gilthead seabream (*Sparus aurata* L.) and European sea bass (*Dicentrarchus labrax* L.) (Akyol and Ertosluk, 2010). In the meantime, the common dentex (*Dentex dentex* L.) is considered as one of the most attractive candidates for aquaculture due to its high commercial value (Loir et al., 2001; Chemmam-Abdelkader et al., 2007). Also, it is known that it shows easy reproduction in captivity and high growth rate (Loir et al., 2001; Tomás et al., 2009).

There are still several constraints for the future development of Mediterranean mariculture, such as disease problems caused by bacterial, viral and parasitic infections (Rodgers and Furones, 1998). Monogeneans have been considered as a factor limiting aquaculture productivity as it frequently causes mixed infections with other parasites and secondary bacterial infections (Cruz e Silva et al., 1997; Antonelli et al., 2010). *Microcotyle* sp. belongs to the Order Monogenea, Suborder Polyopisthocotylea, which has caused high mortality (Sanz, 1992). The symptoms of *microcotyle* sp. infections are anemia and asphyxia due to over production of mucus (Sanz, 1992). There has been a report about the loss related to *Microcotyle* sp. in aquaculture (Paperna, 1960). *Microcotyle* sp. infections have been reported from several countries such as the Americas, Asia, and Israel

E-mail: advancewoo@snu.ac.kr. Tel.: +82 2 880 1282. Fax: +82 2 880 1213.

in several fish species including rabbitfish (*Siganus luridus* and *Siganus virulatus*), gilthead seabream (*Sparus aurata*) and seabass (*Dicentrarchus labrax*) (Paperna, 1983; Sanz, 1992). To date, the importance of molecular analysis has been increased for the rapid and efficient phylogenetic study of parasite. The partial sequences of the 28S rRNA gene have been used for the phylogenetic study of monogeneans (Mollaret et al., 2000; Jovelin and Justine, 2001). The aim of the present study was to isolate *Microcotyle* sp. (Monogenea) from common dentex, sequence the 28S rRNA gene of isolate, compare it with the 28S rRNA genes of other Monogenea, and investigate the phylogenetic characteristics.

MATERIALS AND METHODS

From March to May 2015, a total of 10 common dentex were purchased from fishermen at Heraklion Bay (35°20′N, 25°08′E), Crete, Greece in Mediterranean Sea. Fish were kept in plastic bags with ice and transferred to the diagnostic facility within 1 h. Skin, fins and gills of the fish were examined immediately after arrival. For the examination of parasites, gill arches were removed and observed using a stereo microscope. More than 50 parasites were observed from infected fish and preserved in 2.5% glutaraldehyde for further anaylsis.

DNA extraction was conducted using the DNeasy® Blood & Tissue Kit (QIAGEN) according to the manufacturer's instruction. The 28S rRNA gene was amplified by PCR using C1/D2 primer pair as previously reported (Chisholm et al., 2001). The automated sequencing was carried out using the Automatic Sequencer 3730xl DNA analyzer (Applied Biosystems). Sequence identities were determined with the BLAST search. The 28S rRNA sequences of Monogenea which were used in the current study were downloaded from the GenBank and used for phylogenetic analyses (Table 1). These sequences were aligned with ClustalW and analysed with the MEGA6 (Tamura et al., 2013). Phylogenetic analyses were conducted with: (1) neighbour-joining (NJ) method (Saitou and Nei, 1987); (2) minimum evolution (ME) method (Whittington et al., 2004); (3) maximum likelihood (ML) method (Hasegawa et al., 1985); and (4) maximum parsimony (MP) method (Swofford and Olsen, 1990). Bootstrap values were calculated for each method, with 1,000 replicates. *Merizocotyle icopae*, *Troglocephalus rhinobatidis* and *Neoheterocotyle rhinobatidis* were used as outgroup.

RESULTS AND DISCUSSION

Parasites (2-6 mm in length) attaching to the gills of fish were observed in the central part of gill filaments (data not shown). In the current study, the prevalence of infection of *Microcotyle* sp. was 60% (sixinfected fish out of 10 in total), which is similar to the result reported by González et al. (2004). González et al. (2004) previously reported the incidence of gill parasites of common dentex from Mediterranean Sea. In the previous study, *Microcotyle erythrini* was isolated from 57% of the examined common dentex (González et al., 2004). Also, for the infection with gill monogenean parasite, *Microcotyle sebastis* has been considered as a problem associated with rockfish (*Sebastes schlegeli*) aquacultured in Korea (Kim and Choi, 1998). According to the previous report (Kim and Choi, 1998), high cumulative mortality of juvenile rockfish related to *M. sebastis* infection had been observed in many farms. Even higher mortality caused by *Microcotyle* sp. infection was observed in the aquarium fish; the mortality of 90% was reported (Mellen, 1928).

Phylogenetic analyses based on morphological and molecular genetic data have played an important role in parasitological studies. Although the value of morphological analysis cannot be underestimated, molecular analysis has increased its importance for phylogenetic study as a more rapid, efficient, and cost-effective method due to progress in sequencing techniques (Perkins et al., 2010). There have been many methods developed for the construction of phylogenetic tree, but there is no systematically better method than the others and the result can be improved by combining methods (Guindon and Gascuel, 2003). Although NJ method is known to be better than MP method, it may give the expected result as long as a proper distance measure is used, which depends on the situation encountered (Jin and Nei, 1990).

Choi et al. (2009) carried out a molecular phylogenetic analysis for the evolutionary study of an annexin gene from *Microcotyle sebastis* in their previous report; phylogenetic trees were constructed by the neighbour-joining (NJ) method and it showed the result of evolutionary analysis between the annexin gene of *M. sebastis* and the annexin genes already known. In the current study, the 28S rRNA sequence of *Microcotyle* sp. (989 bp in length) was deposited in GenBank under the accession number KT191025. The sequence obtained showed 96-97% nucleotide similarity with Microcotylidae, such as *Bivagina pagrosomi*, *Microcotyle arripis*, *Microcotyle erythrinii*, and *Microcotyle sebastis* (Table 1). Phylogenetic analyses were based on the 28S rRNA sequence as previously reported (Mollaret et al., 2000; Jovelin and Justine, 2001).

In this study, NJ, ME and ML method of the Polyopisthocotylea using Monopisthocotylea as the outgroup were arranged in two monophyletic groups as previously reported (Mollaret et al., 2000; Jovelin and Justine, 2001). NJ and ME method presented the same topology (Figure 1A). ML method led to a similar but slightly different topology from NJ or ME method (Figure 1B). NJ and ME method clustered the sequences into four groups: Axinidae, Mazocraeidae and Microcotylidae; Diclidophoridae and Discocotylidae; Hexostomatidae, Microcotylidae and Neothoracocotylidae; Monocotylidae (Figure 1A). ML method clustered the sequences into four groups, but their compositions were slightly different: Axinidae, Mazocraeidae, and Microcotylidae; Diclidophoridae; Discocotylidae, Hexostomatidae, Microcotylidae, and Neothoracocotylidae; Monocotylidae (Figure 1B). Also, the Microcotylidae was grouped in

Table 1. List of the 28S rRNA sequences used in this study.

Species and classification	Host	Source	Sequence identity (%) [a]	GenBank No.
Polyopisthocotylea				
Axinidae				
Zeuxapta seriolae isolate Z5	*Seriola lalandi*	Australia	738/837 (88%)	EF653384
Zeuxapta seriolae	*Seriola lalandi*	Australia	710/824 (86%)	AF026103
Diclidophoridae				
Chalguacotyle mugiloides isolate Ch1a	*Pinguipes chilensis*	Chile	744/904 (82%)	KJ397726
Choricotyle australiensis	*Rhabdosargus sarba*	Australia	769/925 (83%)	AF382046
Diclidophora denticulata	*Pollachius virens*	UK	781/936 (83%)	AY157169
Diclidophora denticulata	*Pollachius virens*	UK	761/914 (83%)	AF382047
Diclidophora minor	*Micromesistius poutassou*	UK	774/939 (82%)	AF382048
Parapedocotyle prolatili isolate Pp1a	*Prolatilus jugularis*	Chile	742/893 (83%)	KJ397731
Urocotyle nibae	-	-	772/934 (83%)	FJ432588
Discocotylidae				
Discocotyle sagittata	*Salmo trutta*	UK	762/901 (85%)	AF382036
Hexostomatidae				
Hexostoma thynni isolate H31	*Thunnus thynnus*	Croatia	724/874 (83%)	EF653383
Mazocraeidae				
Probursata brasiliensis	*Oligoplites* sp.	Brazil	806/925 (87%)	AF382049
Microcotylidae				
Bivagina pagrosomi	*Sparus auratus*	Australia	863/894 (97%)	Z83002
Cynoscionicola branquialis	*Umbrina xanti*	Mexico	817/900 (91%)	AF382050
Diplostamenides sciaenae	-	-	827/925 (89%)	FJ432589
Kahawaia truttae	*Arripis truttacea*	Australia	812/890 (91%)	GU263831
Kahawaia truttae	*Arripis trutta*	Australia	792/870 (91%)	GU263832
Microcotyle arripis	*Arripis georgianus*	Australia	814/850 (96%)	GU263830
Microcotyle erythrinii	*Pagellus erythrinus*	France	884/919 (96%)	AM157221
Microcotyle sebastis	*Sebastes* sp.	UK	865/897 (96%)	AF382051
Neomicrocotyle pacifica	*Caranx hippos*	Mexico	747/905 (83%)	AF382043
Polylabris sillaginae	*Sillaginodes punctatus*	Australia	792/888 (89%)	GU289509
Unclassified Microcotylidae				
Microcotylidae gen. sp. MAF-2012	*Argyrops spinifer*	Oman	880/907 (97%)	JN602095
Microcotylidae sp. M10	*Sebastes* sp.	UK	839/871 (96%)	EF653385
Neothoracocotylidae				
Mexicotyle sp. Brazil	*Scomberomorus* sp.	Brazil	761/925 (82%)	AF382041
Paradewesia sp. Brazil	*Scomberomorus* sp.	Brazil	767/929 (83%)	AF382042
Monopisthocotylea				
Monocotylidae				
Merizocotyle icopae	*Rhinobatos typus*	Australia	-	AF026113
Neoheterocotyle rhinobatidis	*Rhinobatos typus*	Australia	-	AF026107
Troglocephalus rhinobatidis	*Rhinobatos typus*	Australia	-	AF026110

[a]Sequence identity (%) means 'Identity of the 28S rRNA sequence of *Microcotyle* sp. isolated in this study to other 28S rRNA sequences available in GenBank'.

three in the ML analysis: *Neomicrocotyle pacifica*; *Cynoscionicola branquialis* and *Diplostamenides sciaenae*;

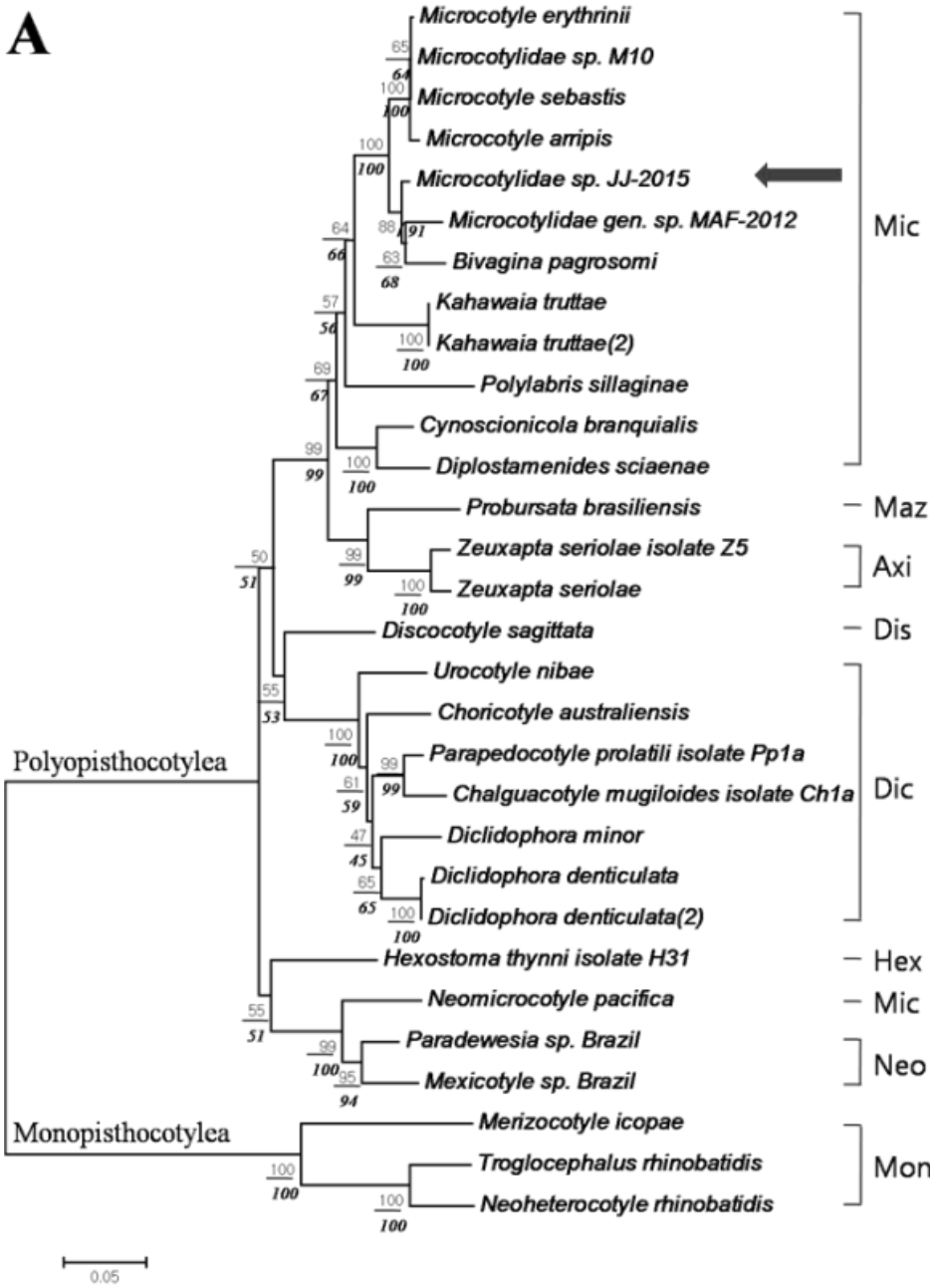

Figure 1. Phylogenetic tree based on the 28S rRNA sequence of the Monogenea. **A)** Neighbour-joining (NJ) and minimum evolution (ME) method. The same topology was found by NJ and ME. Bootstrap values obtained by NJ/*ME* (*italic*) are indicated above the branch. **B)** Maximum likelihood (ML) method. Bootstrap values are presented. **C)** Maximum parsimony (MP) method. Bootstrap values are shown. Axi, Axinidae; Dic, Diclidophoridae; Dis, Discocotylidae; Hex, Hexostomatidae; Maz, Mazocraeidae; Mic, Microcotylidae; Mon, Monocotylidae; Neo, Neothoracocotylidae were presented. The arrow represents *Microcotyle* sp. isolated in this study.

the other Microcotylidae members (Figure 1B). MP method resulted in a totally different topology from the other methods (Figure 1C). In all analyses, *Neomicrocotyle pacifica* was found to be a distant group separated from the other Microcotylidae members (Figure 1). Based on the phylogenetic tree results, *Microcotyle* sp. isolated in

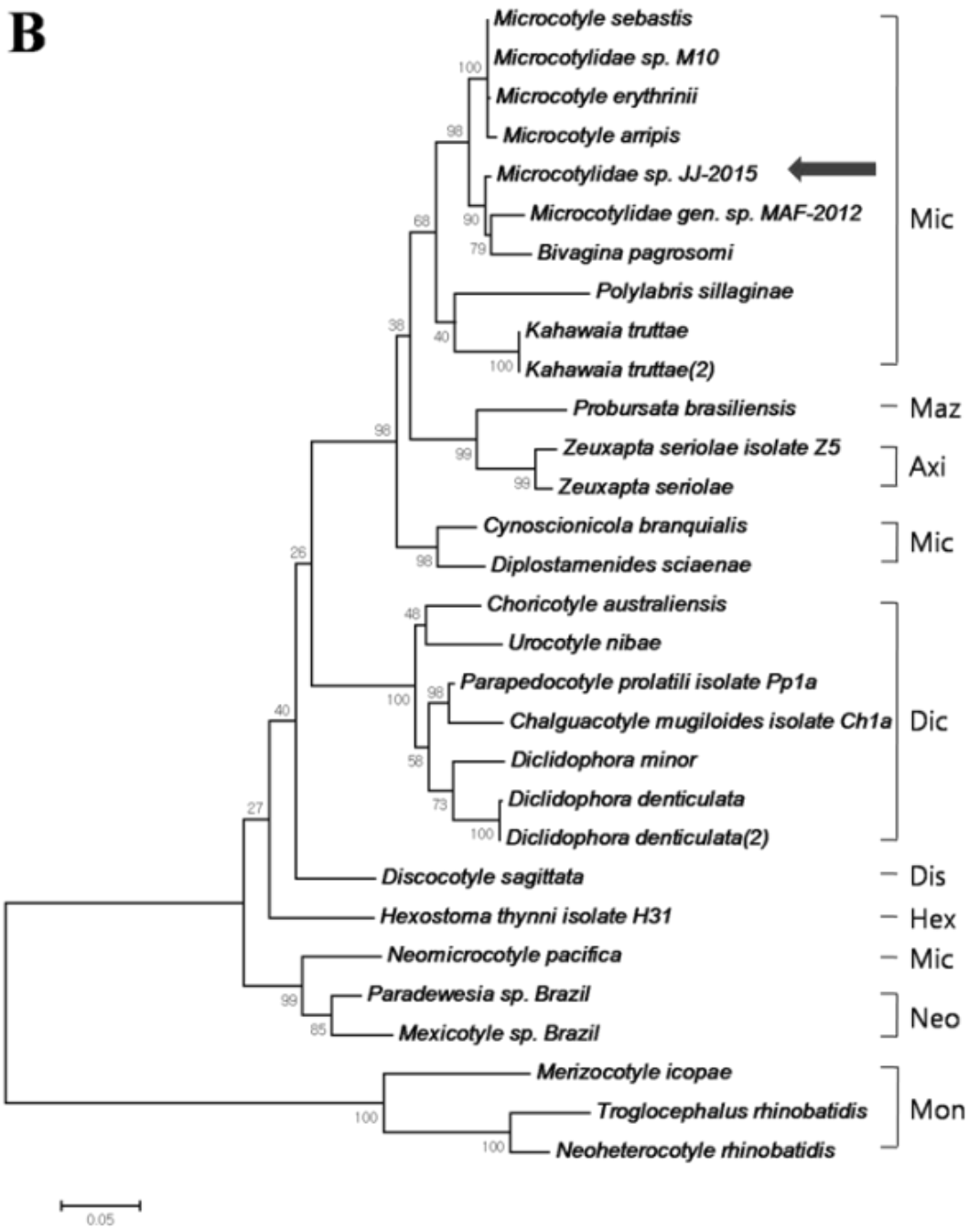

Figure 1. Contd.

this study was clustered with other Microcotylidae members (Figure 1). Also, it was most closely related to Microcotylidae gen. sp. MAF-2012 and *Bivagina pagrosomi* (Figure 1). In all analyses, no relationship was found between geographic region and phylogenetic tree, or between host specificity and phylogenetic tree although several different methods were applied to observe meaningful relationship. However, further research on *Microcotyle* sp. such as its potential impact on common dentex aquaculture is advised because parasites can cause high mortality under intensive aquaculture conditions (Papoutsoglou et al., 1996).

Conflict of interests

The authors did not declare any conflict of interest.

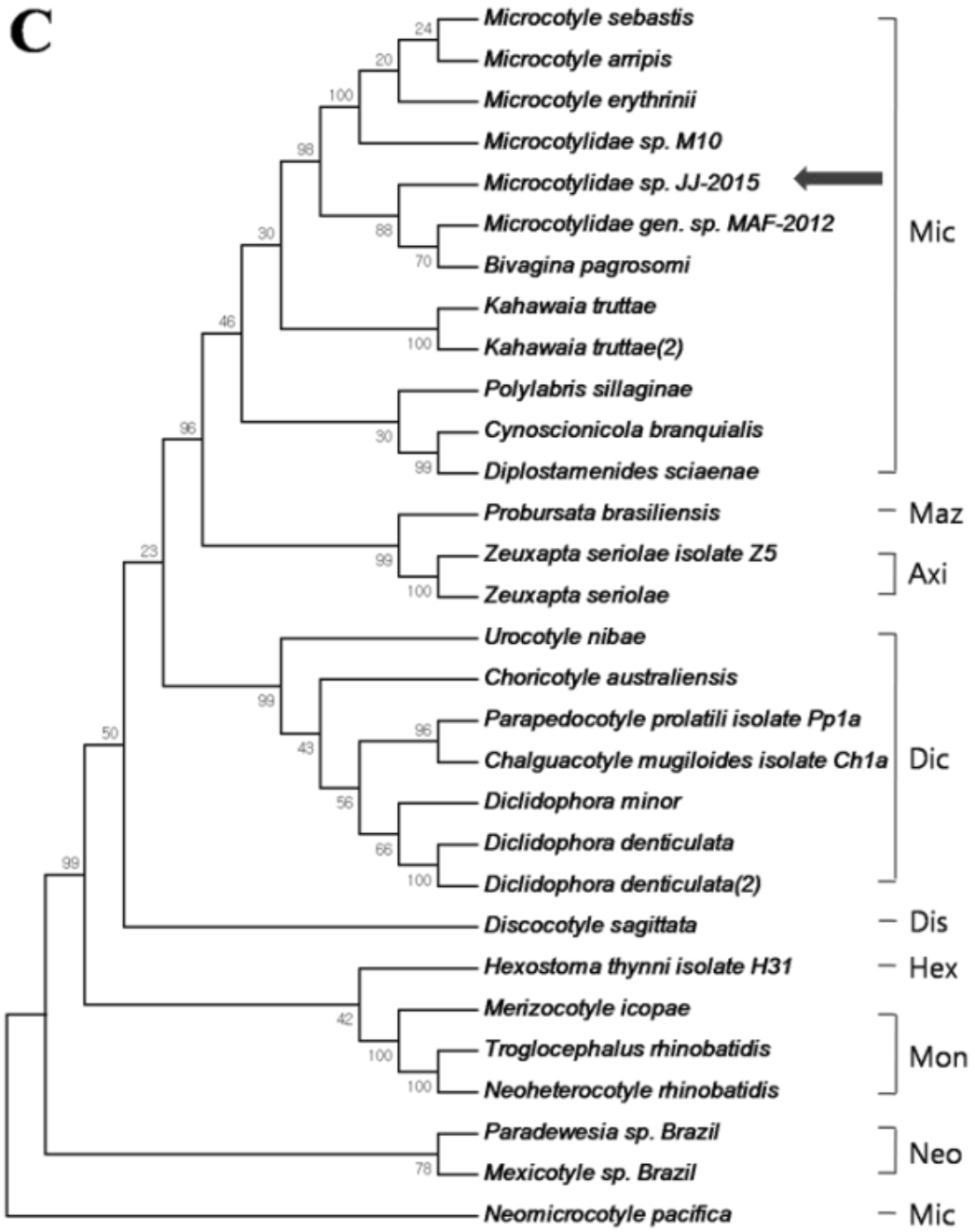

Figure 1. Contd.

REFERENCES

Akyol O, Ertosluk O (2010). Fishing near sea-cage farms along the coast of the Turkish Aegean Sea. J. Appl. Ichthyol. 26: 11-15.

Antonelli L, Quilichini Y, Marchand B (2010). *Sparicotyle chrysophrii* (Van Beneden and Hesse 1863) (Monogenea: Polyopisthocotylea) parasite of cultured gilthead sea bream *Sparus aurata* (Linnaeus 1758) (Pisces: Teleostei) from Corsica: ecological and morphological study. Parasitol. Res. 107: 389-398.

Chemmam-Abdelkader B, Ezzeddine-Najaî S, Kraiem MM (2007). Etude de l'etat du stock de *Dentex dentex* (Linnaeus, 1758) (Teleostei, Sparidae) des côtes sud tunisiennes. Bull. Inst. Natn. Scien. Tech. Tabarka. 12: 55-59.

Chisholm LA, Morgan JAT, Adlard RD, Whittington ID (2001). Phylogenetic analysis of the Monocotylidae (Monogenea) inferred from 28S rDNA sequences. Int. J. Parasitol. 31: 1537-1547.

Choi SH, Kwon SR, Lee EH, Kim KH (2009). Molecular cloning, functional characterization and localization of an annexin from a fish gill fluke *Microcotyle sebastis* (Platyhelminthes: Monogenea). Mol. Biochem. Parasitol. 163:48-53.

Cruz e Silva MP, Freitas MS, Orge ML (1997). Co-infection by monogenetic trematodes of the genus *Microcotyle*, Beneden and

Hese 1863, *Lamellodiscus ignoratus* Palombi, 1943, the protozoan *Trichodina* sp. Ehrenber, 1838 and the presence of *Epitheliocystis*, *Vibrio algynoliticus* and *V. vulnificus* in cultured seabream (*Sparus aurata* L.) in Portugal. Bull. Eur. Assoc. Fish Pathol. 17: 40-42.

González P, Sánchez MI, Chirivella J, Carbonell E, Riera F, Grau A (2004). A preliminary study on gill metazoan parasites of *Dentex dentex* (Pisces: Sparidae) from the western Mediterranean Sea (Balearic Islands). J. Appl. Ichthyol. 20: 276-281.

Guindon S, Gascuel O (2003). A simple, fast, and accurate algorithm to estimate large phylogenies by maximum likelihood. Syst. Biol. 52: 696-704.

Hasegawa M, Kishino H, Yano T (1985). Dating of the human-ape splitting by a molecular clock of mitochondrial DNA. J. Mol. Evol. 22: 160-174.

Jin L, Nei M (1990). Limitation of the evolutionary parsimony method of phylogenetic analysis. Mol. Biol. Evol. 7: 82-102.

Jovelin R, Justine JL (2001). Phylogenetic relationships within the polyopisthocotylean monogeneans (Platyhelminthes) inferred from partial 28S rDNA sequences. Int. J. Parasitol. 31: 393-401.

Kim KH, Choi ES (1998). Treatment of *Microcotyle sebastis* (Monogenea) on the gills of cultured rockfish (*Sebastes schelegeli*) with oral administration of mebendazole and bithionol. Aquaculture 167:115-121.

Loir M, Le Gac F, Somarakis S, Pavlidis M (2001). Sexuality and gonadal cycle of the common dentex (*Dentex dentex*) in intensive culture. Aquaculture 194: 363-381.

Mellen IM (1928). The treatment of fish diseases. Zoopathologica 2:1-31.

Mollaret I, Jamieson BGM, Justine JL (2000). Phylogeny of the Monopisthocotylea and Polyopisthocotylea (Platyhelminthes) inferred from 28S rDNA sequences. Int. J. Parasitol. 30: 171-185.

Paperna I (1960). The influence of monogenetic trematodes on fish breeding economy. Bamidgeh 12: 40-48.

Paperna I (1983). Review of diseases of cultured warm-water marine fish. Réun. Cons. Int. Explor. Mer. 182: 44-48.

Papoutsoglou S, Costello MJ, Stamou E, Tziha G (1996). Environmental conditions at sea-cages, and ectoparasites on farmed European sea-bass, *Dicentrarchus labrax* (L.), and gilt-head sea-bream, *Sparus aurata* L., at two farms in Greece. Aquacult. Res. 27: 25-34.

Perkins EM, Donnellan SC, Bertozzi T, Whittington ID (2010). Closing the mitochondrial circle on paraphyly of the Monogenea (Platyhelminthes) infers evolution in the diet of parasitic flatworms. Int. J. Parasitol. 40:1237-1245.

Rodgers CJ, Furones MD (1998). Disease problems in cultured marine fish in the Mediterranean. Fish Pathol. 33:157-164.

Saitou N, Nei M (1987). The neighbor-joining method: a new method for reconstructing phylogenetic trees. Mol. Biol. Evol. 4: 406-425.

Sanz F (1992). Mortality of cultured seabream (*Sparus aurata*) caused by an infection with a trematode of the genus *Microcotyle*. Bull. Eur. Assoc. Fish Pathol. 12: 186-188.

Swofford DL, Olsen GJ (1990). Phylogeny reconstruction. In: Molecular Systematics. Sinauer, Sunderland: pp. 411-501.

Tamura K, Stecher G, Peterson D, Filipski A, Kumar S (2013). MEGA6: Molecular Evolutionary Genetics Analysis Version 6.0. Mol. Biol. Evol. 30: 2725-2729.

Tomás A, Martínez-Llorens S, Jover M (2009). The effect of dietary soybean meal on growth, nutrient utilization efficiency, and digestibility of juvenile common dentex, *Dentex dentex* (Actinopterygii: Perciformes: Sparidae). Acta Ichtyol. Pisc. 39: 19-25.

Whittington ID, Deveney MR, Morgan JAT, Chisholm LA, Adlard RD (2004). A preliminary phylogenetic analysis of the Capsalidae (Platyhelminthes: Monogenea: Monopisthocotylea) inferred from large subunit rDNA sequences. Parasitology 128:511-519.

academicJournals

Vol. 14(33), pp. 2539-2546, 19 August, 2015
DOI: 10.5897/AJB2015.14757
Article Number: 87EDC6D54967
ISSN 1684-5315

http://www.academicjournals.org/AJB

African Journal of Biotechnology

Full Length Research Paper

Status of cassava mosaic disease and whitefly population in Zambia

P. C. Chikoti[1]*, M. Tembo[1], M. Chisola[1], P. Ntawuruhungu[2] and J. Ndunguru[3]

[1]Zambia Agriculture Research Institute, Mt. Makulu Research Station, P/B 7 Chilanga, Zambia.
[2]International Institute of Tropical Agriculture, P.O. Box 310142 Chelston, Lusaka, Zambia.
[3]Mikocheni Agricultural Research Institute (MARI), P.O. Box 6226, Dar es Salaam, Tanzania.

Received 26 May, 2015; Accepted 27 July, 2015

Cassava mosaic disease is the most important disease affecting cassava in Zambia. A study was conducted through a survey to determine the status of cassava mosaic disease incidence, severity and whitefly abundance in farmers' fields in six provinces: Lusaka, Northern, North-Western, Luapula, Eastern and Western between March and May 2014. The study reveals that cassava mosaic disease incidence was highest in Lusaka (70.0%) and Eastern (69.2%) and lowest in Luapula (45.1%) and Northern (48.5%) provinces. Disease symptom severity was moderate to severe in Lusaka (3.48) and Eastern (3.14) and low in the rest of the provinces. Adult whitefly (*Bemisia tabaci*) populations were highest in Western Province (2.71) and lowest in Luapula Province (0.02). Polymerase chain reaction results using specific primers for African cassava mosaic virus and East African cassava mosaic virus detected single infections of African cassava mosaic virus and East African cassava mosaic virus in 67.9 and 6.8% of the positive reactions, respectively. Dual infections of African cassava mosaic virus and East African cassava mosaic virus were detected in 25.6% of the samples tested. Cassava brown streak virus was not detected in any of the samples and no symptoms suggestive of cassava brown streak disease were observed in the surveyed fields.

Key words: Disease, incidence, severity, whitefly.

INTRODUCTION

Cassava is one of the most important root crops in Africa. It is a staple crop in many African countries including Zambia, Mozambique, Tanzania, Malawi, Democratic Republic of Congo (DRC) and Nigeria. The crop is widely grown in the tropical regions in Africa, Asia and Latin America; and cultivated mostly by smallholder farmers. Production of cassava varies from country to country with varying yields. In Zambia, the average yield is around 4.9 t ha^{-1}, which is below that of Africa at 11.1 t ha^{-1} (FAOSTAT, 2015).

Cultivation of cassava in Africa and Zambia in particular, is constrained by a number of biotic factors of which diseases are the most important. The diseases include cassava mosaic disease (CMD), cassava anthracnose disease (CAD), cassava bacterial blight (CBB) and cassava brown streak disease (CBSD). CMD

*Corresponding author. E-mail: chizachikoti@hotmail.com.

Table 1. Primer pairs used for amplification of cassava mosaic begomoviruses.

Primer	Sequence (5' - 3')	Specificity	Strand	DNA component
JSP001[a]	ATGTCGAAGCGACCAGGAGAT	ACMV	Sense	AV1/CP
JSP002[a]	TGTTTATTAATTGCCAATACT	ACMV	Antisense	AV1/CP
EAB555/F[a]	TACATCGGCCTTTGAGTCGCATGG	EACMV	Sense	DNA-B
EAB555/R[a]	CTTATTAACGCCTATATAAACACC	EACMV	Antisense	DNA-B
UV-AL1/F[b]	TGTCTTCTGGGACTTGTGTG	EACMV-UgV	Sense	AV1/CP
ACMV-CP/R3[b]	GCCTCCTGATGATTATATGTC	EACMV-UgV	Antisense	AV1/CP

[a]Primers used for the study are as described by Fondong et al. (1998) and [b]Zhou et al., 1997.

and CBSD are the major diseases of economic importance. CMD is caused by several distinct whitefly transmitted viruses [African cassava mosaic virus (ACMV), East African cassava mosaic virus (EACMV), East African cassava mosaic Cameroon virus (EACMCV), East African cassava mosaic Zanzibar virus (EACMZV), East African cassava mosaic Malawi virus (EACMMV), East African cassava mosaic Kenya virus (EACMKV) and South African cassava mosaic virus (SACMV)] (Bull et al., 2006). Two other species have recently been described: African cassava mosaic Burkina Faso virus (ACMBFV) and Cassava mosaic Madagascar virus (CMMGV) (Tiendrébéogo et al., 2012).

The viruses exhibit diverse infection dynamics in terms of symptom expression, progression, recovery, severity, and as well as host range (Bull et al., 2007; Patil and Fauquet, 2009). The genome of each of the viruses consists of two subgenomic DNA components, DNA-A and DNA-B. DNA-A and DNA-B, each of about 2.8 kbp (Stanley et al., 2004), with different roles in the infection process. DNA-A encodes genes responsible for viral replication [AC1 (*Rep*), and AC3 (*Ren*)], regulation of gene expression [AC2 (*Trap*)] and particle encapsidation [AV1 (*CP*)] while DNA-B encodes two proteins, BC1 (*MP*) and BV1 (*NSP*) involved in cell-to-cell movement within the plant, host range and symptom modulation (Stanley et al., 2004).

Co-infections of EACMV and ACMV in cassava have been reported in Zambia, Nigeria and Tanzania (Chikoti et al., 2013; Harrison et al., 1997; Ogbe et al., 2003). Of the two viruses, ACMV was reported to be the most predominant and widely distributed wherever cassava is grown in Zambia (Chikoti et al., 2013). With the reemergence of severe form of CMD in East Africa, a new virus strain, the East African cassava mosaic virus Uganda variant (EACMV-UgV) was described (Zhou et al., 1997). Since EACMV-UgV has been reported to occur in DRC, Angola (Kumar et al., 2009), and Tanzania (Ndunguru et al., 2005), the virus is moving southwards towards the border with Zambia. The rapid spread of EACMV-UgV from Uganda to some of the Southern Africa Development Community (SADC) countries such as Tanzania and DRC necessitated this study. Therefore the study was carried out to give an update on the CMD incidence, severity and whitefly population in Zambia.

MATERIALS AND METHODS

Study area

The study was conducted in six provinces: Luapula, North-Western, Northern, Lusaka, Western and Eastern. Luapula, Northern and North-Western are located in agroecological region III, a high rainfall area which experiences rainfall above 1000 mm per year. Eastern, Western, and Lusaka provinces are located in agroecological region II and experiences rainfall between 800 to 1000 mm per year.

Sample collection and propagation

The cassava stem cuttings were collected from plants expressing CMD symptoms from farmers' fields. Plants expressing mild and severe symptoms and from the same variety were targeted. Collection of samples from the field was done through walking in the field using an 'X' pattern. A total of 30 plants were assessed per field, 15 from each diagonal. The whiteflies were also counted from the top most fully expanded leaves from the same plants assessed for disease symptoms. The stem cuttings were labeled and geocoordinates (latitude, longitude and altitude) taken using a global positioning system (Garmin, etrex, summit HC). The collected stem cuttings were transferred to Zambia Agricultural Research Institute (ZARI), Mt. Makulu Research Station and planted in the screenhouse at temperatures between 20 and 30°C. The stem cuttings were planted in insect proof screenhouse in two liter black polythene bags and watering was done when necessary. Monocrotophos insecticide was applied weekly using a knapsack sprayer to control cassava mealybug, cassava green mite and whitefly.

DNA extraction and PCR

Total plant DNA was extracted from cassava leaves expressing CMD symptoms using the Dellaporta method (Dellaporta et al., 1983). Fresh leaf samples were ground with mortar and pestle and virus specific primers (Table 1) were used to detect ACMV, EACMV and EACMV-UgV in 278 virus isolates collected during the survey. Polymerase chain reaction (PCR) was performed using a thermorcycler (Technen 500). PCR conditions were 94°C for 2 min followed by 30 cycles of 94°C for 1 min, 55°C for 1 min, 72°C for 1 min and an extension cycle of 10 min at 72°C. The PCR products were visualised by electrophoresis in 1% agarose gel in TAE buffer (10 mM tris-acetate, 1mM NaEDTA, pH 8.0).

Data analysis

Disease incidence was determined as the proportion of diseased

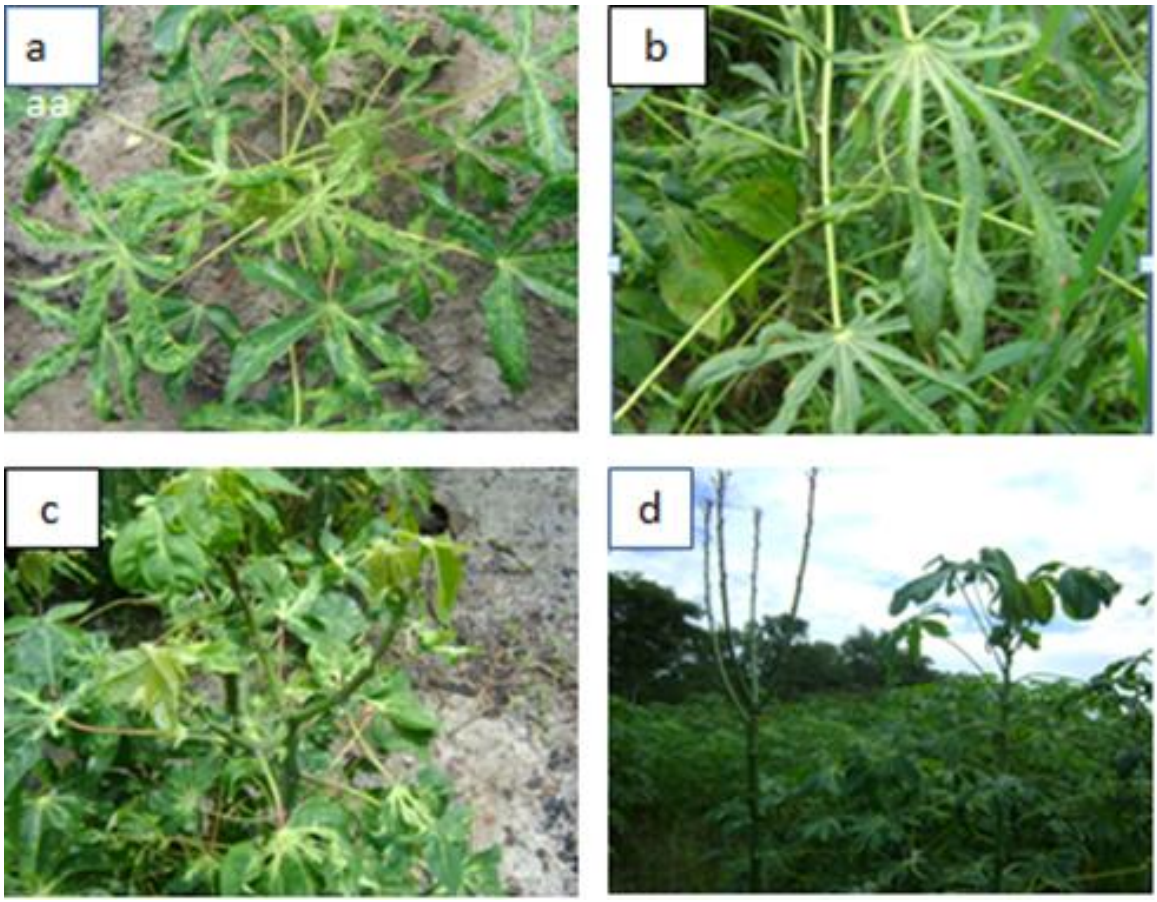

Figure 1. Cassava mosaic disease symptoms. **a)** Light green and yellow patches. **b)** Leaf narrowing. **c)** Leaf curling. **d)** 'Candle stick' symptoms on the left with a normal plant on the right.

plants expressed as a percentage of total number of plants observed per field. Disease symptom severity data were edited to remove plants which showed no symptoms (score 1) and the analysis conducted for the CMD-infected plants (score 2 to 5) per field. Means for incidence, severity and whitefly counts were separated using a one-way analysis of variance (ANOVA) using the Statistical Package for Social Sciences (SPSS). Geo-coordinates (longitude, latitude and altitude) data were used to map the geographical distribution of the cassava viruses using DIVA GIS version 7.5.

RESULTS

Assessment of CMD symptoms

From a total of 245 cuttings collected, 237 were successfully established in the screenhouse. The cassava stem cuttings reproduced similar symptoms observed in the field. Mild and severe CMD symptoms were observed in the surveyed farmers' cassava fields (Figure 1). Mild symptoms comprised patches of yellow and green sectors with less leaf distortion while plants with severe symptoms had deformed leaves and showed stunted growth. Plants with "candle stick" symptoms were also observed (Figure 1).

Cassava mosaic disease severity and incidence

Cassava mosaic disease severity differed significantly ($P<0.044$, $F=2.7$, $df=5$) among the surveyed provinces and averaged 2.95. Lusaka (3.48) and Eastern (3.14) provinces recorded the highest disease severity. The lowest (2.79) was recorded in Northern and Western provinces (Table 2). There were no significant differences for disease incidence among the six provinces surveyed. However, in some fields in Lusaka and Western provinces disease incidence was almost 100%.

Adult whitefly population

Although there were no significant differences in the mean adult whitefly population, Western (2.71) and North-Western (1.16) provinces recorded the highest whitefly population. The lowest (0.02) was recorded in Luapula Province. In the two provinces which recorded high whitefly population, sooty mould was also observed on the middle and lower leaves of healthy and CMD infected plants (Figure 2).

Table 2. Incidence, symptom severity and whitefly populations on cassava crop in six provinces (March/May 2014).

Province	Incidence (%)	Mean of symptom severity (scale 1-5)[a]	Mean of adult whitefly population
Lusaka	70.0	3.48	0.26
Luapula	45.1	2.88	0.02
Northern	48.5	2.79	0.04
North-Western	58.4	2.87	1.16
Western	62.7	2.79	2.71
Eastern	69.2	3.14	0.67
Mean	57.4	2.95	0.89
P-value (5%)	0.487	0.044	0.092
F-statistic	0.995	2.700	1.336

[a]Scale (1-5) 1, no symptoms observed; 2, mild chlorotic pattern over entire leaflets or mild distortion at the base of leaflets only with the remainder of the leaflets appearing green and healthy; 3, moderate mosaic pattern throughout the leaf, narrowing and distortion of the lower one-third of leaflets; 4, severe mosaic, distortion of two thirds of the leaflets and general reduction of leaf size; 5, severe mosaic distortion of the entire leaf.

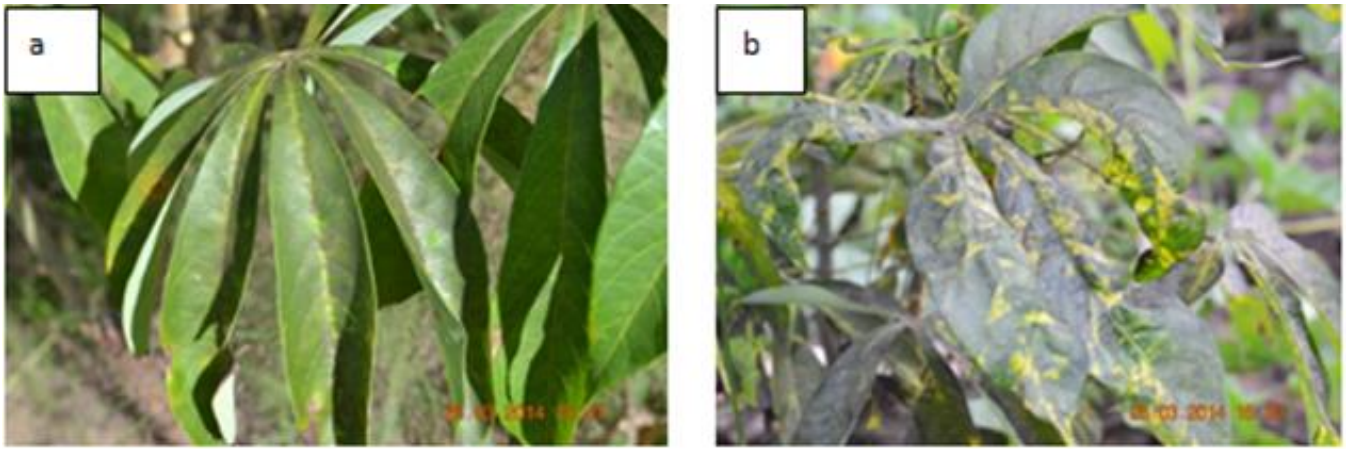

Figure 2. Sooty mould on (a) healthy CMD free plant and (b) CMD infected plant.

Detection of cassava mosaic begomoviruses

PCR amplification products were observed for all the cassava mosaic geminivirus isolates tested using JSP001/2 and EAB555F/R primers. DNA-A (744 kbp) and DNA-B (544 to 560 kbp) partial fragments were amplified by PCR using primers JSP001/2 and EAB555-F/R (Figure 3). There was no amplification for EACMV-UgV, CBSV and UCBSV isolates.

Distribution of virus species in Zambia

A total of 237 samples were analyzed by PCR and of these 219 (92.4%) partial fragments of 774 bp (DNA-A AV1/CP) for ACMV and 556 bp (DNA-B) for EACMV were amplified. Single infections of ACMV occurred in 67.6% (148/219) of the samples, while EACMV occurred in 6.8% (15/219). Mixed infections of ACMV+EACMV were detected in only 25.6% (56/219) of the positive samples (Table 3).

ACMV was widely distributed in all the provinces in which the survey was conducted. Co-infections of EACMV and ACMV occurred in all the provinces except for North-Western Provinces (Figure 4). Single infection of EACMV was detected in Lusaka, Northern and Eastern provinces.

DISCUSSION

This study constitutes the most current survey of cassava mosaic disease in Zambia. The survey was carried out between March and May 2014 in six provinces (Lusaka, Northern, North-Western, Luapula, Eastern and

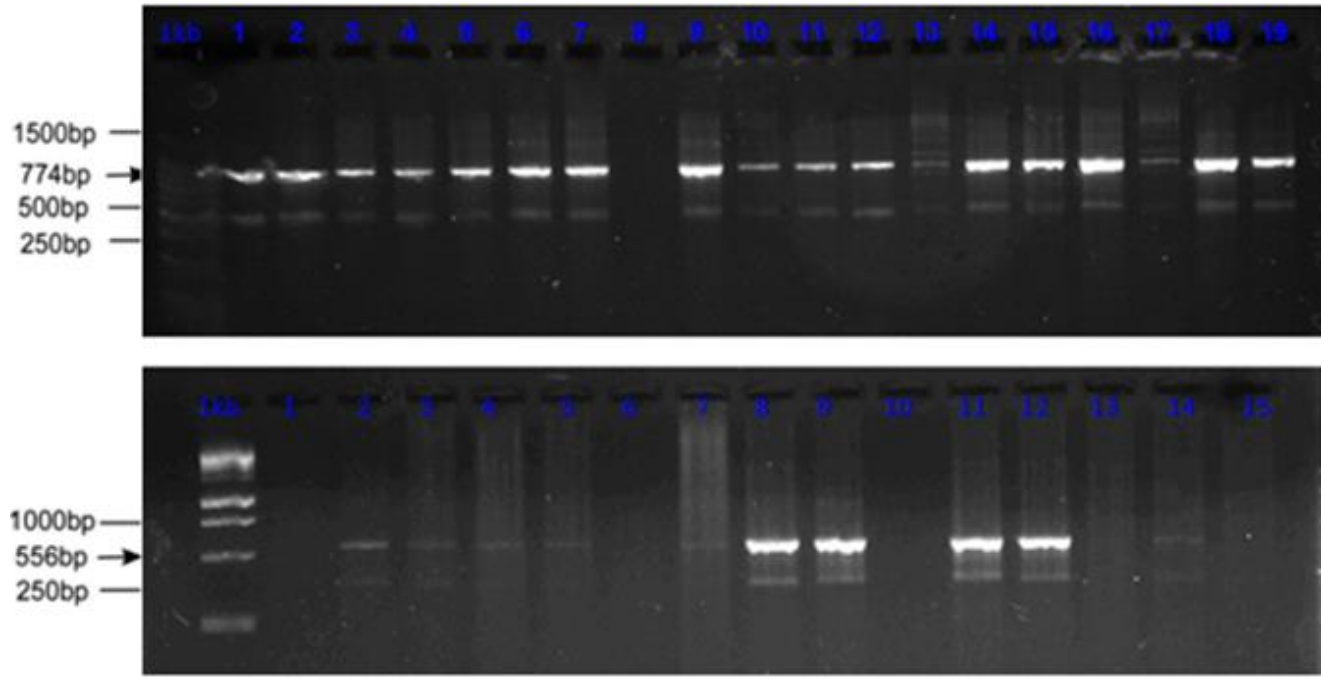

Figure 3. PCR amplification of coat protein of ACMV (774 bp) and EACMV (556 bp) from cassava samples using specific primers JSP001/2 and EAB555F/R, respectively and a DNA 1Kb Ladder

Table 3. Distribution of cassava virus isolates in the six provinces of Zambia.

Province	Number of samples	ACMV[a]	Cassava mosaic begomoviruses	
			EACMV[b]	ACMV + EACMV
Lusaka	15 (6.8%)	7 (4.7%)	2 (13.3%)	6 (10.7%)
Luapula	14 (6.4%)	12 (8.1%)	0 (0.0%)	2 (3.6%)
Northern	52 (23.7%)	25 (16.9%)	3 (20.0%)	24 (42.9%)
North-Western	10 (4.6%)	10 (6.8%)	0 (0.0%)	0 (0.0%)
Western	71 (32.4%)	69 (46.6%)	0 (0.0%)	2 (3.6%)
Eastern	57 (26.0%)	25 (16.9%)	10 (66.7%)	22 (39.3%)
Total	219	148 (67.6%)	15 (6.8%)	56 (25.6%)

[a]Africa cassava mosaic virus. [b]East Africa cassava mosaic virus.

Western). Severe and mild symptoms were observed in all the areas visited. The presence of severe symptoms could be as a result of planting susceptible materials by the farmers. Few farmers have adopted improved varieties bred by the Zambia Agriculture Research Institute which are resistant to CMD. Other reasons could be recycling of seed by the farmers and as a result of virus co-infections. Co-infection with ACMV and EACMV has been reported to cause severe symptoms due to synergistic interactions (Fondong et al., 2000). In Lusaka and Eastern provinces, incidence and severity were high as evidenced from the results obtained. 'Candle stick' symptoms which are characteristic of plants infected with EACMV-UgV were observed. What caused the candle stick appearance in the field calls for further investigations.

The adult whitefly population in the current survey averaged 0.89 slightly higher than what was reported by Chikoti et al. (2013) which reported 0.64 whiteflies per shoot in a survey of 2009. However, the whitefly numbers are lower compared to what has been reported in East and West Africa (Legg and James, 2005). This could be attributed to the long dry climatic conditions which Zambia experiences for most of the year unlike in East and West Africa which experience bimodal rainfall pattern. Climatic factors have been reported to have significant effects on whitefly population (Legg, 1994).

In the current survey, Luapula and Northern provinces

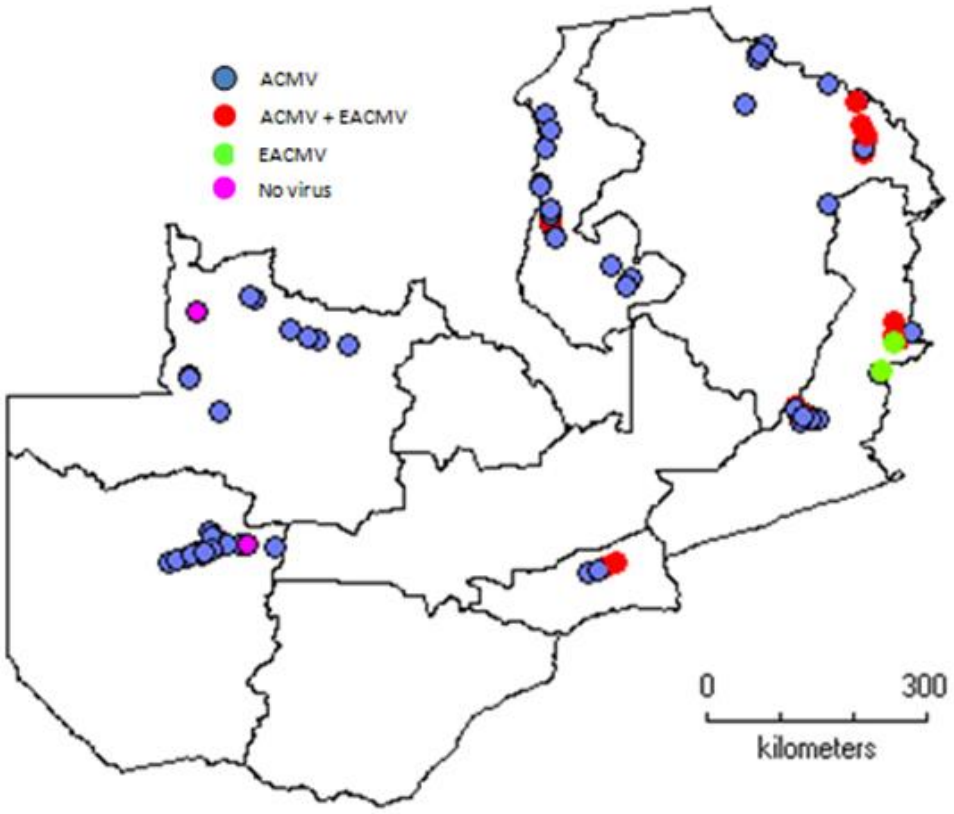

Figure 4. Distribution of cassava mosaic begomoviruses isolates in the surveyed provinces.

recorded the lowest whitefly population compared to what has been observed in previous studies (Chikoti, 2011). In Western and North-Western provinces, high whitefly populations observed in some fields is similar to earlier surveys by Muimba-kankolongo (1997). The high whitefly population in these provinces is not clearly understood. However, we think that it could be due to different whitefly biotypes that exist in these ecologies.

The presence of sooty mould was indicative of high whitefly populations particularly in Western, North-Western and some parts of Eastern Province. Sooty mould is not common in Zambia unlike in East Africa (Omongo et al., 2012). The large whitefly populations has effects on cassava plants; direct feeding damage by whiteflies and the production of honey dew, which falls onto the lower leaves. This is subsequently colonised by black sooty mould (Bellotti and Arias, 2001; Legg et al., 2004), which reduces the ability of the leaves to photosynthesize and contributes to yield losses.

It is apparent from the results of this study that single infections of ACMV were more common compared to those of EACMV. Previous studies (Ogbe et al., 1997) have also reported high frequency of single infections of ACMV compared to EACMV. Similarly, co-infections were also lower than infections of ACMV alone. This could be due to farmers leaving out severely infected plants when selecting cuttings for planting. The occurrence of co-infections in all the provinces surveyed except North-Western Province could be fueled by movement of infected cassava planting materials which are not tested for virus presence in the country.

Our study confirms the occurrence of EACMV as single infections in Western and Eastern provinces as previously reported (Chikoti et al., 2013). However, absence of single infection of EACMV in Luapula Province could be that the fields which had the virus could have been missed when the study was conducted. Detection of ACMV and EACMV in dual infected plants and single infection (EACMV) in Northern Province suggests that the occurrence of the two viruses (ACMV and EACMV) is wide spread than previously thought. These findings agree with previous studies (Were et al., 2003) which reported the presence of the viruses in the province.

Candle stick symptoms synonymous with EACMV-UgV (Alabi, 2011) were observed in the fields. However, the Ugandan variant was not detected in all the samples collected from the surveyed areas. The absence of EACMV-UgV from the current and earlier surveys confirms that Zambia is still free of the Ugandan variant. The fact that EACMV-UgV was not detected in samples from the surveyed areas is not surprising given the long

distance between Zambia and the Democratic Republic of the Congo (northern neighbour) where the virus has been reported to occur (Bulubulu et al., 2015). Most of the land between the common borders of the two countries is covered by forests and is sparsely populated.

It was observed from this study that disease incidence has increased to 57.4% from the previously reported 41.0% in the 1996 study (Muimba-Kankolongo et al., 1997). This could be that farmers are still recycling infected planting materials. The increase in whitefly population in Western and North-Western province could have contributed to the increase in the levels of disease incidence. In the 1990s during the pandemic in East Africa, high whitefly populations were seen as the driver of high CMD incidence. In Uganda, high whitefly population has been observed to increase CMD incidence (Sserubombwe et al., 2005). The decrease of the severity disease scores in Luapula, Northern, North-Western, and Western provinces in this study compared to previous survey (Chikoti et al., 2013) could be attributed to the farmers selecting health cassava planting materials. There have also been campaigns by agriculture extension agents, non- governmental organizations (NGOs), and Research Institutes sensitizing and encouraging farmers to use disease free planting materials.

In conclusion, our study has shown that CMD is still widely distributed in most of the cassava growing provinces. We have established the existence of ACMV and EACMV in single and coinfections in Northern Province. This study demonstrates that ACMV is still wide spread and it also highlights the urgent need for more information. The high incidence recorded in this survey is also of concern given that farmers mostly obtain cassava cuttings for planting from own fields or their neighbours which are not tested. Therefore, there is need to sensitize institutions involved in distribution of cassava planting materials to test them before selling them to the farmers. Future efforts should also aim at characterizing the cassava mosaic begomoviruses in the country in order to have a clear understanding of the existing types of strains.

Conflict of interests

The authors did not declare any conflict of interest.

ACKNOWLEDGEMENTS

Mr. Jackson Mwenya, Mr. Suwilanje Schilima and Ms. Judith Malumo are appreciated for the laboratory assistance. We acknowledge Mikocheni Agriculture Research Institute for the provision of diagnostic facilities. Africa Development Bank (AfDB) and United States Agency for International Development (USAID) are appreciated for the financial assistance.

REFERENCES

Alabi OJ, Kumar PL, Naidu RA (2011). Cassava mosaic disease: A curse to food security in Sub-Saharan Africa. Online, APS*net* Features. doi:10.1094/APSnetFeature-2011-0701. Retrieved on 12 January 2015 from http://www.apsnet.org/publications/apsnetfeatures/Pages/cassava.aspx

Bellotti AC, Arias B (2001). Host plant resistance to whiteflies with emphasis on cassava as a case study. Crop Prot. 20:813-823.

Bull SE, Briddon RW, Sserubombwe WS, Ngugi K, Markham PG, Stanley J (2006). Genetic diversity and phylogeography of cassava mosaic viruses in Kenya. J. Gen. Virol. 87:3053-3065.

Bull SE, Bridon RW, Sseubombwe WS, Ngugi K, Markham PG, Stanley J (2007). Infectivity, pseudorecombination and mutagenesis of Kenyan cassava mosaic begomoviruses. J. Gen. Virol. 88:1624-1633.

Bulubulu OF, Diamuini NA, Kikakedimau NF, Mbaya NA, Mutambel H, Lumande K, Luyindula N, Rufflard G, Lepoivre P (2015). PCR and ELISA detection of cassava mosaic virus in a Congolese cassava landrace. Int. J. Biotechnol. Food Sci. 3: 10-16

Chikoti PC (2011). Development of cassava (*Manihot esculenta* Crantz) cultivars for resistance to cassava mosaic disease in Zambia. PhD thesis, University of KwaZulu-Natal.

Chikoti PC, Ndunguru J, Melis R, Tairo F, Shanahan P, Sseruwagi P (2013). Cassava mosaic disease and associated viruses in Zambia: occurrence and distribution. Int. J. Pest Manag. 59: 63-72

Dellaporta SL, Wood J, Hisks JB (1983). A plant DNA minipreparation: version II. Plant Mol. Biol. Rep. 1:19-21.

FAOSTAT (2015). Food and Agriculture Organisation of the United Nations. Retrieved 10 March 2015 from http://faostat3.fao.org/download/Q/QC/E

Fondong V N, Pita JS, Rey C, Fauquet AC (1998). First Report of the Presence of East African Cassava Mosaic Virus in Cameroon. Plant Dis. 82:1172

Fondong VN, Pita JS, Rey ME, de Kochko A, Beachy RN, Fauquet CM (2000). Evidence of synergism between African cassava mosaic virus and a new double-recombinant geminivirus infecting cassava in Cameroon. J. Gen. Virol. 81:287-297

Harrison BD, Zhou X, Otim-Nape GW, Liu Y, Robinson DJ (1997). Role of a novel type of double infection in the geminivirus-induced epidemic of severe cassava mosaic in Uganda. Ann. Appl. Biol. 131:437-448

Kumar LP, Akinbade SA, Dixon AGO, Mahungu NM, Mutunda MP, Kiala D, Londa L, Legg JP (2009). First report of the occurrence of East African cassava mosaic virus-Uganda (EACMV-UG) in Angola. Plant Pathol. *58*:402

Legg J (1994). Bemisia Tabaci: the whitefly vector of cassava mosaic geminiviruses in Africa: an ecological perspective. Afr. Crop Sci. J. 2:437-448

Legg J, James B (2005). Conclusions and recommendations. In: Whitefly and whitefly-borne viruses in the tropics: Building a knowledge base for global action. Edited by Pamela K. Anderson & Francisco J. Morales; with the collaboration of Annie L. Jones and Richard H. Centro Internacional de Agricultura Tropical (CIAT), 2005. 351 p.

Legg JP, Sseruwagi P, Brown J (2004). *Bemisia* whiteflies cause physical damage and yield loss to cassava in Africa. In: Sixth International Scientific Meeting of the Cassava Biotechnology Network, 8-14 March, 2004, CIAT, Cali, Colombia. p. 78

Muimba-Kankolongo A, Chalwe A, Sisupo P, Kang MS (1997). Distribution, prevalence and outlook for control of cassava mosaic disease in Zambia. Roots 4:2-7.

Ndunguru J, Legg JP, Aveling, TAS, Thompson G, Fauquet CM (2005). Molecular biodiversity of cassava begomoviruses in Tanzania: evolution of cassava geminiviruses in Africa and evidence for East Africa being a center of diversity of cassava geminiviruses. Virol. J. 2:21.

Ogbe FO, Legg JP, Raya MD, Muimba-Kankalongo A, Theu MP, Kaitisha G, Phiri NA, Chalwe A (1997). Diagnostic survey of cassava mosaic viruses in Tanzania, Malawi and Zambia. Roots 12-15

Ogbe FO, Thottappilly G, Dixon AGO, Atiri GI, Mignouna HD (2003).

Variants of East African cassava mosaic virus and its distribution in double infections with African cassava mosaic virus in Nigeria. Plant Dis. 87:229-232

Omongo CA, Kawuki R, Bellotti AC, Alicai T, Baguma Y, Maruthi MN, Bua A, Colvin J (2012). African Cassava Whitefly, *Bemisia tabaci*, Resistance in African and South American Cassava Genotypes. J. Integr. Agric. 11:327-336

Patil BL, Fauquet CM (2009). Cassava mosaic geminviruses: actual knowledge and perspectives. Mol. Plant Pathol. 10:685-701

Sserubombwe W, Thresh M, Legg J, Otim-Nape W (2005). Progress of Cassava Mosaic Disease in Ugandan Cassava Varieties and in Varietal Mixtures. In: Whitefly and whitefly-borne viruses in the tropics: Building a knowledge base for global action. (In: by Pamela, K.A. Francisco, J., Annie, L., Jones & Richard, H.M. Cali, Colombia, Centro Internacional de Agricultura Tropical (CIAT). p. 351.

Stanley J, Bisaro DM, Briddon RW, Brown JK, Fauquet CM, Harrison BD, Rybicki EP, Stenger DC (2004). Geminiviridae. In Virus Taxonomy, VIIIth Report of the ICTV. 8th edition. Edited by Fauquet CM, Mayo MA, Maniloff J, Desselberger U and Ball LA. Elsevier/Academic Press. 2004:301-326.

Tiendrébéogo F, Lefeuvre P, Hoareau M, Harimalala MA, De Bruyn A, Villemot J, Traoré VSE, Konaté G, Traoré AS, Barro N, Reynaud B, Traoré O, Lett JM (2012). Evolution of African cassava mosaic virus by recombination between bipartite and monopartite begomoviruses. Virol. J. 9:67

Were HK, Winter S, Maiss E (2003). Distribution of begomoviruses infecting cassava in Africa. J. Plant Pathol. 85:145-151

Zhou X, Liu Y, Calvert L, Munoz C, Otim-Nape GW, Robinson DJ, Harrison BD (1997). Evidence that DNA-A of a geminivirus associated with severe cassava mosaic disease in Uganda has arisen by interspecific recombination. J. Gen. Virol. 78:2101-2111.

academicJournals

Vol. 14(33), pp. 2547-2553, 19 August, 2015
DOI: 10.5897/AJB2015.14777
Article Number: BF0A34954968
ISSN 1684-5315

http://www.academicjournals.org/AJB

African Journal of Biotechnology

Full Length Research Paper

Polymers selection for a liquid inoculant of *Azospirillum brasilense* based on the Arrhenius thermodynamic model

Cortés-Patiño Sandra and Bonilla Ruth Rebeca*

Corporación Colombiana de Investigación Agropecuaria -Corpoica. Km 14 via Mosquera, Cundinamarca, Colombia.

Received 4 June, 2015; Accepted 6 August, 2015

Plant growth promoting bacteria (PGPB) enhances the growth of their hosts and can protect them from biotic and abiotic stresses. Bacterial inoculants contain one or more of these beneficial strains in a carrier material, which must be able to maintain the viability of the cells during the time of storage, and also guarantee the biological activity of the strains once applied in the soil. These inoculants can be solid, liquid, gel or oil-based, depending on the characteristics of the strains and the shelf life expected by the producers. In this study, we used a method of accelerated degradation to select a polymer and a concentration to maintain cell stability of a liquid inoculant based on the strain C16 *Azospirillum brasilense.* A screening at 45°C was made to compare the protectant effect of five polymers on the viability of the strain (p/v): carrageenan (1.5%), sodium alginate (1%), trehalose (10 mM), polyvinylpyrrolidone (2%), glycerol (10 mM) and phosphate saline buffer as control. Carrageenan and sodium alginate showed significant differences in cell viability over the use of other polymers ($P < 0.05$). We evaluated cell viability with these two polymers at three concentrations and three different temperatures (4, 28 and 45°C) for 60 days and determined the bacterial degradation rates. Based on the Arrhenius thermodynamic model, we calculated the time required to reduce cell concentration in three log units, and observed that the protectant activity of each polymer and each concentration depends on the temperature of storage. Cell viability was best preserved in all treatments at 4°C. In general, alginate prolonged cell viability at 28°C, and carrageenan at 45°C. Alginate at 1% and carrageenan at 0.75% showed a stable behavior (superior to the control) in the three evaluated temperatures, so we conclude that they can be used for a formulation of a liquid inoculant based on the strain C16 of *A. brasilense.*

Key words: Energy of activation, degradation, cell death, kinetics, formulation.

INTRODUCTION

Plant growth promoting bacteria (PGPB) are able to enhance the growth of their hosts by increasing the supply or availability of primary nutrients, producing beneficial compounds and protecting them from biotic

*Corresponding author. E-mail: rbonilla@corpoica.org.co. Tel/Fax: +5714227300.

Abbreviations: PGPB, Plant growth promoting bacteria.

and abiotic stresses (Vessey, 2003). Bacterial inoculants contain one or more of these beneficial strains in an easy-to-use and economical carrier material (Bashan, 1998), which must be able to maintain the viability of the cells and protect them from the stresses they face once applied into the soil or plant surfaces. There is no universal carrier, and choosing the proper formulation is a strain-specific process as important as the selection of the bacteria itself (Rivera et al., 2014). Solid, liquid, oil and gel based formulations have been developed, each with their own advantages and limitations. Liquid inoculants are an economical technology, usually consisting in the addition of one or more polymers to the broth culture. These polymers are used to protect bacterial cells from stresses and help their establishment into the host (Albareda et al., 2008; Mugilan et al., 2011; Amalraj et al., 2013*)*. Their major disadvantage is that they cannot be stored at room temperature for long periods without compromising the viability of the bacteria and their efficacy. Here, the physical and chemical properties of polymers protect cells against desiccation and sedimentation, which is directly related to cell death (Sivasakthivelan and Saranraj, 2013; Rouissi et al., 2011).

Stability tests are used to determine the viability and biological activity of the bacteria inside these formulations, helping to establish the point where they are no longer viable and will not be of any use to the farmers. In the first steps of formulating a bacterial inoculant, methods of accelerated thermal degradation are used to select -in a short period of time, the components which will best preserve the viability of the strains. These models rely on the effect of temperature over cell viability, and with first-order kinetics, determine the experimental values of cell degradation rates. Prediction models like Arrhenius are used to calculate the energy of activation and determine the time required for cell death in the bacterial inoculant (Krumnow et al., 2009).

In this study, we aimed to select a polymer and concentration for a liquid inoculant based on the strain C16 of the PGPB *Azospirillum brasilense,* evaluating the effect of five polymers on cell viability and using the Arrhenius thermodynamic model to predict the shelf-life of the selected formulations. *A. brasilense*, a member of the alpha-proteobacteria, is one of the most studied PGPR (Steenhoudt and Vanderleyden, 2000; Okon and Labandera-Gonzalez, 1994; Baudoin et al., 2009) and its beneficial effects have been widely known in more than a hundred plant species (Bashan and Bashan, 2010), and are attributed to various mechanisms, especially nitrogen fixation and hormone production, such as auxins, cytokinins and gibberellins (Cassaan et al., 2014; Fibach-Paldi et al., 2011). Determining the best conditions to maintain the viability of the bacteria in the formulation can lead to a steady behavior in field, which will help to promote plant growth in crops of socio-economical interest.

MATERIALS AND METHODS

Bacterial strain and culture conditions

The strain C16 was isolated from *Panicum maximum*, identified as *A. brasilense,* and cryopreserved on glycerol (50%) (Cardenas et al., 2010). For its activation, the strain was incubated at 30°C for three days on Potato Agar Medium (Components g/L: potatoes peeled and sliced, 200; DL-malic acid, 2.5; KOH, 2.0; sucrose, 2.5; vitamin solution, 1.0 ml; micronutrient solution, 2 ml; bromothymol blue, 2 drops; agar, 15.0). Cellular suspensions were made in 10 ml of ABRA medium (Moreno et al., 2012), a strain-specific medium designed in our laboratory for biomass production. After 27 h, cell concentration was adjusted (OD 600 nm = 0.5).

Evaluation of the polymeric protectant effect under stress conditions

Five polymers were selected based on their use as additives in other liquid inoculant formulations (Table 1). Treatments were (w/v): alginate 1%; carragenaan 1.5%; polyvinylpyrrolidone 2%; trehalose 10 mM, glycerol 10 mM, and phosphate saline buffer (components g/l: NaCl 8.0, KCl 0.2, Na_2HPO_4 x $7H_2O$ 1.15, KH_2PO_4 0.2; pH 7.3) as a control. Flasks with ABRA medium were inoculated at 1% with the cellular suspensions and incubated for 27 h and 120 rpm. Each polymer was added at 10% of the total volume of the flasks -each flask consisting in one replicate. Three replicates per treatment were made, and the content of the flasks was dispensed in microtubes (1.5 ml) with a total of five microtubes per flask. Finally, the microtubes were incubated at 45°C for 15 days. During this time, cell concentration was determined by serial dilutions, plating 20 µL on BMS medium at 0, 7 and 15 days. At the end of the evaluation time, two polymers were selected based on their protectant effect on the preservation of cell viability.

Cell viability prediction with the Arrhenius thermodynamic model

For the two polymers chosen, three different concentrations were selected. The same procedure described above was used to mix the polymers within the cell suspensions. Three temperatures were selected to evaluate their effect: 4, 28 and 45°C, each one representing refrigeration, environmental and stress conditions, respectively. Treatments were carrageenan at 0.75, 1.5 and 3%; alginate at 0.5, 1 and 2%, and phosphate saline buffer as a control. All of them were incubated at the three temperatures mentioned above, with a total of 21 treatments. Cell concentration was measured at 0, 15, 30, 45 and 60 days. Knowing that bacterial degradation rate at constant temperature can be described by first-order kinetics, cell concentration versus time was plotted to determine the experimental values of cell death rate (k) based on Equation 1:

$$\mathrm{Log}\frac{N}{No} = -2.303 \times kt \quad (1)$$

First-order kinetics equation, where N_o is the initial concentration of cells, N is the cells concentration at a specific time, k represents the first-order rate constant and t, the time of the thermal degradation.

The first-order cell death rate (k) was replaced in the Arrhenius Equation 2, where A is the pre-exponential Arrhenius factor (1/day), Ea is the apparent activation energy (cal/mol), R is the

Table 1. Previous reports of the selected polymers for the screening with strain C16 *Azospirillum brasilense*

Polymer	Concentration	Microorganisms	References
Sodium alginate	1%	*Azospirillum brasilense, Pseudomonasfluorescens Rhizobium* sp.	Bashan and Gonzales (1999), Rivera (2014), Yabur et al. (2007)
Carragenaan	1.5%	*Azotobacter chroococcum*	Rojas-Tapias et al. (2013)
Polyvinylpirrolydone	2%	*Bradyrhizobium, japonicum Azorhizobium, caulinodans Mesorhizobium cicero Azospirillum brasilense*	Tittabutr et al. (2007), Kumaresan and Reetha (2011)
Trehalose	10 mM	*Pseudomonasfluorescens, Azospirillum brasilense*	Manikandan et al. (2010)
Glycerol	10 mM	*Pseudomonasfluorescens*	Manikandan et al. (2010)

universal gas constant (1.985 cal/ mol K), and T is temperature (K):

$$k = Ae^{-\frac{Ea}{RT}} \quad (2)$$

Taking the logarithm of the Arrhenius equation and plotting log k versus the reciprocal of temperature (1/T), the experimental value for the energy of activation was obtained (Equation 3):

$$\text{Log } k = -\frac{Ea}{2.303R} \times \frac{1}{T} + \text{Log } A \quad (3)$$

Finally, the time required to reduce cell concentration in three log units was estimated using the first-order kinetics equation.

Statistical analysis

The experimental design consisted in a complete randomized design with 21 treatments where polymers, concentrations and temperature were the factors of evaluation. The data of the screening was analyzed using the ANOVA and HSD Tukey test. To calculate the rate of cell death, the Arrhenius equation was used as reported by Sorokulova et al. (2008). Figures were made using Sigmaplot 13.0.

RESULTS

Screening under stress conditions

The first seven days of evaluation, cell viability showed no significant differences, but that tendency changed at day fifteenth, where cell concentrations differed significantly among treatments (Figure 1). Carrageenan and alginate showed the higher cell counts compared with the use of other polymers. Cells concentrations were maintained at least one log unit above, meaning that these two polymers protected cells against heat and desiccation and reduced the rate of cell death. Trehalose and glycerol also showed a protectant effect superior to polyvinylpyrrolidone, which was only similar to the control. All polymers proved to significantly protect cells against high temperature (45°C) with the exception of polyvinylpyrrolidone, but in this study, the strain C16 was more compatible with carrageenan and alginate. The observed behavior of polyvinylpyrrolidone contrasts with previous reports, where its good rheological properties, high water activities, and ability to limit heat transfer, helped to preserve cell viability of *Azospirillum, Azotobacter* and *Bacillus* strains (Leo Daniel et al., 2013; Kumaresan and Reetha, 2011). Here, the concentration of the polymer and its interaction with the liquid medium may have affected its performance (Albareda et al., 2008; Velineni and Brahmaprakash, 2011) which was also seen in glycerol and trehalose. Carrageenan and alginate demonstrated that, as seen by other authors, they have desirable characteristics as additives in liquid formulations. The viscosity and water holding capacity of these hydrophilic polymers reduced the drying rate and helped to protect cells from environmental stresses. Similar results were obtained with carrageenan on *Azotobacter chroococcum* (Rojas-Tapias et al., 2015), and alginate with *Rhizobium* and *Bradyrhizobium* strains (Tittabutr et al., 2007; Rivera et al., 2014). It is important to establish that these two polymers are used in other type of formulations like microencapsulation, which have been proved to maintain cell viability of nitrogen fixing bacteria for over fourteen years (Bashan and Gonzalez, 1999).

Cell viability prediction using the Arrhenius thermodynamic model

Figure 2 shows the dependence of cell viability as a function of time at the evaluated temperatures, where

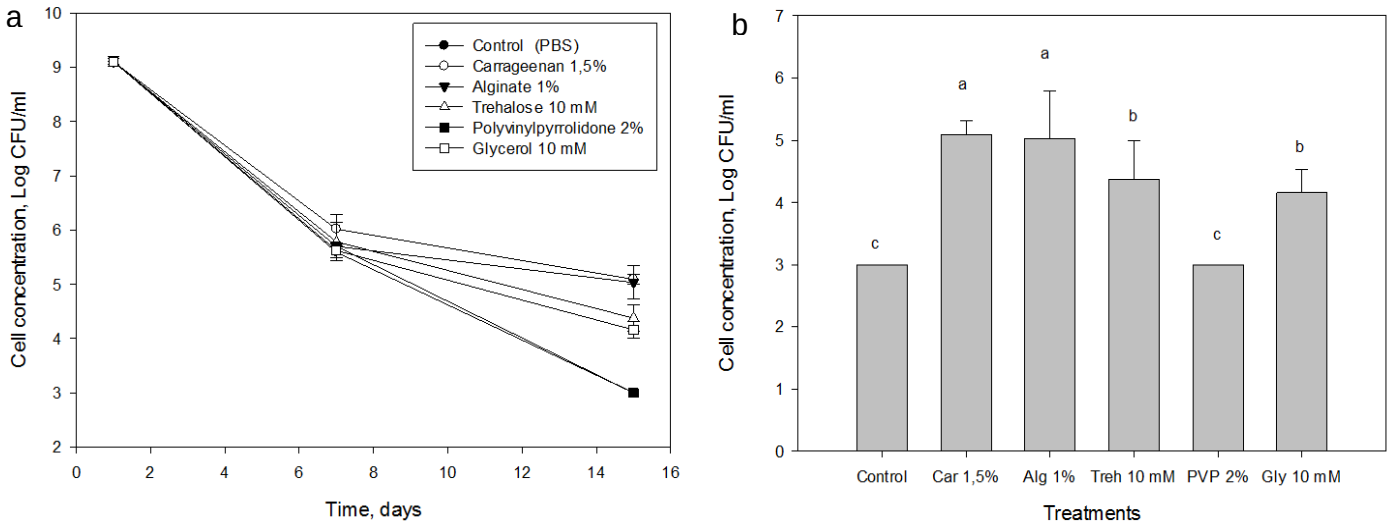

Figure 1. Effect of high temperature on cell concentration. a) Cell concentration during the assay. b) Final cell concentration at fifteenth day. Letters indicate sub homogeneous groups obtained using the HSD Tukey test.

degradation rates followed a first-order kinetics across all temperatures. At 4 and 28°C, cell viability was similar in all treatments, with a reduction of only one log unit regarding the polymer used and its concentration. At 45°C, cell viability decreased about four log units for the treatments with polymers and five log units for the control. At this temperature, we observed that carrageenan at 1.5 and 3% allowed a major viability of the strain. The apparent first-order degradation rate constants increased with temperature, with the highest values at 45°C for all treatments, as shown in Figure 3. At 4°C, alginate at 2% and control showed the highest degradation rates, as well as carrageenan at 0.75% at 28°C. On the highest temperature (45°C), carrageenan at 1.5 and 3% showed the lowest rates. Once the apparent rates of constant degradation was obtained, we used the Arrhenius equation to calculate the experimental values of the energy of activation (Table 2) and observed that, at the three concentrations used for carrageenan, the energy of activation was very similar. Alginate at 0.5%, had the highest value for energy of activation, and the control (PBS) the lowest, followed by alginate at 2%. Data of bacterial death during time helped to determine the apparent rate constants of degradation for each polymer, and the energy of activation was determined in a plot where the log of the rate is linearly related to the inverse of absolute temperature. In terms of viability, the energy of activation is the energy barrier needed to overcome cell degradation (Rojas-Tapias et al., 2015). The protectant effect of polymers was observed because the energy of activation increased when compared with the control (PBS), meaning that it takes more energy and time for cells to start degrading. The experimental values of the activation energy in our study (with a maximum value of 13.2 kcal/mol) were inferior to those described by other authors for *Azotobacter* (22.07 kcal/mol) and *Bacillus* spores (19.7 kcal/mol) when they were evaluating the effect of carrageenan, alginate and acacia gum over cell viability (Rojas-Tapias et al., 2015; Sorokulova et al. 2008), but is necessary to highlight that, *Azospirillum* is much more sensitive to temperature than those microorganisms, and *Bacillus* spores are more resistant to any kind of stress. According to Dell et al. (2007) and Huey and Kingsolver (2011), the use of the Arrhenius model is well accepted for biological processes, fitting in about 80 to 90% the behavior of thermal sensitivity among plants, microbes and animals. Although, some deviations of the model have been developed (Aquilanti et al., 2010), the results of this study show clearly that it can be useful in the selection of the components of bacterial inoculants.

The data obtained was fitted to the first-order kinetics equation to predict the necessary time to reduce cell concentration of the strain in three log units (Table 3). The time needed for this reduction at 4°C was more than a year in all treatments with the exception of alginate at 2% and the control treatment. Alginate at 1% was the only treatment predicted to prolong cell viability more than two days than the control treatment at 28°C. Interestingly, carrageenan at 1.5 and 3% are predicted to preserve cell viability at 4 and 45°C, but at 28°C the time of reduction is similar to the control. Even though the control treatment has a predicted life time lower than the others, the time needed for the reduction shows that cells can survive long periods only in the culture medium at room temperature.

The addition of polymers had a strong effect in the rate of cell death in all temperatures, and according to the

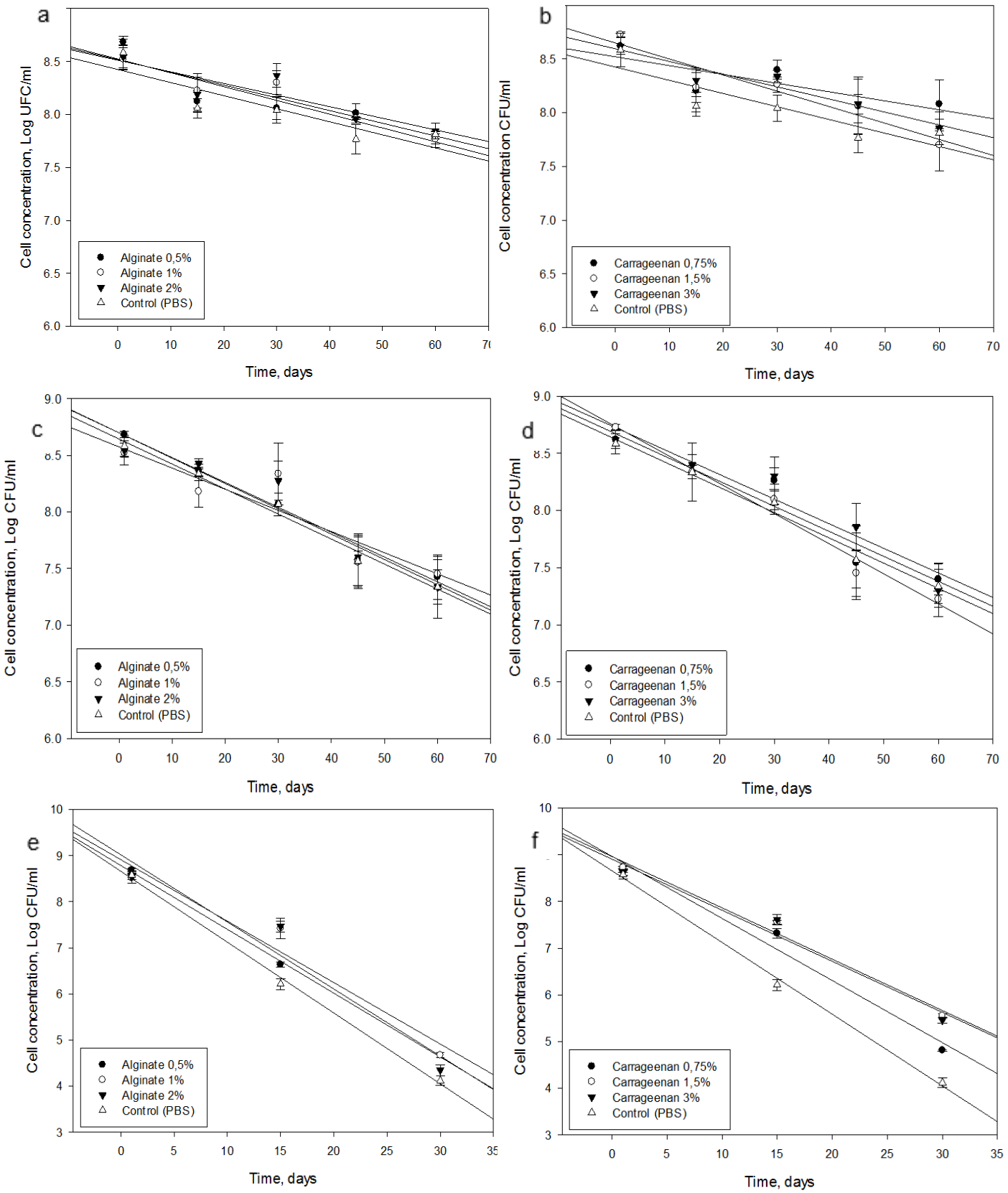

Figure 2. Apparent first order-kinetics of degradation for strain C16 *Azospirillum brasilense* with different alginate and carrageenan concentrations during storage. Experimental data of cell degradation rate at 4ºC (a, b); 28ºC (c, d) and 45ºC (e, f).

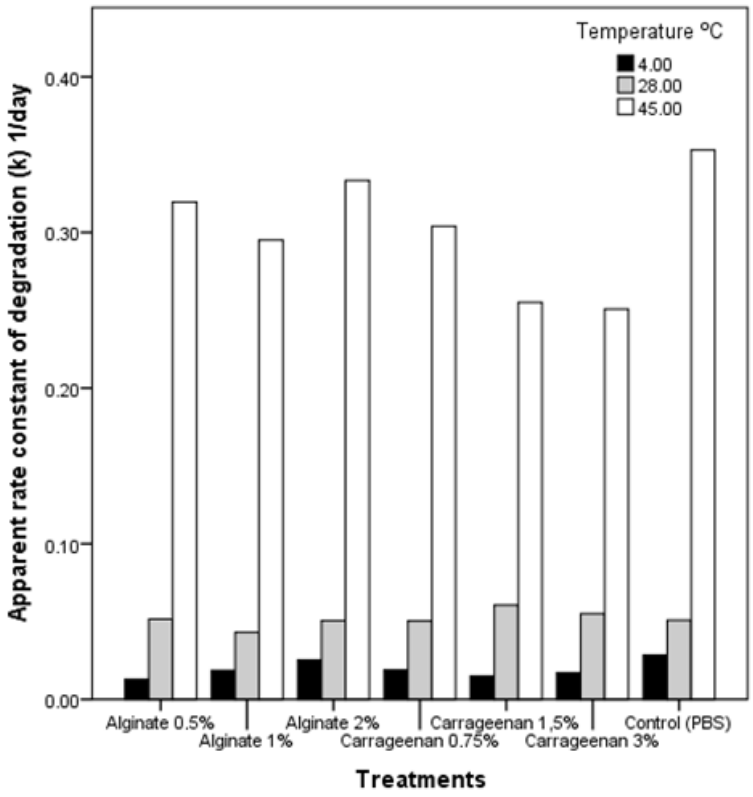

Figure 3. Apparent first-order constant of degradation of strain C16 with carrageenan and alginate at different temperatures and concentrations.

Table 2. Experimental values for energy of activation of strain C16 in all treatments. R^2 corresponds to the determination coefficient. Values of slope are the result of plotting Log (k) vs. 1/K. Ea meaning energy of activation.

Treatment (%)	R²	Slope	Ea (Kcal/mol)
Alginate 0.5	R² = 0.9538	2.90	13.233
Alginate 1	R² = 0.8763	2.46	11.197
Alginate 2	R² = 0.8507	2.28	10.423
Carrageenan 0.75	R² = 0.9104	2.49	11.384
Carrageenan 1.5	R² = 0.9794	2.59	11.873
Carrageenan 3	R² = 0.956	2.43	11.134
Control (PBS)	R² = 0.8213	2.21	10.122

Table 3. Predicted time to reduce cell concentration in three log units based on the Arrhenius equation.

Treatment (%)	4ºC	28ºC	45ºC
Alginate 0.5	568	143	23
Alginate 1	397	172	25
Alginate 2	292	146	22
Carrageenan 0.75	391	147	24
Carrageenan 1.5	492	122	29
Carrageenan 3	429	134	29
Control (PBS)	260	145	21

predicted time they can prolong shelf-life of liquid inoculants in more than 200 days at 4°C, 30 days at 28°C and 8 days at 45°C. These results are similar to those obtained by Kumaresan and Reetha (2011) and Manikandan et al. (2010), where they found that the polymers like glycerol, trehalose, and gum arabica doubled the shelf life of liquid inoculants of *A. brasilense,* and *Pseudomonas fluorescens.* Leo Daniel et al. (2013) also found that the addition of polymers as additives and adjuvants maintain cell concentration in liquid inoculants of *A. brasilsense, Bacillus megaterium* and *Azotobacter chroococcum,* reducing just two or three log units in 480 days at room temperature.

The Arrhenius prediction model allowed us to observe that, liquid inoculants can have a long shelf-life when refrigerated, but they can also survive enough time at room temperature (28°C), taking on average five months to reduce cell viability in three log units. Shelf-life prediction showed that, in general, at any concentration, carrageenan and alginate can prolong cell viability, but alginate at 1% and carrageenan at 0.75% preserved cell

viability and increased the shelf life of the formulations at the three temperatures evaluated. So, we conclude that they can be used in the formulation of a liquid inoculant based on the strain C16 *A. brasilense*.

Conflict of interests

The authors did not declare any conflict of interest.

ACKNOWLEDGEMENTS

We thank the Colombian Department for Science and Technology Colciencias, and its program "Jovenes investigadores e innovadores" and also, the Colombian Corporation of Agricultural Research Corpoica, for their funding and support.

REFERENCES

Albareda M, Rodríguez-Navarro D, Camacho M, Temprano FJ (2008). Alternatives to peat as a carrier for rhizobia inoculants: Solid and liquid formulations. Soil Biol. Biochem. 40(11):2771-2779.

Aquilanti V, Carlos K, Elango M, Kleijn S, Kasai T (2010). Temperature dependence of chemical and biophysical rate processes: Phenomenological approach to deviations from Arrhenius law. Chem. Phys. Lett. 498(1-3):209-213.

Bashan Y (1998). Inoculants of plant growth-promoting bacteria for use in agriculture. Biotechnol. Adv. 16(4):729-770.

Bashan Y, Gonzalez LE (1999). Long-term survival of the plant-growth-promoting bacteria *Azospirillum brasilense* and *Pseudomonas fluorescens* in dry alginate inoculant. Appl. Microbiol. Biotechnol. 51(2):262-266.

Bashan Y, Gonzalez LE (2010). How the Plant Growth-Promoting Bacterium Azospirillum Promotes Plant Growth — A Critical Assessment. Adv. Agron. 1(108):77-136.

Baudoin E, Nazaret S, Mougel C, Ranjard L, Moënne-Loccoz Y (2009). Impact of inoculation with the phytostimulatory PGPR *Azospirillum lipoferum* CRT1 on the genetic structure of the rhizobacterial community of field-grown maize. Soil Biol. Biochem. 41(2):409-413.

Cardenas DM, Garrido MF, Bonilla R, Baldani V (2010). Aislamiento e identificación de cepas de Azospirillum *sp*. en pasto guinea (*Panicum maximum* Jacq.) del Valle del Cesar. Pastos Y Forrajes 33:3.

Cassaan F, Vanderleyden J, Spaepen S (2014). Physiological and Agronomical Aspects of Phytohormone Production by Model Plant-Growth-Promoting Rhizobacteria (PGPR) Belonging to the Genus Azospirillum. J. Plant Growth Regul. 33(2):440-459.

Dell AI, Pawar S, Savage VM (2011). Systematic variation in the temperature dependence of physiological and ecological traits. PNAS 108(26):10591-10596.

Fibach-Paldi S, Burdman S, Okon Y (2012). Key physiological properties contributing to rhizosphere adaptation and plant growth promotion abilities of *Azospirillum brasilense*. FEMS Microbiol. Lett. 326(2):99-108.

Huey RB, Kingsolver JG (2011). Variation in universal temperature dependence of biological rates. PNAS 108(26): 10377-10378.

Krumnow AA, Sorokulova IB, Olsen E, Globa, L, Barbaree JM, Vodyanoy VJ (2009). Preservation of bacteria in natural polymers. J. Microbiol. Methods 78(2):189-194.

Kumaresan G, Reetha D (2011). Survival of *Azospirillum brasilense* in liquid formulations amended with different chemical additives. J. Phytol. *3*(10):48-45

Leo Daniel A, Venkateswarlu B, Desai S, Hassan M, Meenakshi T (2013). Physiology and pathology effect of polymeric additives, adjuvants, surfactants on survival, stability and Plant-Growth-Promoting ability of liquid bioinoculants. J. Plant Physiol. Pathol. 1(2):2-6.

Manikandan R, Saravanakumar D, Rajendran L, Raguchander T, Samiyappan R (2010). Standardization of liquid formulation of *Pseudomonas fluorescens* Pf1 for its efficacy against *Fusarium* wilt of tomato. J. Biol. Control 54(2):83-89.

Moreno-Galván A, Rojas-Tapias DF, Bonilla R (2012). Development and evaluation of an alternative culture medium for mass cultivation of *Azospirillum brasilense* C16 using sequential statistical designs. Revista Corpoica 13(2):201-206.

Mugilan I, Gayathri P, Elumalai EK, Elango R (2011). Studies on improve survivability and shelf life of carrier using liquid inoculation of *Pseudomonas striata*. JPBA 2(4):1271-1275.

Okon Y, Labandera-González C (1994). Agronomic applications of *Azospirillum*: an evaluation of 20 years of worldwide field inoculation. Soil Biol. Biochem. 6:1591-1601

Rivera D, Obando M, Barbosa H, Rojas Tapias D, Bonilla R (2014) Evaluation of polymers for the liquid rhizobial formulation and their influence in the Rhizobium-Cowpea interaction. Univ. Sci. 19(3): 265-275.

Rojas-Tapias D, Ortega O, Rivera D, Bonilla R (2015). Preservation of *Azotobacter chroococcum* vegetative cells in dry polymers. Univ. Sci. 20(2):201-207.

Rojas-Tapias D, Ortiz-Vera M, Rivera D, Kloepper J, Bonilla R (2013). Evaluation of three methods for preservation of *Azotobacter chroococcum* and *Azotobacter vinelandii*. Univ. Sci. 18(2): 129-139.

Rouissi T, Tyagi RD, Brar SK, Prevost D, John RP, Surampalli RY (2011). Efficient and simple method for determination of suspendibility of bio-inoculant suspensions. Bioresour. Technol. 102(22): 10754-10758.

Sivasakthivelan P, Saranraj P (2013). Azospirillum and its Formulations: A Review. Int. J. Microbiol. Res. 4(3): 275-287.

Sorokulova IB, Krumnow AA, Pathirana S (2008). Novel Methods for Storage Stability and Release of Bacillus Spores. Biotechnol. Prog. 24: 1147-1153.

Steenhoudt O, Vanderleyden J (2000) Azospirillum, a free-living nitrogen-fixing bacterium closely associated with grasses: Genetic, biochemical and ecological aspects. FEMS Microbiol. Rev. 24(4):487-506.

Tittabutr P, Payakapong W, Teaumroong N, Singleton PW, Boonkerd N (2007). Growth, survival and field performance of bradyrhizobial liquid inoculant formulations with polymeric additives. Sci. Asia 33(1):69-77

Velineni S, Brahmaprakash GP (2011). Survival and phosphate solubilizing ability of *Bacillus megaterium* in liquid inoculants under high temperature and desiccation stress. J. Agric. Sci. Technol. 13(5):795-802.

Vessey JK (2003) Plant growth promoting rhizobacteria as biofertilizers. Plant Soil 255:571-586.

academicJournals

Vol. 14(33), pp. 2554-2567, 19 August, 2015
DOI: 10.5897/AJB2015.14692
Article Number: EBC7E4F54969
ISSN 1684-5315

http://www.academicjournals.org/AJB

African Journal of Biotechnology

Full Length Research Paper

Biosynthesis of silver nanoparticles by plants crude extracts and their characterization using UV, XRD, TEM and EDX

Vishwajeet Singh[1*], Ankita Shrivastava[2] and Nitin Wahi[3]

[1]Department of Botany, Raja Balwant Singh, College, Dr B.R. Ambedkar University, Agra-282002, U.P., India.
[2]New Era Research Foundation, Agra-282007, India, U.P., India.
[3]Department of Biotechnology, GLA University, Mathura-281406, U.P., India.

Received 4 May, 2015; Accepted 13 July, 2015

Plant extracts are very cost effective and eco-friendly, thus, can be an economic and efficient alternative for the large-scale synthesis of nanoparticles. The preparation of stable, uniform silver nanoparticles by reduction of silver ions with *Emblica officinalis*, *Terminalia catappa* and *Eucalyptus hybrida* extract is reported in the present paper. It is a simple process of global research interest for obtaining silver nanoparticles in least amount of time. These nanoparticles were characterized with UV-Vis spectroscopy, X-ray diffraction (XRD), transmission electron microscopy (TEM) and energy diffraction X- ray (EDX analysis which revealed that the silver nanoparticles are polydisperse and of different morphologies ranging from 20 to 80 nm in size. XRD results reveal that these nanostructures exhibit a face-centered cubic crystal structure. The UV/Vis spectra absorption peak confirms their production. Pioneering of reliable and eco-friendly process for synthesis of metallic nanoparticles biologically is an important step in the field of application of nanobiotechnology. Thus, these silver nanoparticles (Ag-NPs) may prove as a better candidate for drugs and can potentially eliminate the problem of chemical agents because of their biogenic nature. The indiscriminate use of antibiotics has fuelled the development of drug resistance at an alarming rate. To overpower this burning problem, the Ag-NPs may prove to be a universal solution.

Key words: Nanobiotechnology, silver nanoparticles (Ag-NPs), *Emblica officinalis*, *Terminalia catappa* and *Eucalyptus hybrida.*

INTRODUCTION

Nanotechnology (NT) is the engineering of functional systems at the molecular scale. NT is the ability to work at the atomic, molecular and supramolecular levels (on a scale of 1 to 100 nm) in order to understand, create and use material structures, devices and systems with fundamentally new properties and functions resulting from their small structure. NT provides the tools and technology platforms for the investigation and trans-

*Corresponding author. E-mail: officervishu@gmail.com. Tel: 8410829626.

formation of biological systems, and biology offers inspiration models and bio-assembled components to NT (Mihail, 2003). Silver is used in the medical field as a topical bactericide (Yamanaka et al., 2005). With the progress of NT, production of the nanoparticle possesses more surface atoms than microparticles, which greatly improves the particles physical and chemical characteristics. There are some physical and chemical methods available for silver nanoparticle (Ag-NP) synthesis but these are so tedious; they consume lot of energy to maintain high pressure and temperature. Involvement of toxic chemicals in the synthesis process may be harmful to human beings (Chen et al., 2003). With the emergence and increase of microbial organisms resistant to multiple antibiotics, and the continuing emphasis on health-care costs, many researchers have tried to develop new, effective antimicrobial reagents free of resistance and cost. Recently, resistance to commercially available antimicrobial agents by pathogenic bacteria and fungi is increasing at an alarming rate and has become a global threat. Drug resistance is one of the most serious and widespread problems in all developing countries (Stevanovic et al., 2012). Such problems and needs have led to the resurgence in the use of Ag-based antiseptics that may be linked to broad-spectrum activity and far lower propensity to induce microbial resistance than antibiotics (Jones et al., 2004). The antibacterial effects of Ag salts have been noticed since antiquity (Silver and Phung, 1996), and Ag is currently used to control bacterial growth in a variety of applications, including dental work, catheters, and burn wounds (Catauro et al., 2004; Crabtree et al., 2003). In fact, it is well known that Ag ions and Ag-based compounds are highly toxic to microorganisms, showing strong biocidal effects on as many as 12 species of bacteria including *Escherichia coli* (Zhao and Stevens, 1998).

The development of cost efficient and ecologically benign methods of synthesis of nanomaterials still remains a scientific challenge as metal nanoparticles are of use in various catalytic applications, viz electronics, biology and biomedical applications, material science, physics, environmental remediation fields (Gonzalez and Noguezm, 2007; Gross et al., 2007; Kim et al., 2003; Parak et al., 2003; Schultz, 2003; Smith et al., 2006; Wei et al., 2005; Wang et al., 2007). It is well known that the toxicity of nanomaterials essentially depends on the structural features such as size, shape, composition and the surface chemistry. To prolong the life span of metal nanoparticles it is vital to select stabilizing agents and pathways that are environmentally friendly, non-toxic and easy to implement. Novel methods of ideally synthesizing NPs are thus being thought which are formed at ambient temperatures, neutral pH, low costs and environmentally friendly fashion. Keeping these goals in view nano-materials have been synthesized using various routes. Among the biological alternatives, plants and plant extracts seem to be the best option. In this paper, we report a green method for the synthesis of silver nanoparticles at room temperature by using plant extracts of *Emblica officinalis*, *Terminalia catappa* and *Eucalyptus hybrida*. These nanoparticles were characterized with UV-Vis spectroscopy, XRD, TEM and EDX analyses. Furthermore, we will use these Nanoparticles to evaluate *in-vitro* antimicrobial activity for the development of nanosilver-phytochemical composite formulation.

MATERIALS AND METHODS

Synthesis of silver nanoparticles using leaves extract of *E. officinalis, E. hybrida and T. catappa*

Fresh leaves of *E. officinalis, E. hybrida* and *T. catappa* were collected and were washed thoroughly with distilled water. About 50 g of leaves were cut into small pieces. Finely cut leaves were dipped into a beaker containing 200 ml distilled water. After that the mixture was boiled for 10 to 12 min. The extract was filtered using Whatmann filter paper and filtrate was collected. Synthesis of silver nanoparticles using extract of these leaves was mixed with aqueous solution of 1 mM Silver nitrate (99.99%) in 1:4 ratios in conical flask under aseptic conditions. The pH was adjusted to 8.0. The conical flasks were then agitated at 100 rpm in dark at 25°C on shaker for 1 to 2 h. A change in the color of the solution was observed. Control set (only extract) without $AgNO_3$ was also run side by side. Another negative control containing only 1 mM $AgNO_3$ were maintained under the same conditions. Silver nanobioconjugates were characterized by various methods.

Characterization of the synthesized silver nanoparticles

UV–visible spectroscopy

The detection of Ag-NPs was primarily carried out by visual observation by colour change of the cell filtrate after treatment with silver nitrate (1 mmol $^{-l}$). A further characterization of synthesized Ag-NPs was carried out with the help of UV–Visible spectrophotometer by scanning the absorbance spectra in 250 to 800 nm range of wavelength. It was observed that upon addition of the extract into the flask containing the aqueous silver nitrate solution, the colour of the medium changed to brown within 2 min. This indicated the formation of silver nanoparticles. The solution containing the signatory colour of AgNPs (dark brown) was then poured out into Petri-dishes and left in the oven for drying at 50°C for 24 h. The formation and quality of compounds were checked by XRD technique. The X-ray diffraction (XRD) pattern measurements of drop- coated film of AgNPs on glass substrate were recorded in a wide range of Bragg angles θ at a scanning rate of 2° min^{-1}, carried out on a XRD Diffractometer (PANalytical-XPERT PRO diffractometer system) that was operated at a voltage of 40 kV and a current of 30 mA with CuKα radiation (1.5405 Å). High Resolution Transmission Electron Microscopy (HRTEM) was per- formed by TECHNAIG20-STWIN (200 KV) machine with a line resolution 2.32 (in angstrom). These images were taken by drop coating AgNPs on a carbon-coated copper grid. Energy Dispersive Absorption Spectroscopy photograph of AgNPs were carried out by the HRTEM equipment.

Scanning electron microscopy

Scanning electron micrographs were taken. Samples were

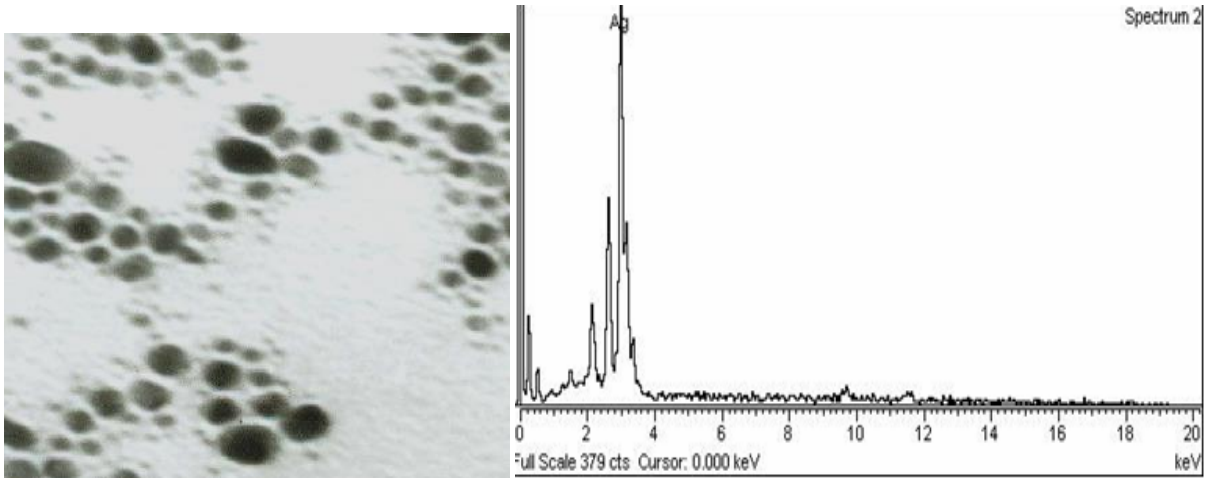

Figure 1. Synthesis of nanoplates by crude *Emblica*, (80 to 300 nanometers) of silver by reducing Ag ions EDX spectrum recorded from drop-coated films of silver nanoparticles.

prepared by fixing with 2Æ5% glutaraldehyde overnight at room temperature. The fixed sample was dehydrated with gradient alcohol (10 to 95%), incubated for 20 min in each gradient and dipped in absolute alcohol for 2 to 5 min. Finally, specimen was prepared by placing a drop of dehydrated sample on a glass slide, followed by coating with monolayer platinum for making the surface conducting.

XRD measurements

The purified powders of silver nanoparticles of varying interaction times were subjected to XRD measurements using an XRD Diffractometer (PANalytical-XPERT PRO diffractometer system). The target was Cu K α with a wavelength of 1.54060 A°. The generator was operated at 40 kV and with a 30 mA current. The scanning range was selected between 10 and 100°C. The crystallite size was also determined using the Debye Scherrer equation.

Transmission electron microscopy (TEM)

The samples for transmission electron microscopy (TEM) analysis were prepared by drop-casting the Silver Nano Bio Conjugates solution on a carbon-coated copper TEM grid. Before casting to the grid the Silver Nano Bio Conjugates solution was centrifuged at 10000 rpm for 5 min and the isolated silver Nano Bio Conjugates were dispersed in 100 µl double distilled water and sonicated in a bath sonicator for 15 min. The TEM images were recorded on a high resolution electron microscope (HRTEM: JEOL JEM 2010) operating at an accelerating voltage of 200 kV. Fast Fourier transform (FFT) images were recorded with built-in software for the FFT algorithm for image processing in HRTEM: JEOL JEM 2010 instrument at NPL, New Delhi.

Energy diffraction X- ray (EDX) measurements

The EDX analysis was carried out using JEOL JSM 7600F.

Fourier transform infrared spectroscopy

For FTIR spectrum analysis the silver nano bioconjugates were centrifuged at 15,000 rpm for 15 min to remove free proteins or other compounds present in the solution. The filtrate after complete reduction of Ag+ ions was subjected to repeated centrifugation at 15,000 rpm for 15 min, and supernatant was replaced by distilled water each time to concentrate Ag-NPs. The process was repeated for three times and finally the centrifuged part containing silver nano bioconjugates were redispersed in double distilled water and subjected to FTIR spectroscopy. The presence of unreacted silver ions leads to white precipitation on addition of sodium chloride. However, no precipitate was formed after addition of sodium chloride indicating the absence of unreacted silver in the nanoparticle solution. FTIR measurements were carried out to identify the possible biomolecules responsible for the reduction of the Ag+ ions and capping of the bioreduced silver nanoparticles synthesized by the leaf broth. The Fourier transform infrared spectroscopy (FTIR) spectrum of the sample was recorded on a Perkin-Elmer FTIR spectrum in the range 450 to 4000 cm^{-1} at resolution of 4 cm^{-1}.

RESULTS AND DISCUSSION

Synthesis of silver nanoparticles using leaves extract of *E. officinalis, E. hybrida* and *T. catappa*

Synthesis of silver nanobioconjugates was done using leaves extract of *E. officinalis, E. hybrida* and *T. catappa.* By *Emblica* crude *emblica*, synthesis of nanoplates (80 to 300 nm) of silver by reducing Ag ions EDX spectrum was recorded from drop-coated films of silver nanoparticles (Figure 1). UV-vis spectra was recorded from the aqueous silver nitrate and *E. hybrida* leaf extract. It was observed that the silver surface plasmon resonance band occurs at 440 nm and steadily increases in intensity as a function of time of reaction without any shift in the peak wavelength (Figure 2). The frequency and width of the surface plasmon absorption depends on the size and shape of the metal nanoparticles as well as on the dielectric constant of the metal itself and the surrounding medium. SEM images of reduction of Ag+ to silver

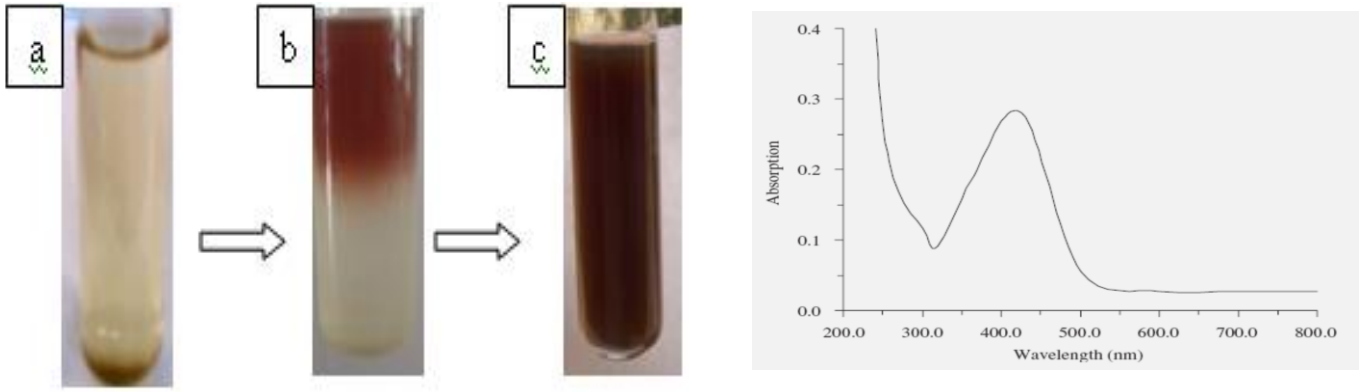

Figure 2. Pictures showing the color changes before (a), during (b) and after the process of reduction of Ag+ to Ag nanoparticles (c).

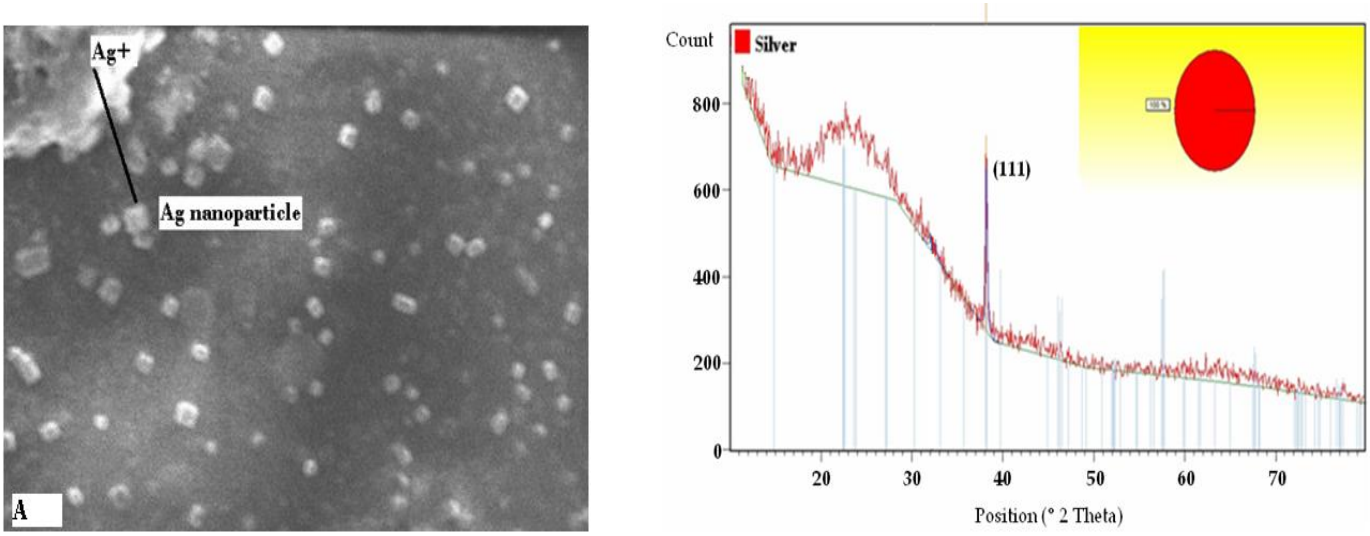

Figure 3. SEM images of reduction of Ag+ to Silver nanoparticles.

nanoparticles in solution by exposing 5 ml of *E. hybrida* leaves extract to 45 ml of 1 mM aqueous $AgNO_3$ at 26°C were done (Figure 4). XRD patterns were recorded from drop-coated films on glass substrate of silver nanoparticles synthesized by treating *E. hybrida* leaf extract with $AgNO_3$ aqueous solutions. The Bragg reflections are indexed on the basis of the fcc silver structure. XRD patterns obtained for silver nanoparticles synthesized using *E. hybrida* leaf extract in Figure 3, it shows characteristic peaks (at $2\theta = 30.8°$), marked with (111). A number of Bragg reflections corresponding to the (111) sets of lattice planes are observed which may be indexed based on the face-centred cubic structure of silver. The XRD pattern thus clearly shows that the silver nanoparticles are crystalline in nature. The XRD pattern of pure silver ions is known to display peaks at $2\theta = 7.9$, 11.4, 17.8, 30, 38, and 44°. The value of the pure silver lattice constant has been estimated to be a = 4.081, a value that is consistent with a = 4.0862 A° reported by the JCPDS file n^{o}4-0783. This estimation confirmed the hypothesis of particle monocrystallinity. *Terminalia* leaf extract in Figure 5 shows the UV-Vis spectra, EDAX and HR-TEM micrograph of synthesized Ag nanoparticles (20 to 80 Nanometers; spherical and triangle shaped).

Characterisation of silver nanobioconjugates

UV-vis spectroscopy

It is well known that silver nanoparticles exhibit yellowish-brown color in water. These colors arise due to excitation of surface plasmon vibrations in the metal nanoparticles which occur in the range 380 to 440 nm in an aqueous

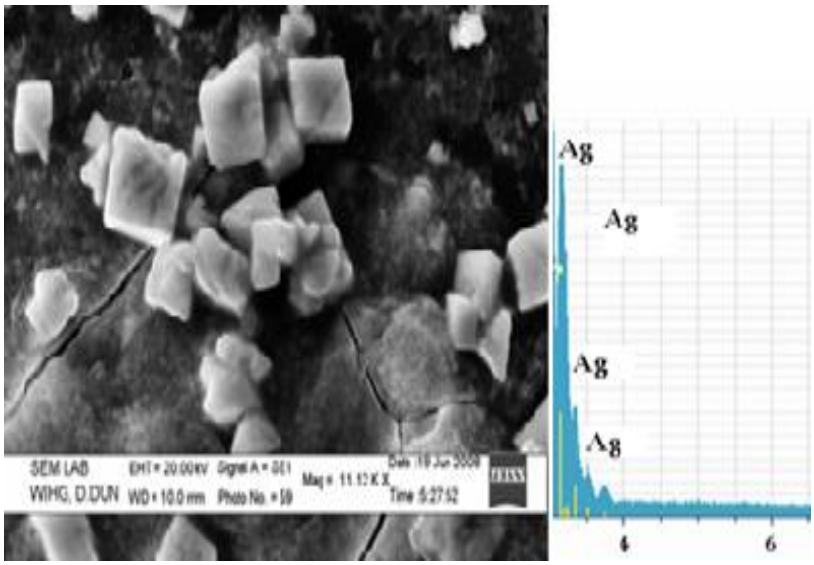

Figure 4. SEM image of the silver nanoparticles synthesized by treating *Eucalyptus hybrida* leaf extract with $AgNO_3$ aqueous solutions. Silver nanoparticles formed were predominantly cubical with uniform size, EDX spectrum recorded from a film, after formation of silver nanoparticles. Different X-ray emission peaks are labelled.

medium. From the inset of Figure 6, it shows that the silver nitrate treated with *E. officinalis*, *E. hybrida* and *T. catappa* biomass turned dark reddish-brown after 1 to 3 h due to the formation of silver nanoparticles extracellularly. This shows that it was a quite fast process. This color is due to the SPR signal generated in the region 340 to 450 nm of silver nano bio conjugates by UV-visible spectroscopy. An increase in absorbance in the region 340 to 450 nm with time indicated the synthesis of Silver Nano Bio Conjugates. However, no change in color was observed in control sets.

The intensity of the surface plasmon band is seen to saturate after 2 h of reaction

XRD measurements

Figure 7 shows the XRD pattern obtained for Silver Nano Bio Conjugates synthesized using the *E. hybrida*, *T. catappa* and *E. officinalis* extract represented by the curve. A number of Bragg reflections are observed for the silver nanoparticles synthesized with each of the *T. catappa* and *E. officinalis* extract, which may be indexed based on the fcc structure of silver and is shown in Table 1. The XRD pattern thus clearly shows that the silver nanoparticles formed by the reduction of Ag+ ions by the *T. catappa*, *E. hybrida*, and *Emblica officinalis* extract are crystalline in nature. From the calculated d spacing values corresponding to each 2θ values, it appears that the (101), (111), (200), and (220) lattice spacing are broadened as compared to the bulk form and this phenomenon is more pronounced in case of the (111) planes. In addition to the Bragg peaks representative of fcc silver nanocrystals (JCPDS—International Center for Diffraction Data, PCPDFWIN v. 1.30, 31-1238) corresponding to the lattice planes (101), (111), (200) and (220), respectively. The XRD pattern of pure silver ions is known to display peaks at 2θ = 7.9, 11.4, 17.8, 30, 32, 38, and 44°. This estimation confirmed the hypothesis of particle monocrystallinity. The sharpening of the peaks clearly indicates that the particles are in the nanoregime. The XRD pattern thus clearly shows that the silver nanoparticles are crystalline in nature.

Transmission electron microscopy (TEM)

Figure 8 shows TEM images recorded from drop-coated films of the Silver Nano Bio Conjugates synthesized with *T. catappa* leaf extract. At low magnification (Figure 8), a very large density of silver nanoparticles can be seen and the silver nanoparticles are quite polydisperse and ranged in size from 10 to 40 nm with an average size ca. 20 nm. At higher magnification, the morphology of the silver nanoparticles is more clearly seen (Figures 8B and C). The particles are predominantly spherical with a small percentage being elongated. The assembly of the silver particles in the manner observed might be driven by the presence of the bioorganic molecules. While the TEM pictures do not provide direct evidence of the presence of a bioorganic material on the silver nanoparticles, it is

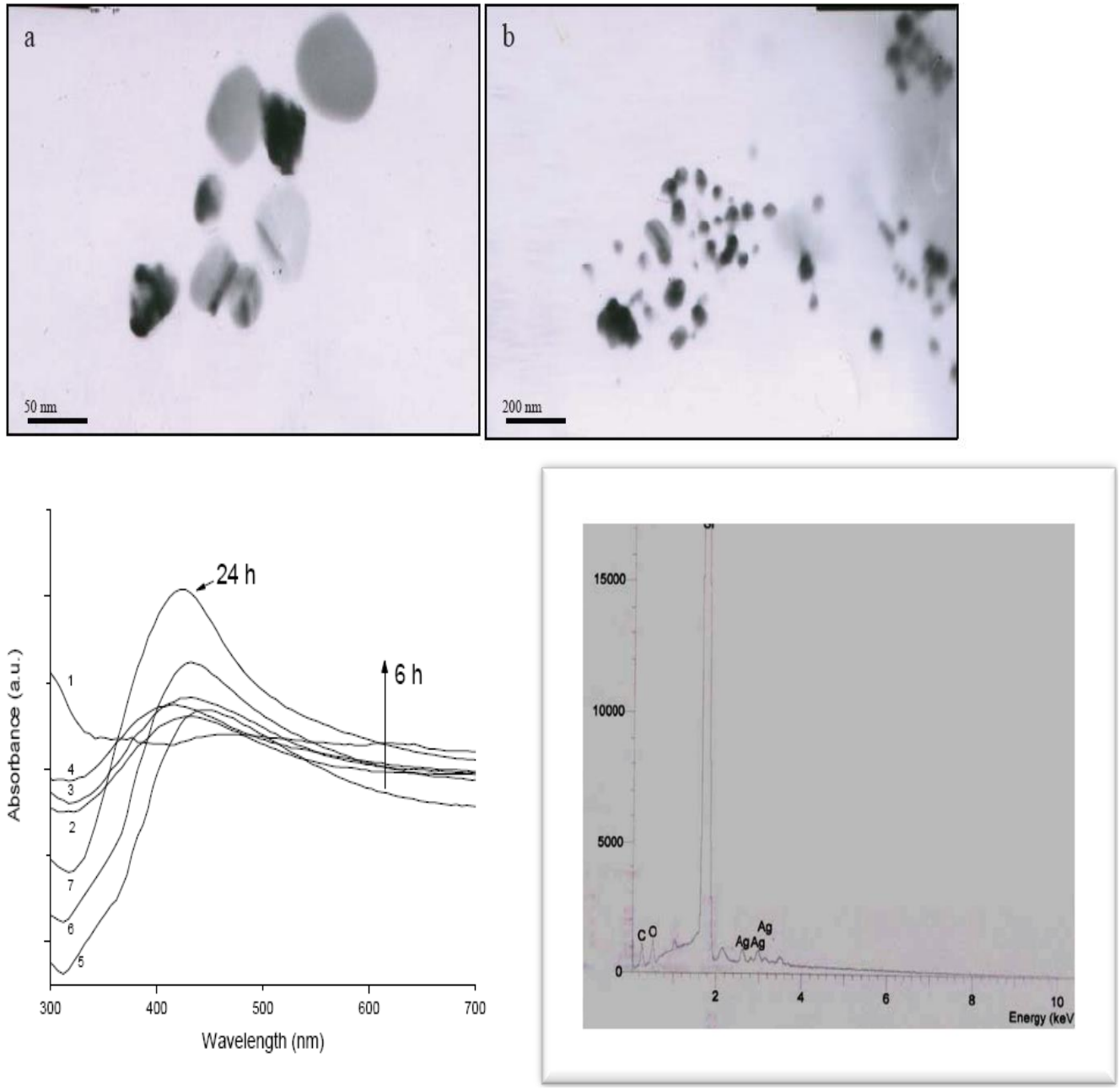

Figure 5. UV-Vis spectra, EDAX and HR-TEM micrograph of synthesized Ag nanoparticles (20-80 Nanometers; spherical and triangle shaped) by *Terminalia* leaf extract.

interesting to note that most of the particles in the TEM pictures are not in physical contact but are separated by a fairly uniform inter-particle distance. From the higher magnification TEM images (Figure 8D) it can be seen that each silver nanoparticle is surrounded by a material with a lower contrast as indicated by an arrow for one of the particles. We believe that this coating material with an average thickness of 5 nm is a bioorganic component of the *T. catappa* extract acting as a stabilizing agent for the nanoparticles. Figure 9 shows TEM images recorded for the Silver Nano Bio Conjugates synthesized by treating $AgNO_3$ solution with *E. officinalis* extract. The silver nanoparticles are observed to range in size from 10 to 30 nm with an average size of ca. 15 nm (Figure 9A).

The morphology of the Ag nanoparticles is predominantly spherical. Few of the particles indicated by the arrows in Figure 9B, appear to have core shell like structure. As stated before, morphology of some of the particles appear to be disc like, while an exact estimate of the thickness of these apparent flat, disc-like particles

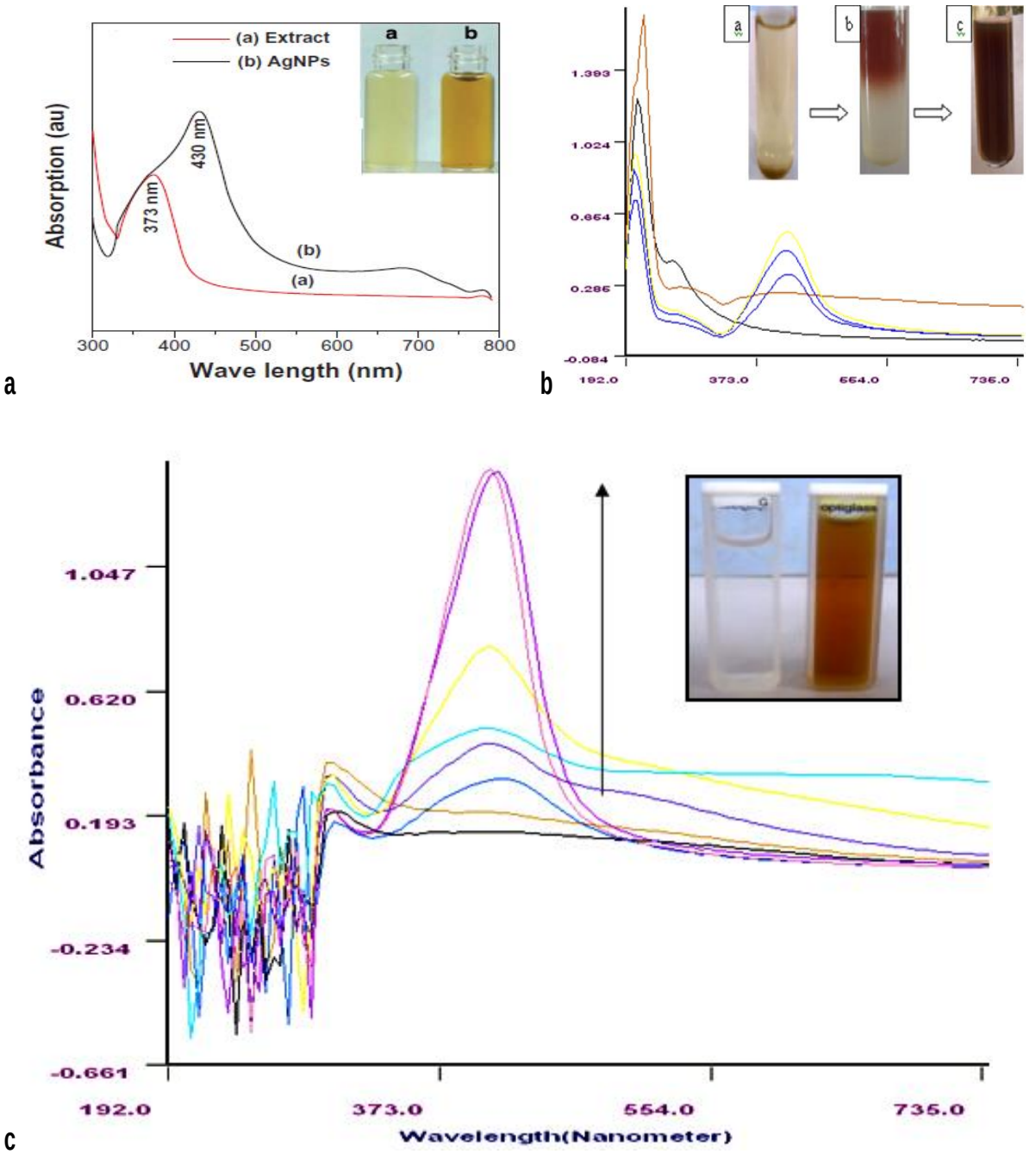

Figure 6. Shows the UV-vis spectra recorded as a function of time of reaction of Ag+ ions with *Emblica officinalis, Eucalyptus hybrida* and *Terminalia catappa* extract. The band corresponding to the surface Plasmon vibrations of Ag nanoparticles is observed at 430 nm. The intensity of the surface plasmon band is seen to saturate after 2 h of reaction. **(a)** UV-vis *spectra of Emblica officinalis* extract, **(b)** UV-vis *spectra of Eucalyptus hybrid* extract, **(c)** UV-vis *spectra of Terminalia catappa* extract.

could not be made; the fact that the thickness of these structures is less than that of the spherical particles is inferred from the increased contrast in places where such nanoparticles overlap. A typical TEM image of silver nano bio conjugates (Figure 10a and b) revealed the presence of maximum number of spherical shapes. The average diameter of 252 particles measured in TEM was 11.10 ± 6.40 nm. A high resolution TEM (HRTEM) image of Silver Nano Bio Conjugates synthesized by eucalyptus (Figure 10c) showed the well resolved interference fringe patterns separated by 0.24 nm which corresponded well to the spacing between (111) plane of fcc silver crystal

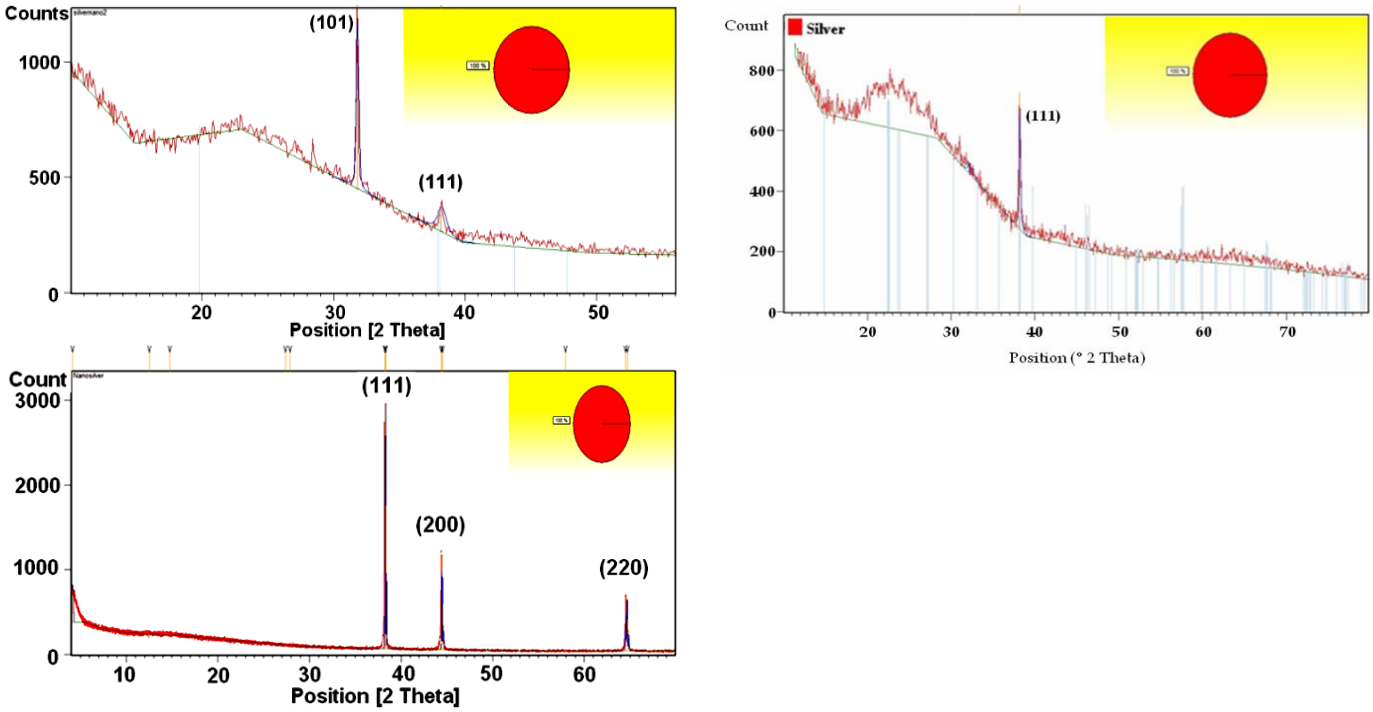

Figure 7. XRD patterns recorded from drop-coated films on glass substrate of silver nanoparticles synthesized by treating *Emblica officinalis, Eucalyptus hybrida* and *Terminalia catappa* leaf extract with $AgNO_3$ aqueous solutions.

Table 1. Lattice spacing values calculated from the 2θ values obtained from the XRD pattern of silver nanoparticles synthesized using *Terminalia catappa* leaf, Eucalyptus hybrid and *Emblica officinalis*.

Pos. [°2Th.]	Lattice Planes (hkl)	Standard Ag (A^o)	*Terminalia catappa* -Ag (A^o)	*Emblica officinalis* Ag (A^o)	*Eucalyptus A*g (A^o)
32	(101)	2.815	-	2.81446	-
38	(111)	2.359	2.35291	2.35567	2.2111
45	(200)	2.044	2.03897	-	-
65	(220)	1.445	1.44446	-	-

(JCPDS. No.01-087-0597). The patterns of SAED (Figure 10d) were indexed according to (111), (200), (220) and (311) reflections of fcc silver crystal on the basis of their d-spacing of 2.47, 2.13, 1.49 and 1.27 A°.

Energy diffraction X- ray (EDX) measurements

The EDX analysis was carried out using JEOL JSM 7600F. Figure 11 shows the energy dispersive analysis by X- rays (EDAX) spectrum of the plain *T. catappa* and *E. officinalis* extract and it is observed that the both extract consists of a number of inorganic ions apart from the presence of carbon and oxygen originating from the bioorganic component of the extract. *T. catappa* leaf extract and *E. officinalis* extract also contains potassium, calcium and magnesium in appreciable amounts. Presence of magnesium possibly indicates that the extract also consists of considerable amount of chlorophyll in it. Figure 12 shows the energy dispersive analysis by X- rays (EDAX) spectrum of the silver nano bioconjugates from *T. catappa* leaf and *E. officinalis* extract confirming the presence of elemental silver signal of silver nanoparticles. The vertical axis displays the number of x-ray counts whilst the horizontal axis displays energy in KeV. Identification lines for the major emission energies for silver (Ag) are displayed and these correspond with peaks in the spectrum, thus giving confidence that silver has been correctly identified.

Fourier transform infrared (FTIR) spectroscopy

Components from *T. catappa* leaf showed that alkaloids,

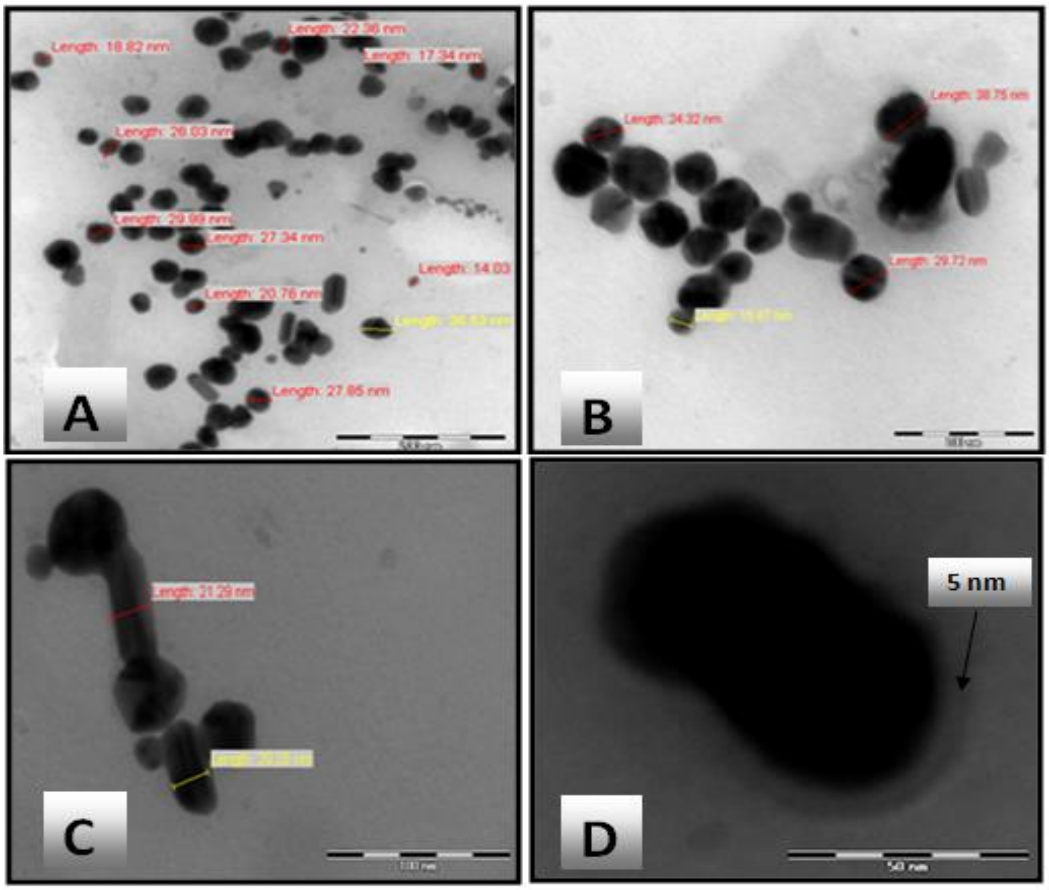

Figure 8. TEM images of silver nano bio conjugates synthesized by *Terminalia catappa* extract.

tannin, flavonoid, and glycosides exist in leaf. FTIR absorption spectra of the dried biomass of *T. catappa* leaf before and after bioreduction, are shown in Figure 13 (i); other information regarding the chemical change of the functional groups were involved in bioreduction. Some absorbance bands centred at 1109, 1244, 1317, 1384, 1446, 1517, 1631 and 1726 cm^{-1} were observed in the region 1000 to 1800 cm^{-1}. Among them, the absorbance bands at 1109, 1631 and 1726 cm^{-1} were associated with the stretch vibration of –C–O, –C=C, RHC=O, respectively. To a large extent, the band at 1109 cm^{-1} might be contributed by the –C–O groups of the polyols such as flavones and polysaccharides in the biomass. It could be figured out by comparison of (a), and (b) that the disappearance of the band at 1109 cm^{-1} after bioreduction shows that the polyols are mainly responsible for the reduction of silver ions. For silver nanoparticles, the absorption at about 1384 cm^{-1} (a) was notably enhanced in that NO^{-3} existed in the residual solution. To a large extent, the bonds or functional groups, such as –C–O–C–, –C–O–, –C=C– and –C=O, derive from the heterocyclic compounds that are water-soluble components in biomass. Therefore, it is thought that the water soluble heterocyclic compounds, for example, alkaloids and flavones, are the capping ligands of the nanoparticles.

FTIR absorption spectra of *E. officinalis* extract before and after reduction of silver are shown in Figure 13 (ii). Extract shows hydroxyl group in alcoholic and phenolic compound which is supported by the presence of a strong peak at approximately 3300 cm^{-1}. This sharp peak representing O–H bond is not seen in *E. officinalis* extract after bioreduction. This indicates that the polyols are mainly responsible for reduction of Ag+ into silver nanoparticles. This may lead to the disappearance of the O–H bond. We could observe free hydroxyl groups in the FTIR of silver nanoparticles at 3600 cm^{-1}. The absorbance bands at 2931, 1625, 1404 and 1143 cm^{-1} are associated with the stretch vibrations of alkyl C–C, conjugated C–C with a benzene ring, bending of C–O–H and C–O stretch in saturated tertiary or secondary highly symmetric alcohol in *E. officinalis* extract, respectively. The presence of peaks at 3749 and 1523 cm^{-1} indicate that the silver nanoparticles may be surrounded by amines, because the peaks indicate $–NH_2$ symmetric stretching and N–O bonds in nitro compounds. The intense broad band at 3384 cm^{-1} is due to the O−H stretching mode and at 2921 cm^{-1} due to the aldehydic

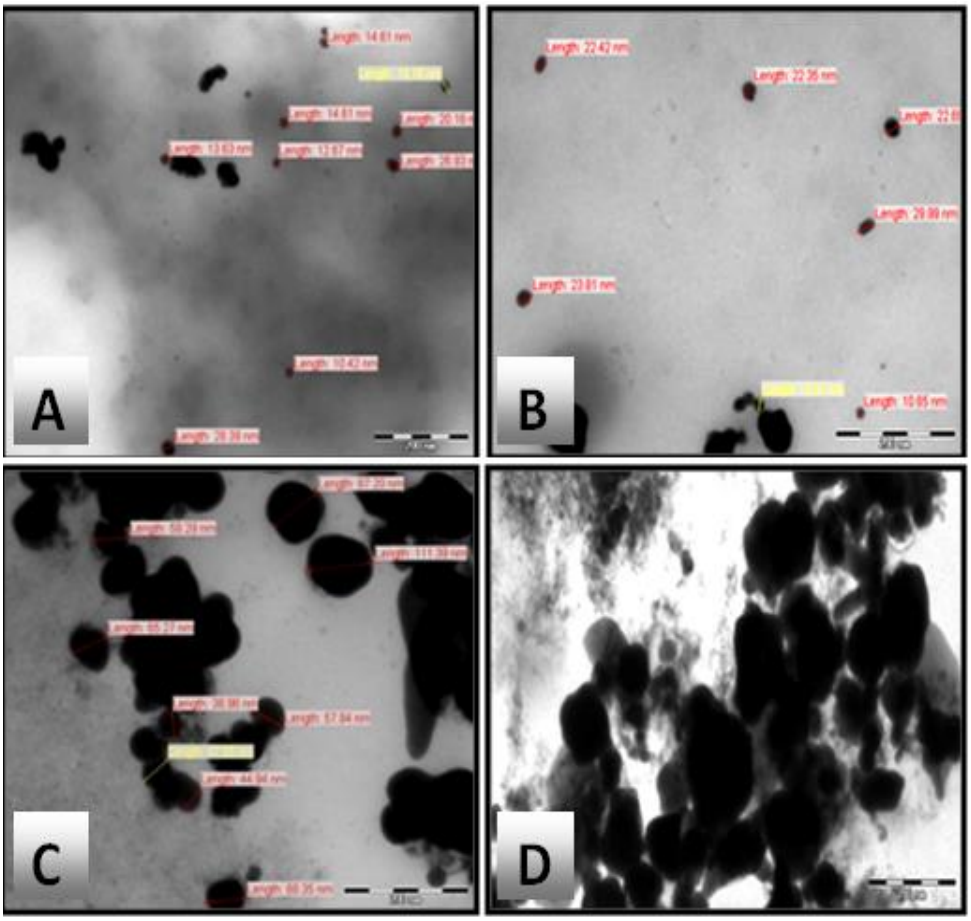

Figure 9. TEM images of Silver Nano Bio Conjugates synthesized by *Emblica officinalis* extract.

C−H stretching mode. The peak at 1078 cm^{-1}, which is absent for the AgNP FTIR spectrums, is the bending vibration of the C−O stretch and could be due to the stabilization of AgNP through this group. The peak of C=C group (at 1406 cm^{-1}) absent for AgNP is possible, due to the reduction of $AgNO_3$ to Ag. It is corresponding to the results of the UV-vis spectroscopy that the extract played a role as the reducing and stabilizing agent in the preparation of AgNP. This indicated the presence of extracts as a capping agent for AgNP, which increases the stability of the nanoparticles synthesized.

In the present scenario, Ag-NPs as antibacterial agents have come up as a promising candidate in the medical field (Duran et al., 2007). The extremely small size of nanoparticles exhibits enhanced or different properties when compared with the bulk material. There are different physical and chemical methods (Chen et al., 2003) for the synthesis of nanoparticles, but there is always need for the development of eco-friendly route for the synthesis process (Ingle et al., 2008). Hence, our current study proves to be an important step in this direction. In the current work of synthesis of Ag- NPs using plant leaf extracts, the colour of the filtrate changed from pale yellow to dark brown after addition of silver nitrate (1 $mmol^{-1}$). Our results show resemblance to that reported by Gade et al. (2008), who reported the formation of brown colour of the cell filtrate of *Aspergillus niger* after treatment with silver nitrate (1 $mmol^{-1}$).

The UV-Vis spectrophotometer analysis showed the absorbance at around 440 nm in the form of sharp peak, which was specific for the synthesis of Ag-NPs; these findings corroborate with the findings of Wang et al. (2007) who reported the same results, in which they observed that when *Capsicum annum* L. extract was challenged with aqueous silver ions, the reaction mixture containing Ag-NPs showed the absorption peak at about 440 nm because of the excitation of longitudinal Plasmon resonance vibration.

In similar study, silver nanoparticles were synthesized using flower broth of *Tagetes erecta* as reductant by a simple and eco-friendly route. The aqueous silver ions when exposed to flower broth were reduced and resulted in green synthesis of silver nanoparticles. The silver nanoparticles were characterized by UV-visible spectroscopy, zeta potential, Fourier transform infra-red spectroscopy (FTIR), X-ray diffraction, transmission

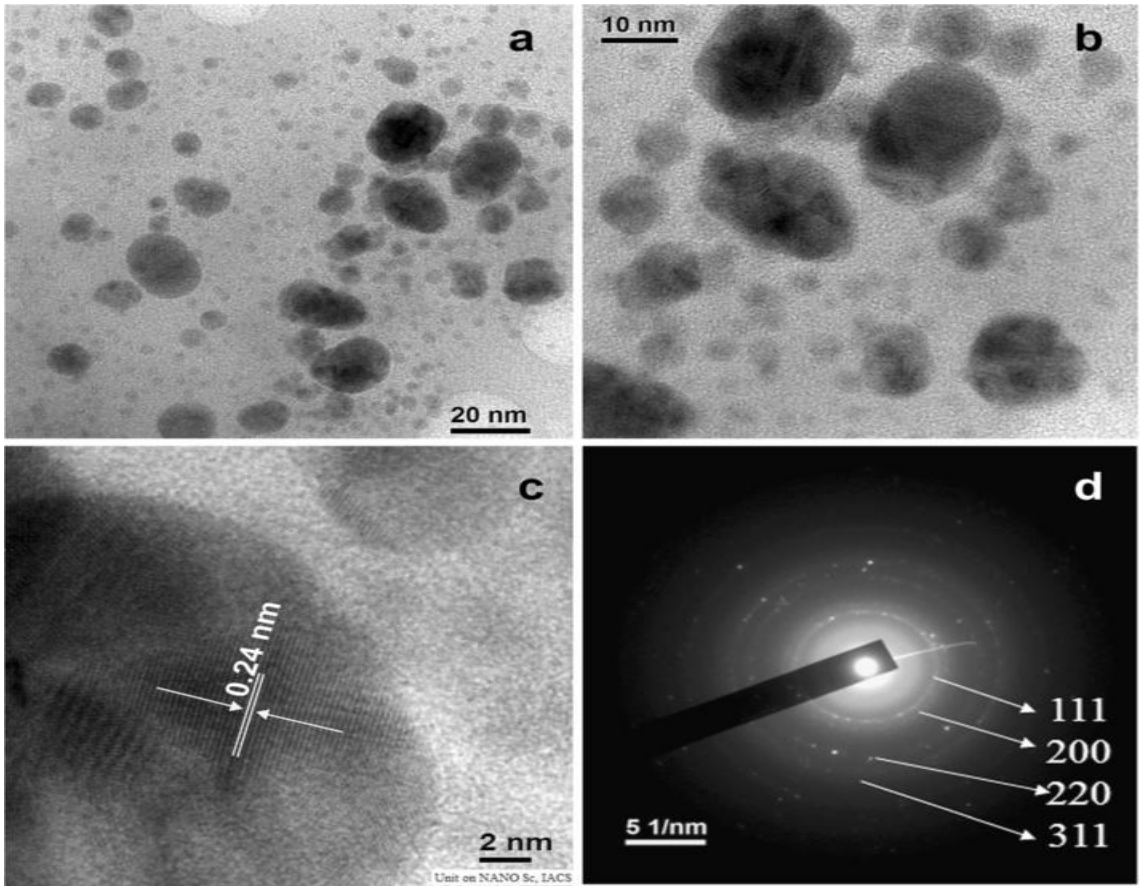

Figure 10. TEM images of silver nano bio conjugates synthesized by *Eucalyptus hybrid* extract.

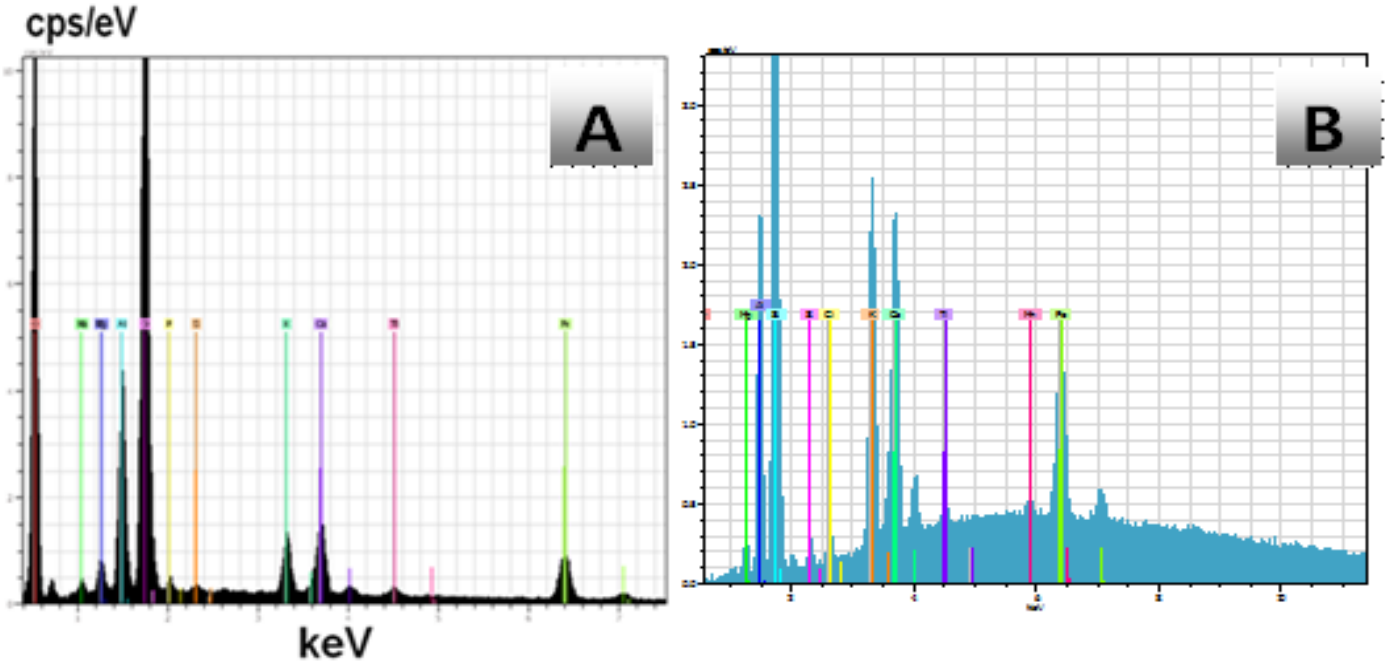

Figure 11. EDX of crude extract of (A) *Terminalia catappa* and (B) *Emblica officinalis* in absence of any external additive.

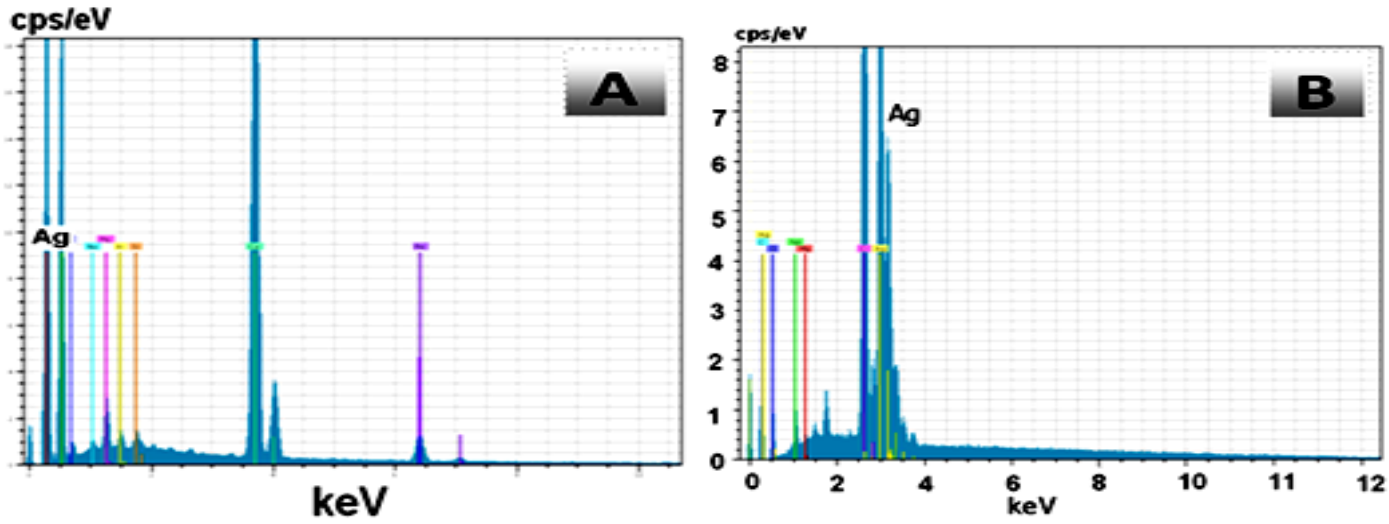

Figure 12. EDX spectrum recorded from a film, after formation of silver nano bioconjugates from (A) *Terminalia catappa* and (B) *Emblica officinalis* extract. Different X-ray emission peaks are labeled.

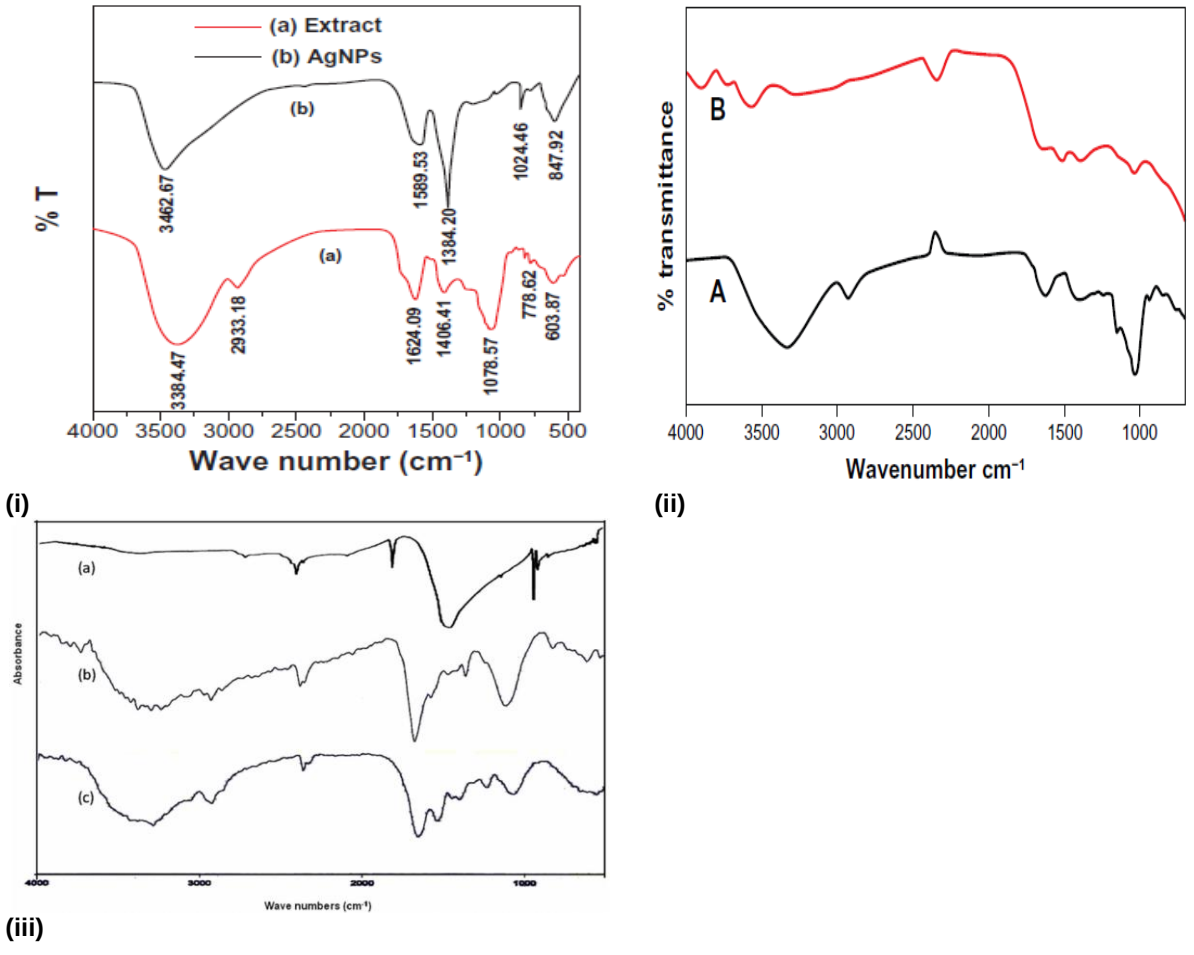

Figure 13. Typical FTIR absorption spectra of the (i) *Terminalia catappa* leaf biomass before bioreduction (a), after bioreduction of silver ions (b). (ii*) Emblica officinalis* biomass before bioreduction (a), after bioreduction of silver ions (b). (iii) Fourier transform infrared absorption spectra of Eucalyptus hybrida extract (A) $AgNO_3$, (b) before bioreduction and (c) after complete bioreduction of Ag+ ions at 50°C.

electron microscopy (TEM) analysis, Energy dispersive X-ray analysis (EDX) and selected area electron diffraction (SAED) pattern. UV–visible spectrum of synthesized silver nanoparticles showed maximum peak at 430 nm. TEM analysis revealed that the particles were spherical, hexagonal and irregular in shape and size ranging from 10 to 90 nm and Energy dispersive X-ray (EDX) spectrum confirmed the presence of silver metal. Synergistic antimicrobial potential of silver nanoparticles was evaluated with various commercial antibiotics against Gram positive (*Staphylococcus aureus* and *Bacillus cereus*), Gram negative (*E. coli* and *Pseudomonas aeruginosa*) bacteria and fungi (*Candida glabrata, Candida albicans, Cryptococcae neoformans).* The antifungal activity of AgNPs with antibiotics was better than antibiotics alone against the tested fungal strains and Gram negative bacteria, thus signification of the present study is in production of biomedical products (Hemali et al., 2014).

AgNPs from *Annona squamosa* leaf extract were spherical in shape with an average size ranging from 20 to 100 nm (Vivek et al., 2012) while Thirunavokkarasu et al. (2013) reported spherical nanoparticles with size ranging from 8 to 90 nm in *Desmodium gangeticum*. The sharp signal peak of silver strongly indicated the reduction of silver ion by *T. erecta* into elemental silver. Metallic silver nanoparticles generally show typical optical absorption peak approximately at 2.6 keV due to surface plasmon resonance. There were spectral signals for C and Cu because of the TEM grid used. From EDX spectrum, it was clear that *T. erecta* had percent yield of 71.31% of AgNPs and synthesized nanoparticles were composed of high purity AgNPs. TEM images showed that the surfaces of the AgNPs were surrounded by a black thin layer of some material which might be due to the capping organic constituents of flower broth as also reported by Rafiuddin (2013).

Thakur et al. (2013) and Niraimathi et al. (2013) also reported antibacterial activity of AgNPs. The AgNPs plus antibiotics could successfully inhibit the fungal strains under investigation while acetone extract plus antibiotics could not. Antifungal activity of AgNPs with commercial antibiotics is also reported by Kim et al. (2009) and Gajbhiye et al. (2009). However, they have reported against only fungi and only with two antibiotics, that is, fluconazole and amphotericin B, respectively. The mechanism of inhibitory effects of silver ions on microorganisms is somewhat known. Some studies have reported that positive charge on the silver ion is significant for its antimicrobial activity through the electrostatic attraction between negative charge on cell membrane of microorganism and positive charged nanoparticles (Hamouda and Baker, 2000; Dibrov et al., 2002; Chanda, 2014).

In the FTIR analysis, the amide linkages between amino acid residues in proteins give rise to the well-known signatures in the infrared region of the electro-magnetic spectrum. Representative spectra of obtained nanoparticles manifest absorption peaks in the region 1000 to 2000 cm^{-1}. Among them, the absorption peak at around 1025 cm^{-1} can be assigned as absorption peaks of –C–O–C– or –C–O– (Huang et al., 2007). The peak at 1630 cm^{-1} is associated with stretch vibration of –C=C– (Huang et al., 2007) and is assigned to the amide I bonds of proteins (Sastry et al., 2003) in the present FTIR spectrum. The SEM micrograph study showed the presence of spherical nanoparticles in the range of 60 to 80 nm, and aggregates of silver nanoparticles were also observed in the micrograph; these findings corroborate the observations of Sadowski et al. (2008) that the nanoparticles get partially aggregated because of the drying process. However, future studies on antibacterial activity of the influence of these nanoparticles on other Gram-positive and Gram negative bacteria are necessary in order to evaluate it as a better bactericidal material.

Conclusion

In the present study, plant extracts were studied for the synthesis of Ag-NPs. We have reported a simple biological process for synthesizing Ag-NPs. The FTIR analysis confirms capping over Ag-NPs. These capped Ag-NPs will help to enhance the stability of Ag-NPs in a colloidal solution by preventing aggregation of particles. Because they are capped by biomolecules and they may serve as a better candidate for the drug delivery systems. However, synthesis of nanoparticles using plant extracts can potentially eliminate the problem of chemical agents, which may have adverse effects in its application, thus making nanoparticles more biocompatible.

Conflict of interests

The authors did not declare any conflict of interest.

Abbreviations: XRD, X-Ray diffraction; **Ag-NPs,** silver nanoparticles; NT, nanotechnology; **TEM,** transmission electron microscopy; **EDX,** energy diffraction X- ray; **FFT,** fast Fourier transform; **FTIR,** Fourier transform infrared spectroscopy; **SAED,** selected area electron diffraction.

REFERENCES

Catauro M, Raucci MG, De Gaetano FD, Marotta A (2004). Antibacterial and bioactive silver-containing Na2O CaO 2SiO2 glass prepared by sol-gel method. J. Mater. Sci. Mater. Med. 15(7):831-837.

Chanda S (2014). Silver nanoparticles (medicinal plants mediated): a new generation of antimicrobials to combat microbial pathogens – a review. In: Mendez-Vilas, A. (Ed.), Microbial Pathogens and Strategies for Combating Them: Science Technology and Education. FORMATEX Research Center, Badajoz, Spain. pp. 1314-1323.

Chen JC, Lin ZH, Ma XX (2003). Evidence of the production of silver nanoparticles via pretreatment of *Phoma* sp. 3Æ2883 with silver nitrate.

Lett . Appl. Microbiol. 37:105-108.
Crabtree JH, Burchette RJ, Siddiqi RA, Huen IT, Handott LL, Fishman A (2003). The efficacy of silver-ion implanted catheters in reducing peritoneal dialysis-related infections. Perit. Dial. Int. 23(4):368-374.
Dibrov P, Dzioba J, Gosink KK, Hase CC (2002). Chemiosmotic mechanism of antimicrobial activity of Ag (+) in *Vibrio cholera*. Antimicrob. Agents Chemother. 46: 2668-2670.
Duran N, Alves OL, De Souza GIH, Esposito E, Marcato PD (2007). Antibacterial effect of silver nanoparticles by fungal process on textile fabrics and their effluent treatment. J. Biomed. Nanotechnol. 3:203-208.
Gade AK, Bonde PP, Ingle AP, Marcato PD, Duran N, Rai MK (2008). Exploitation of *Aspergillus niger* for fabrication of silver nanoparticles. J. Biobased Mater. Bioenergy 2:243-247.
Gajbhiye M, Kesharwani J, Ingle A, Gade A, Rai M(2009). Fungus-mediated synthesis of silver nanoparticles and their activity against pathogenic fungi in combination with fluconazole. Nanomed. NBM 5:382-386.
Gonzalez AL, Noguezm C (2007). Influence of Morphology on the Optical Properties of Metal Nanoparticles. J. Comput. Theor. Nano-sci. 4 (2): 231-238.
Gross M, Winnacker MA, Wellmann PJ (2007). Electrical, Optical and Morphological Properties of Nanoparticle Indium-Tin-Oxide Layers. Thin Solid Films 515 (24): 8567-8572.
Hamouda T, Baker JR (2000). Antimicrobial mechanism of action of surfactant lipid preparations in enteric Gram-negative bacilli. J. Appl. Microbiol. 89:397-403.
Hemali P, Pooja M, Sumitra C (2014). Green synthesis of silver nanoparticles from marigold flower and its synergistic antimicrobial potential. Arabian J. Chem. (In Press).
Huang J, Chen C, He N, Hong J, Lu Y, Qingbiao L, Shao W, Sun D et al. (2007). Biosynthesis of silver and gold nanoparticles by novel sundried Cinnamomum camphora leaf. Nanotechnology 18:105-106.
Ingle A, Gade A, Pierrat S, Sonnichsen C, Rai M (2008). Mycosynthesis of silver nanoparticles using the fungus *Fusarium acuminatum* and its activity against some human pathogenic bacteria. Curr. Nanosci. 4:141–144.
Jones SA, Bowler PG, Walker M, Parsons D (2004). Controlling wound bioburden with a novel silver-containing Hydrofiber dressing. Wound Repair Regen. 12 (3):288-294.
Kim JY, Kim M, Kim HM, Joo J, Choi JH (2003). Electrical and Optical Studies of Organic Light Emitting Devices Using SWCNTs-Polymer Nanocomposites. Opt. Mater. 21 (1-3):147-151.
Kim KJ, Sung WS, Suh BK, Moon SK, Choi JS, Kim JG, Lee DG (2009). Antifungal activity and mode of action of silver nano-particles on Candida albicans. Biometals 9(22):235-242.
Mihail CR (2003). Nanotechnology: convergence with modern biology and medicine. Curr. Opin. Biotechnol. 14:337-346.
Niraimathi KL, Sudha V, Lavanya R, Brindha P (2013). Biosynthesis of silver nanoparticles using Alternanthera sessilis (Linn.) extract and their antimicrobial, antioxidant activities. Colloids Surf. B Biointerfaces 102:288-291.
Parak WJ, Gerion D, Pellegrino T, Zanchet D, Micheel C, Williams SC, Boudreau R, Le Gros MA, Larabell CA, Alivisatos AP (2003). Biological Applications of Colloidal Nanocrystals. Nanotechnology 14(7):15-27.
Rafiuddin ZZ (2013). Bio-conjugated silver nanoparticles from Ocimum sanctum and role of cetyltrimethyl ammonium bromide. Colloids Surf. B Biointerfaces 108:90-94.
Sadowski Z, Maliszewska IH, Grochowalska B, Polowczyk I, Kozlecki T (2008). Synthesis of silver nanoparticles using microorganisms. Mater. Sci. Pol. 26:419-425.
Sastry M, Ahmad A, Khan MI, Kumar R (2003). Biosynthesis of metal nanoparticles using fungi and actinomycetes. Curr. Sci. 85: 162–170.
Schultz DA (2003). Plasmon Resonant Particles for Biological Detection. Curr. Opin. Biotechnol. 14(1):13-22.
Silver S, Phung LT (1996). Bacterial heavy metal resistance: new surprises. Annu. Rev. Microbiol. 50:753- 89.
Smith AM, Duan H, Rhyner MN, Ruan G, Nie S (2006). A Systematic Examination of Surface Coatings on the Optical and Chemical Properties of Semiconductor Quantum Dots. Phys. Chem. Chem. Phys. 8(33):3895-3903.
Stevanovic MM, Skapin SD, Bracko I, Milenkovic M, Petkovic J, Filipic M (2012). Poly (lactide-co-glycolide)/silver nanoparticles: synthesis, characterization, antimicrobial activity, cytotoxicity assessment and ROS-inducing potential. Polymer 53:2818-2828.
Thakur M, Pandey S, Mewada A, Shah R, Oza G, Sharon M (2013). Understanding the stability of silver nanoparticles biofabricated using Acacia arabica (Babool gum) and its hostile effect on microorganisms. Spectrochim. Acta Part A Mol. Biomol. Spectrosc. 109: 344–347.
Thirunavokkarasu M, Balaji U, Behera S, Panda PK, Mishra BK (2013). Biosynthesis of silver nanoparticles from extract of Desmodium gangeticum (L.) DC. and its biomedical potential. Spectrochim. Acta Part A Mol. Biomol. Spectrosc. 116:424-427.
Vivek R, Thangam R, Muthuchelian K, Gunasekaran P, Kaveri K, Kannan S (2012). Green biosynthesis of silver nanoparticles from Annona squamosa leaf extract and its in vitro cytotoxic effect on MCF-7 cells. Process Biochem. 47:2405-2410.
Wang HY, Li YF, Hua CZ (2007). Detection of ferulic acid based on the plasmon resonance light scattering of silver nanoparticles. Special Issue on China Japan-Korea Environmental Analysis, Talanta 72(5):1698-1703.
Wei GH, Zhou Z, Liu Z. (2005). A Simple Method for the Preparation of Ultrahigh Sensitivity Surface Enhanced Raman Scattering (SERS) Active Substrate. Appl. Surf. Sci. 240(1-4): 260-267.
Yamanaka M, Hara K, Kudo J (2005). Bactericidal actions of a silver ion solution on Escherichia coli, studied by energy-filtering transmission electron microscopy and proteomic analysis. Appl. Environ. Microbiol. 71:7589-7593.
Zhao G, Stevens Jr SE (1998). Multiple parameters for the comprehensive evaluation of the susceptibility of *Escherichia coli* to the silver ion. Biometals 11:27-32.

academicJournals

Vol. 14(33), pp. 2568-2575, 19 August, 2015
DOI: 10.5897/AJB2014.14198
Article Number: DA5F8B754971
ISSN 1684-5315

http://www.academicjournals.org/AJB

African Journal of Biotechnology

Full Length Research Paper

Biochemical profile of cuttings used for *in vitro* organogenesis of *Prunus africana*: An endangered species in Cameroon

Justine Germo Nzweundji[1,2*], Nicolas Niemenak[2], Oumar[3], Julie Judith Tsafack[1], Koffi Konan[4], Leopold Nyochembeng[5], Noumi Christelle[2], Nehemie Donfagsiteli Tchinda[1,2] and Denis Omokolo Ndoumou[2]

[1]Medicinal Plants and Traditional Medicine Research Centre, Institute of Medical Research and Medicinal Plants Studies (IMPM). P. O. Box 6163 Yaounde, Cameroon.
[2]Department of Biological Science, Higher Teacher Training College, University of Yaounde I. P.O. Box 47 Yaounde, Cameroon.
[3]Jay P. J. Biotechnology Laboratory, Institute of Agricultural Research for Development, P.O. Box 25, Buea, Ekona, Cameroon.
[4]IngateyGen LLC, 410 Interpath Parkway Unit J, Elisabeth City North Carolina 27909, USA.
[5]Department of Natural Resources and Environmental Sciences Alabama A&M University, P.O. Box 1208, Normal, 35762, Hunstville Alabama, USA.

Received 21 September, 2014; Accepted 3 August, 2015

Prunus africana **(Kanda stick) is a valuable medicinal tree classified as priority species for domestication in Cameroon. To measure the ability for developing axillary buds and multiple shoots in relation with the origin and state of explants, some biochemical parameters were assessed in eight types of single-node cuttings. These cuttings were treated with different concentrations of kinetin (kin) indole butyric acid (IBA) and thidiazuron (TDZ) and cultured in Murashige and Skoog (MS) medium. The glutelin content (1.13 ± 0.201 µg/mg FW) was higher compared to those of total albumin, globulin and prolamin and most representative at mature vegetative apical stage (MVA). The highest (15.60 ± 1.966 µg/mg FW) and lower (2.82 ± 0.072 µg/mg FW) amount of phenol compound was observed in the mature dormant stages and immature vegetative distal stage (IVD), respectively. Regarding the peroxidases, highest activity (0.453 ± 0.055 OD/mg/ FW.5 min^{-1}) was obtained in mature dormant apical stage. Apart from IVA state, there was no reactive explant cultured *in vitro*. The high percentage of budding and proliferation of budding (100%) and rooting (100%) were achieved with 12 µM Kin and 24 µM IBA, respectively. In the presence of 24 µM TDZ, multiple shoot was induced with a maximum of 5 shoots/explants. Micropropagation success of *P. africana* is influenced by cytokinin, physiological and biochemical status of single node cutting.**

Key words: Biochemical profile, *Prunus africana*, budding, multiple shoots, rooting.

INTRODUCTION

Prunus africana (Hook.f.) Kalman commonly known as *Pygeum*, is a large tree which grows in the afromontane forests between 1500 and 3000 m asl (Betti and Ambara, 2013). It is mainly used for the healing properties of its bark extracts, against benign prostatic hyperplasia (Kadu et al., 2012). Global demand of *P. africana*'s bark is estimated at more than 4000 t per year for a value of finished goods estimated at U.S. $220 million (Cunningham et al.,

2002) and one of the main sources of supply to satisfy this demand consists of Cameroon natural populations (Nsawir and Ingram, 2007).

Unfortunately, much of this exploitation has been irresponsible with entire trees being girdled of their bark and left to die or, in other cases, felled to facilitate easier access to their bark (Betti, 2008). This massive exploitation leads to classify it as an endangered species in Cameroon (Cunningham, 2005). A decrease has therefore been noted in its population over the time in terms of tree density, area of occupation, and habitat quality due to the actual level of exploitation (Amougou et al., 2010). Thus, without the renewal of this culture, extinction may occur during the next decade. The key challenge is therefore to develop different methods of propagation that are both appropriate to the species and easily applicable to local communities.

Propagation by seeds is the main form of regeneration of *P. africana*. This propagation is the easiest and cheapest way usually used to regenerate trees. However, this method of propagation faces two major constraints that hinder access to seeds of *P. africana*: the low aptitude to germinate and the rapid loss of their vigor and viability during storage. To date, the best germination percentage obtained after 06 months of storage at 4°C is 37% (Avana, 2006). Vegetative propagation via cuttings using auxins in rooting media has been also done (Tchoundjeu et al., 2002).

Biotechnologies across *in vitro* micro propagation might be an alternative to produce seeds and planting stock material for plantation. Meanwhile, the success of micro propagation is dependent on the nature, origin, physiological and biochemical state of plant material (Yildiz and Er, 2002). Generally, young cuttings during dormant phase are more reactive than old cuttings in vegetative phase (Auge, 1989). These events are accompanied with some biochemical variations such as the protein and phenol level. Storage proteins are a source of reduced nitrogen, carbon, and amino acids for growing tissues.

Peroxidases are implicated in cell differentiation by cross linking low weight phenolic compounds in the cell wall (Almagro et al., 2009), thus allowing or restricting a cell growth. These phenol components are products of phenol-propanoid pathway. Phenols plays a major role in root process but their effect is under control of the biochemical endogenous level in cuttings. They are the main substrate of peroxidases and their preferential oxidation by peroxidase prevents peroxidase-catalysed oxidation of auxin.

The present investigation was carried out to determine physiological and biochemical status of single-node cutting in relation with their ability to budding and develop axillary buds. In addition, the effect of cytokinin on budding and development of multiple shoots and their rooting with auxin was assessed.

MATERIALS AND METHODS

Study site and harvesting of plant material

This study was conducted from January 2013 to July 2014 both at the Institute of Medical Research and Medicinal Plants Studies in Yaounde, Cameroon (IMPM), in the Centre region with latitude 3° 51' N and longitude 11° 25' E., approximately 813 m asl., average rainfall 1692 mm (Segalen, 1967) and at Alabama A&M University in Alabama State, USA (latitude 34.7846° N and longitude 86.5700° W). The plant materials were cuttings (approximately 2 cm length) of *P. africana* at eight growth stages: mature cutting at dormant stage (Apical and Distal part: MDA, MDD); mature cutting at vegetative stage (Apical and Distal part: MVA, MVD); immature cutting at dormant stage (Apical and Distal part: IDA, IDD); immature cutting at vegetative stage (Apical and Distal part: IVA, IVD). Mature cuttings were harvested on 10 years old trees at Odza, Yaounde while immature cuttings were harvested from seedlings of one month old obtained in the Alabama A&M University nursery.

Enzyme preparation and reserve protein assay

Proteins were extracted according to the modified Voigt et al. (1993) method. To avoid an irreversible denaturation of storage proteins by oxidation products of polyphenols during extraction, the acetone dry powder (AcDP) was extracted each time at 4°C successively with 10 mM Tris-HCl (pH 7.5, 2 mM EDTA), 0.5 M NaCl (containing 2 mM EDTA and 10 mM Tris-HCl pH 7.5), 70% (v/v) ethanol and 0.1 N NaOH, to obtain the albumin, globulin, prolamin and glutelin fractions, respectively, and centrifuging at 6000 rpm for 30 min. All these solvents contained 5 mM sodium ascorbate. Protein concentrations were determined according to Bradford (1976) using bovine serum albumin as the standard and the absorbance was measured at 595 nm.

Enzyme preparation and peroxidase assay

Proteins were extracted according to the modified Voigt et al. (1993) method. Cuttings were ground in mortar with 10 ml of Tris Hcl buffer 50 mM, pH 7 added 0.25 M mannitol and 1 mM $MgCl_2$. The homogenate was centrifuged at 4°C for 30 min at 6000 *g* and the supernatant was taken off. The pellet was re-suspended in Tris Hcl buffer and recentrifuged under the same conditions as before, and the new supernatant was added to the first. Peroxidase activity was determined according to Thorpe and Gaspar (1978) by monitoring the formation of guaïacol at 420 nm. Five 5 ml of

*Corresponding author. E-mail: nzweundji@gmail.com.

Abbreviations: MS, Murashige and Skoog; **Kin,** kinetin; **IBA,** indole butyric acid; **MVA,** mature vegetative apical; **IVD,** immature vegetative distal; TDZ , Thidiazuron.

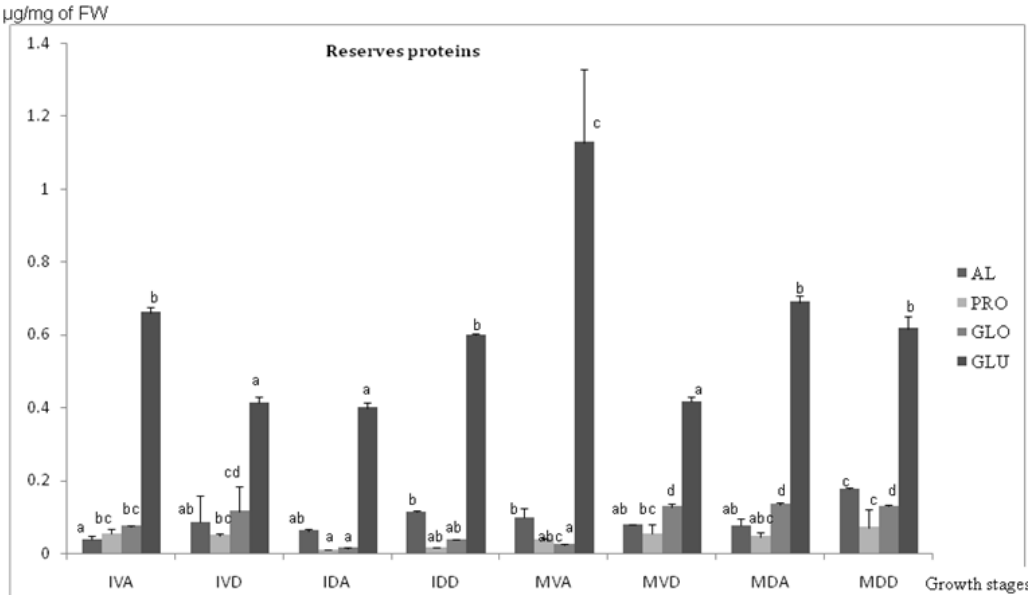

Figure 1. Variations of reserve proteins (albumin, prolamin, globulin, glutelin) in different cutting growth stages of *P. africana.* Values having the same letter(s) in the same column are not significantly different according to Duncan. Test at P< 0.05. Values were means ± standard deviation.

reaction mixture (1 V of 0.2% H_2O_2; 2 V of 1% guaïacol; 5 V of 1/15 M phosphate buffer pH 6) was added to 10 µl of extract.

Phenol extraction and assay

Phenols were extracted by homogenizing 1 g of grounded cuttings in 5 ml methanol (80%). The homogenate was then centrifuged for 20 min at 6000 *g* and the supernatant was collected. The pellet was re-suspended in 3 ml methanol (80%) and re-centrifuged under the same conditions as before and the new supernatant was added to the first. The quantity of phenol was determined as described by Bray and Thorpe (1954) using Folin-Ciocalteu reagent. The reaction mixture was incubated at 40°C for 20 min and absorbance read at 725 nm. Total phenol content was expressed as µg/mg of fresh weight.

Preparation of cuttings and development of axillary bud

The cuttings (1 to 1.5 cm long) were washed under running tap water for 15 min, and then surface sterilized with 15% (v/v) bleach for 20 min and gently agitated once or twice. Hereafter, they were washed three times in sterilized deionised water. The explants were cultured in MS medium (Murashige and Skoog, 1962) supplemented with 100 mg l/L glutamine, 30 g/L sucrose, 3 g /L of gellan gum and different concentrations of kinetin (kin) at 4, 12 and 24 µM. The pH was adjusted to 5.7 with 0.1 N NaOH (1 N) or HCl (0.1 N) followed by autoclaving for 20 min at 115°C. All preparations were kept in a culture room at 25°C under a 16 h photoperiod with 40 mol m^{-2} s^{-1}. After appearance of 3 leaves, the cuttings were subcultured in the same media as described above and supplemented with different growth regulators IBA (4, 12 and 24 µM) for root development.

Preparation of material and multiple shoot production

Seeds were surface sterilized by immersion in 5% (v/v) sodium hypochlorite for 15 min, followed by 3 times rinsing in sterile deionised water, and germinated on Wet Filter Papers in Petri dishes containing 5 ml of deionized water for seedling development. After 10 days, single node cuttings were cultured in MS supplemented with 100 mg l/L glutamine, 30 g/L sucrose, 3 g /L of gellan gum with kinetin and Thidiazuron (TDZ) at 4, 12 and 24 µM respectively. The cultures were subcultured every 10 days in the same media and kept in the same environment as described above. The number of shoots per explants was evaluated.

Statistical analyses

Experiments were replicated three times. The data were subjected to tests of analysis of variance. After rejecting null hypothesis of equal means using ANOVA Duncan-test, was used for comparing treatment group means at P = 0.05. Statistical software used was SPSS 17.0 for Windows. Values were means ± standard deviation.

RESULTS

Biochemical changes of cutting at growing stages

The biochemical studies were conducted on cuttings at different stages during growth process; mature cuttings at Dormant stage (MDA, MDD); Mature cuttings at Vegetative stage (MVA, MVD); Immature cuttings at Dormant stage (IDA, IDD); Immature cuttings at Vegetative stage (IVA, IVD). Results reveal that all the reserve proteins were represented in each developmental stage but with a differential expression. The maximum amount of glutelin (1.13 ± 0.201 µg/mg FW) and albumin (0.178 ± 0.004 µg/mg FW) were observed at mature vegetative apical stage and mature dormant distal phase, respectively (Figure 1). Regarding globulin content,

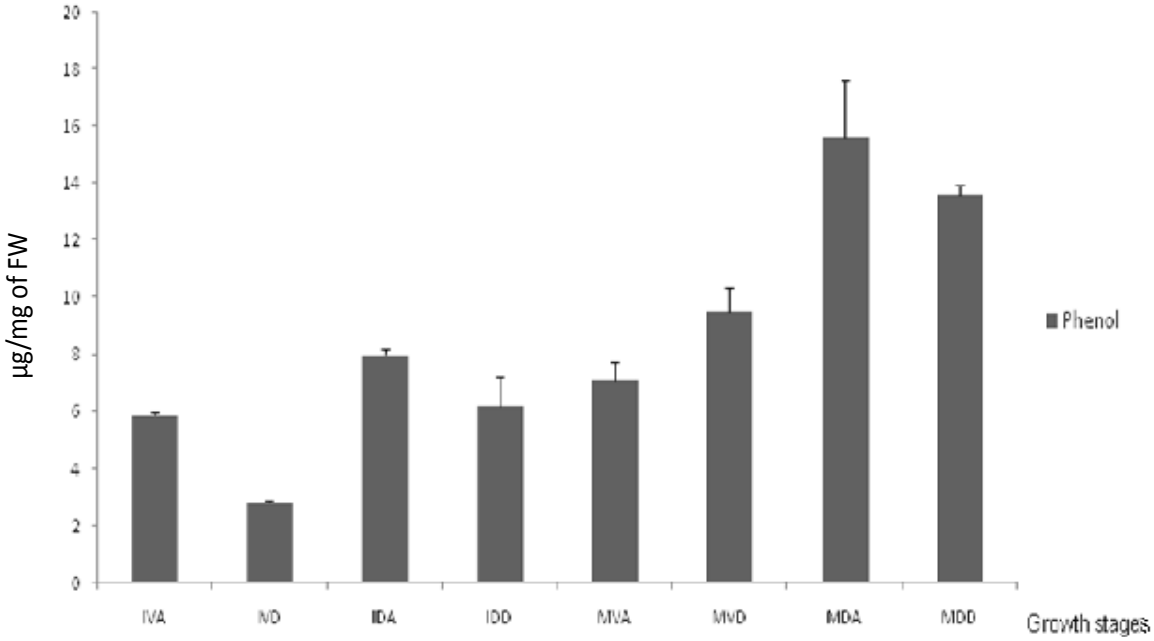

Figure 2. Variation of total phenol in different cutting growth stages of *P. Africana.* Values having the same letter(s) in the same column are not significantly different according to Duncan. Test at P< 0.05. Values were means ± standard deviation.

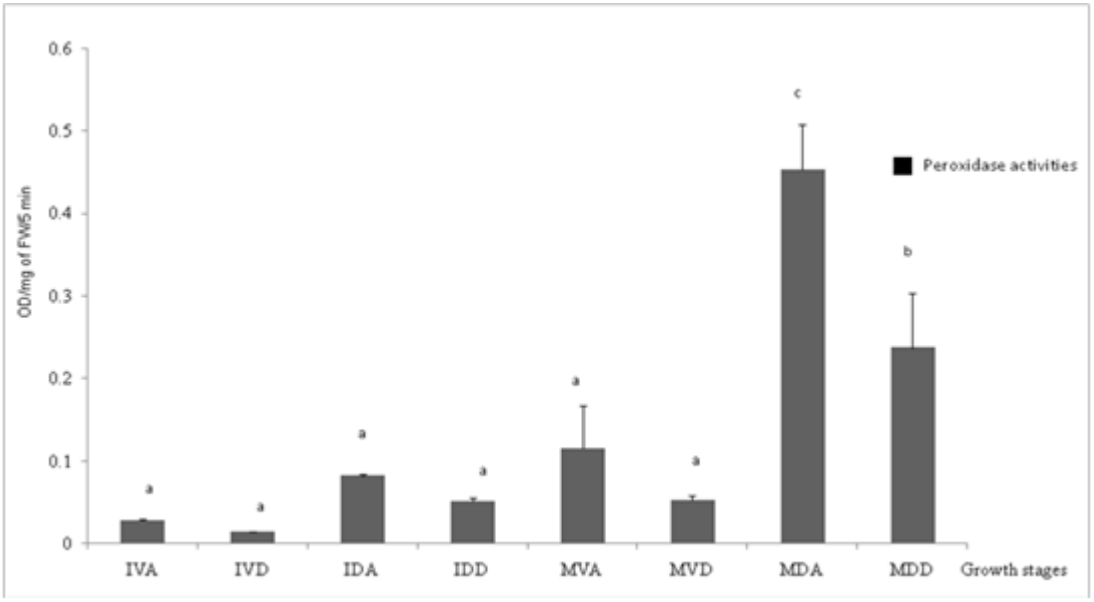

Figure 3. Variation of peroxidase activities in different cutting growth stages of *P. Africana.* Values having the same letter(s) in the same column are not significantly different according to Duncan Test at P< 0.05. Values were means ± standard deviation.

difference was noticed only at the Mature and Immature stages. In addition, for any growing stage, there was not significative difference of prolamin content. The initial level of phenol (5.88 ± 0.06 µg/mg FW) at IVA increase with time during growing stages to reach a maximal value (15.6 ± 1.96) at MDA (Figure 2). Peroxidase activity of the single-node cutting exhibited a low initial value (0.01 ± 0.001 DO/g PF/5 min) in IVD, and generally increased gradually, reaching a maximum level (0.45 ± 0.05 DO/g PF/5 min) in MDA (Figure 3).

Figure 4. Different stages of microcutting in *P. africana.* **a)** Budding and proliferation of leave from axillary bud day 10 in Kin. **b)** Plantlet with a developped callus at the basal part day 20 in Kin. **c)** Plantlet with short and thicking roots in IBA. **d)** Plantlet with well developped root system in IBA.

Budding and development of axillary buds or multiple shoot

Three concentrations of Kin and TDZ (4, 12 and 24 µM) were tested and compared to the control (without phytohormons) for the induction of budding. Among those concentrations, the control had the minimum budding rate (0%) while the maximum budding response (100%) was seen with 12 and 24 µM of Kin after 10 days of culture (Figure 4a). Proliferation of axillary buds gave the well developed plantlets at 4 µM with callus formation at the base 10 days after sub culturing in the same medium (Figure 4b). Well-developed shoots, 2 to 4 cm in length, formed the first roots at the base of their stem 10 days after transferring in MS medium supplemented with different concentrations of IBA (4, 12, 24 µM). Within 3 weeks, plantlets with short and thickness roots were observed with 24 µM of IBA (Figure 4c). IBA 12 µM gave (100%) the maximum rooting (Figure 4d, Figure 5). Single-node cuttings were harvested on 1 month old seedling (Figure 6a and b) and cultured in MS medium supplemented with TDZ and Kin at the same concentration (0, 4, 12 and 24 µM). After the budding (Figure 6c) with a highest rate (100%) at 12 and 24 µM TDZ, proliferation of multiple shoots was observed with a maximum time dependent 2, 3 and 5 shoots per explants (Figure 6d, 6e and 6f) and Table 1.

DISCUSSION

Storage proteins in trees have been examined at cytological, biochemical and molecular levels (De Castro and Marraccini, 2006). The external factors, such as temperature and short days, have been emphasized as key signals in inducing storage proteins accumulation in trees (Martre et al., 2003). In the present study, reserved proteins are present in all the mature or immature stage of cuttings. However, their expression is differential among the different categories of reserved proteins (Rate of glutelin higher compare to those of albumin, prolamin and globulin) and different stages of cutting. Accumulation of proteins with an increasing of total nitrogen content could enhance growth and development of organ from *P. africana* cuttings cultured in MS medium. Unfortunately only cuttings of IVA stage were reactive showing that many other factors influenced the growth of explants. In this experiment, the increasing of initial level of

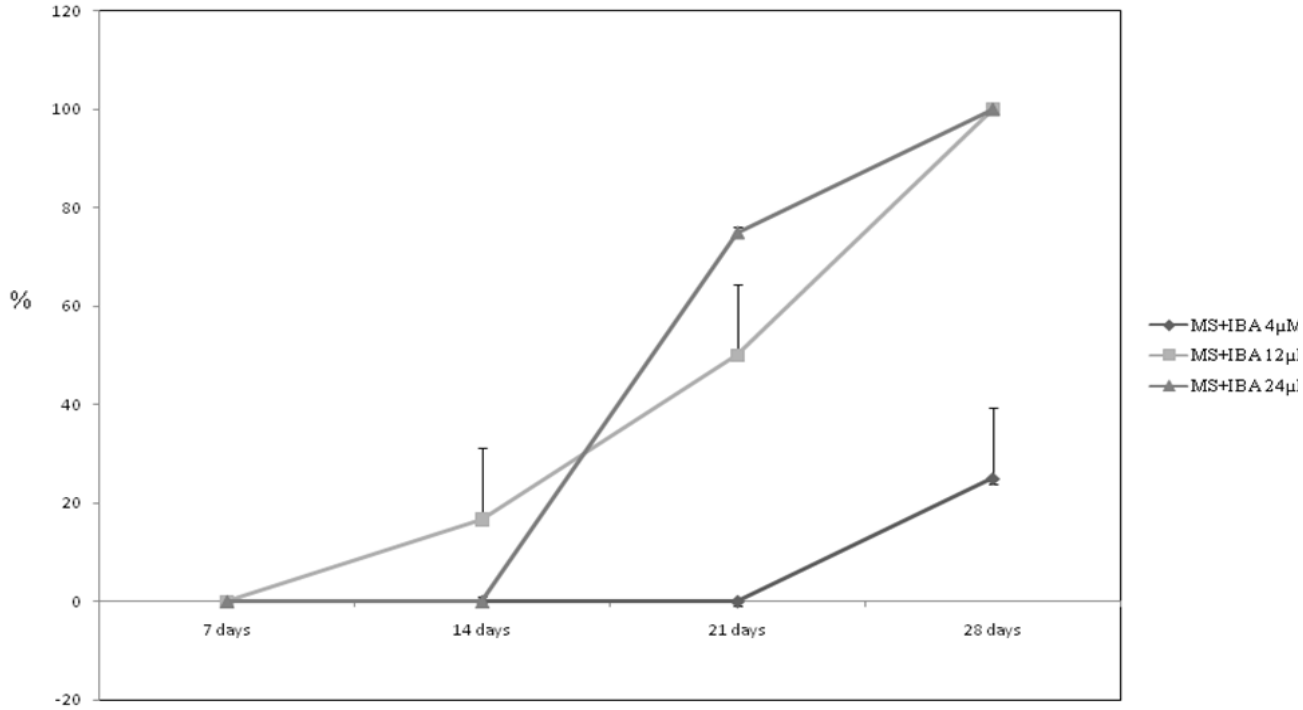

Figure 5. Percentage of cutting rooting of *P. africana* in different concentration of IBA.

Table 1. Budding and multiple shoots percentage and shoot numbers.

Media	Budding	Multiple shoots	Number of shoots
Control without growth regulator	0	0	0
Kin 4 µM	50	0	1
Kin 12 µM	100	25	2
Kin 24 µM	100	50	2
TDZ 4 µM	100	50	3
TDZ 12 µM	100	100	4
TDZ 24 µM	100	100	5

phenols which are the main substrate of peroxidase had a negative effect on *in vitro* cutting development. In fact, phenolic compounds were released from cut surface to the culture medium and were probably responsible of the phytotoxic effect. The oxidized products not only may contribute to failure of the explant development, but also may lead to the death of explants (Liu and al., 2015). Some factors including type of explant, light exposure, age and vigour of the donor plants, source of explant, genotype, size of explant affect the controlling of explants browning (Thomas and Ravindra, 1999). Time of the year at explant collection is also another important factor influences the explants browning. It is possible to alleviate the browning of explant with the selection of growing stage (Thomas and Ravindra, 1999) which is IVA in this study that presented the minimum phenolic compounds.

Different methods developed in this work showed that *P. africana* might be multiply with success from single-node cuttings of young plants. The successful percentage of different steps was assessed depending on the nature and concentration of phytohormons used. We observed a positive action of low concentration of Kin on budding and development of axillary bud. Similar results were obtained by Enjalric (1983) and Fotso et al. (2007) in *Hevea brasiliensis* and *Ricinodendron heudelotii*, respectively. AIB was used for rooting of cutting with 100% of maximal effect at 24 µM. Shiembo (1994) obtained the same results in *R. heudelotii* multiplied *ex vitro* into a propagation system. Maximum rate has been observed with 2 and 4 mg/L of IBA for rooting of *Prunus laurocerasus* L. (Sulusoglu and Cavusoglu, 2010). On the

Figure 6. Multiple shoots from 14 days old seedling of *P. africana.* **a** and **b)** Germinated seed derived-seedling. **c)** Budding of axillary bud; **d,e,f)** Proliferation of 2, 3 and 5 multiples shoots after 7, 10 and 14 days old, respectively.

other hand, propagation of many woody plants such as *Psidium guajava* (Yasseen et al., 1995), *Cola anomala* and *Cola nitida* (Fotso et al., 2002) is limited by the difficulties of rooting. When using TDZ and Kin at high concentration, there had a development of multiple shoots from one axillary bud. These phytohormons have created probably at the level of buds, an antagonist effect of apical dominance of main axillary bud on lateral buds which enter in competition with the principal bud. In contrary, low concentration of Kin treatment promote the budding of principal axillary buds without reducing its dominance which maintain in a dormant state, lateral buds

In conclusion, chemical profile of explants varies from different growing stages and influences its reaction. However, acquired results showed that tissues culture of *P. africana* via micro cutting is promising and could be useful alternative technique for more rapid clonal multiplication of this endangered species. For this reason, acclimatization of plantlets are required.

Conflict of interests

The authors did not declare any conflict of interest.

ACKNOWLEDGEMENTS

This research was supported by the International Foundation for Sciences (IFS), Sweden, through Grant N°: D/4916-1 received by NZWEUNDJI Justine Germo and Unesco l'Oreal Fellowship.

REFERENCES

Almagro L, Gomez Ros LV, Belchi-Navarro S, Bru R, RosBarcelo A, Pedreno MA (2009). Class III peroxidases in plant defense reactions. J. Exp. Bot. 60: 337-390.

Amougou A, Betti JL, Ewusi NB, Mbarga N, Akagou ZHC, Fonkoua C, Essomba ER, Nkouna AC (2010). Preliminary report on sustainable harvesting of *Prunus africana* (Rosaceae) in the North West region of Cameroon. 71 p.

Auge R (1989). Physiological events in relation with the establishment of *in vitro* culture, In: Beauchesne (Ed.). *In vitro* culture and Its Horticultural Applications, 3rd ed. Laballary, France. pp. 1–5.

Avana TML (2006*).* Domestication de *Prunus africana (Hook. F.)* Kalkmam (Rosaceae): étude de la germination et du bouturage. Université de Yaoundé I Cameroun, Thèse de Doctorat.

Betti JL 2008. Non-Detriment Findings Report on *Prunus africana* (Rosaceae) in Cameroon. Report prepared for the International Expert Workshop on Non-Detriment Findings, Mexico. 52 p.

Betti JL, Ambara J (2013). Mass of *Prunus africana* stem barks on Tchabal mbabo and Tchabal Gang Daba Mountain Forests, Cameroon. Afr. J. Environ. Sci. Technol. 7(5):204-221

Bradford MM (1976). Rapid and sensitive method for the quantitation of microgram quantities of protein utilizing the principle of protein-dye binding. Anal. Biochem. 72:248-254.

Bray HG, Thorpe WV (1954). Analysis of phenolic compounds of interest in metabolism. In: Glick, D. (Ed.), Methods of biochemical analysis, Vol 1. Interscience Publisher, New York, pp. 27-52.

Cunningham AB (2005). CITES Significant Trade Review of *Prunus africana*.In Review of Significant Trade in specimens of Appendix-II species. Sixteenth meeting of the Plants Committee, PC16 Doc.10.2. Lima (Peru).

Cunningham AB, Ayuk E, Franzel S, Duguma B, Asanga C (2002). An economic evaluation of medicinal tree cultivation: *Prunus africana* in Cameroon. People and Plants working paper 10. Paris, France: UNESCO.

De Castro RD, Marraccini P (2006). Cytology, biochemistry and molecular changes during coffee fruit development. Braz. J. Plant Physiol. 18(1):175-199.

Enjalric F (1983). Étude sur le microbouturage *in vitro* de *Hevea brasiliensis*. Mull Arg. Thèse de Doctorat de 3 e cycle, Université de Paris-Sud, Orsay, France.

Fotso, Donfagsiteli TN, Mbouna D, Omokolo ND (2007). *In vitro* regeneration of Ricinodendron heudelotii. Fruits 16: 31-36.

Fotso, Omokolo ND, Mbouna D (2002). Comparaison de l'aptitude à la régénération *in vitro* de deux kolatiers : *Cola anomala* et *Cola acuminata*. Cah. Agric. 11: 355-60.

Kadu CAC, Parich A, Schueler S, Konrad H, Muluvi GM, Eyog-Matig O, Muchugi A, Williams VL, Ramamonjisoa L, Kapinga C, Foahom B, Katsvanga C, Hafashimana D, Obama C, Schumacher R and Geburek T (2012). Bioactive constituents in Prunus africana: Geographical variation throughout Africa and associations with environmental and genetic parameters. Phytochemistry 83 : 70–78.

Liu C-P, Yang L, Shen H-L (2015). Proteomic analysis of immature *Fraxinus mandshurica* cotyledon tissues during somatic embryogenesis: effects of explant browning on somatic embryogenesis. Int. J. Mol. Sci. 16:13692-13713.

Martre P, Porter JR, Jamieson PD, Triboï E (2003). Modeling grain nitrogen accumulation and protein composition to understand the sink/source regulations of nitrogen remobilization for wheat. Plant Physiol. 133(4): 1959–1967.

Murashige T, Skoog F (1962). A revised medium for rapid growth and bioassays with tobacco tissue culture. Physiol. Plant. 15: 473-497.

Nsawir AT, Ingram V (2007). *Prunus africana*: Money growing on trees? A plant that can boost rural economies in the Cameroon Highlands. FAO Nature Faune J., 22 "The value of biodiversity".

Segalen (1967). Soil and geomorphology of Cameroon. Written Book of ORSTOM: Pedologic Series, 5(2): 112 pp.

Shiembo P (1994). Domestication of multipurpose tropical plants with particular reference to *Irvingia gabonensis* Baill., *Ricinodendron heudelotii* (Baill.) Pierre ex Pax and *Gnetum africanum* Welw. Edinburgh, Edinburgh.

Sulusoglu M, Cavusoglu A (2010). Vegetative propagation of Cherry laurel (*Prunus laurocerasus* L.) using semi-hardwood cuttings. Afr. J. Agric. Res. 5(23):3196-3202.

Tchoundjeu Z, Avana ML, Leakey RRB, Simons AJ, Asaah E, Duguma B, Bell JM (2002) Vegetative propagation of *Prunus africana*: effects of rooting medium, auxin concentrations and leaf area. Agroforestry Syst. 54:483-492.

Thomas P, Ravindra MB (1999). Shoot tip culture in mango: Influence of medium, genotype, explant factors, season and decontamination treatments on phenolic exudation, explant survival and axenic culture establishment. J. Hort. Sci. 72:713-722.

Thorpe TA, Gaspar T (1978). Changes in isoperoxidases during shoot formation in tobacco callus. *In vitro* 14(6):522-526.

Voigt J, Biehl B, Kamaruddin SSW (1993). The major seed proteins of *Theobroma cacao* L. Food Chem. 47 : 145-151.

Yasseen MY, Barringer SA, Schnell RJ, Splittstoesser WE (1995). *In vitro* shoot proliferation of guava (*Psidium guajava* L.) from germinated seedlings. Plant Cell Rep. 14:525-528.

Yildiz MC, Er C (2002). The effect of sodium hypochlorite solutions on *in vitro* seedling growth and shoot regeneration of flax (*Linumusitatissimum*). Naturwissenschaften 89 : 259-261.

academicJournals

Vol. 14(33), pp. 2576-2582, 19 August, 2015
DOI: 10.5897/AJB2014.13756
Article Number: 90C6E2754972
ISSN 1684-5315

http://www.academicjournals.org/AJB

African Journal of Biotechnology

Full Length Research Paper

Liver histopathology in bovine Fascioliasis

Okoye, I. C.*, Egbu, F. M. I., Ubachukwu, P. O and Obiezue, Nduka R.

Applied Parasitology and Biomedical Research Unit, Department of Zoology and Environmental Biology, University of Nigeria, Nsukka, Nigeria.

Received 24 February, 2014; Accepted 13 August, 2015

The livers of slaughtered cattle were examined by visualization, palpation and incision. Macroscopically, some of the infected livers appeared to be slightly swollen with pale color at the round edges, while some appeared greatly swollen, with a few small irregular whitish areas indicating fibrosis over the parietal surface. In some cases, the capsule was thick and rough with whitish or reddish discoloration and parenchyma was hard due to fibrous tissue. Fibrosis of the bile ducts with numerous small and large patches scattered over the parietal surface and the pipe stem appearance of the liver were noticed. It could be concluded that the histopathological changes in the livers of cattle infected with *Fasciola gigantica* reflected tissue damage, which can amount to significant economic losses in animals and great health problems in man. Serious care and attention are required of both the veterinary workers and the public health planners in the state to ensure that seriously damaged livers are not passed on for human consumption despite their deranged nutritional values and health risk problems. The grazing of cattle should be highly restricted to areas of lesser snail infected site to reduce the rate of animal infection and the consequent economic losses.

Key words: Fascioliasis, *Fasciola gigantica*, histopathology, cirrhosis.

INTRODUCTION

Bovine fascioliasis (liver rot) is an economically important helminth disease caused by two trematodes viz. *Fasciola hepatica* (Linnaeus, 1758) (the common liver fluke) and *Fasciola gigantica* (Cobbold, 1855). This disease belongs to the plant-borne zoonosis. Fascioliasis is generally a disease of ruminants such as sheep, cattle and goats and is also recognized as occasional zoonotic disease of man. Fascioliasis has the widest geographic spread of any emerging vector-borne zoonotic disease and affects an estimated 17 million people in more than 51 countries, worldwide (Marcos et al., 2008). Chronic fascioliasis causes a chronic inflammation of the liver and bile ducts accompanied by loss of condition, digestive disturbances and a general reduction in productivity (Rana et al., 2014). Depending on the disease prevalence in a herd, these reductions can be significant. The direct economic impact of fascioliasis infection is increased condemnation of liver meat, but the far more damaging effects are decreased animal productivity, lower calf birth weight, and reduced growth in effected animals (Hillyer, 2005). The negative impact of the helminth infection on livestock productivity has long been established. Fascioliasis

*Corresponding author. E-mail: ikem.okoye@unn.edu.ng. Tel: +2348069284633.

causes thickening and dilation of the bile ducts and toxic degeneration of the adjacent liver tissues leading to liver condemnation at slaughter. Heavy infections cause serious disease and high mortality in cattle and sheep. In man, fascioliasis causes biliary colic, epigastric pain, nausea, juandice, haemorrhage, anaemia and in very chronic cases liver failure. The disease damages the liver of cattle and makes the liver unsuitable for human consumption.

Recently, fascioliasis has only been recognized as a significant human disease; studies to determine the global morbidity caused by the disease are ongoing. There is the need to intensify meat inspection activities in Nigerian abattoirs and introduce trace-back systems (Ibironke and Fasina, 2010). This study therefore investigated some histopathological responses of cattle naturally infected with fascioliasis and identified the induced changes in the pathological conditions of the liver.

MATERIALS AND METHODS

Study area and population

This research was carried out in Nsukka area, Nigeria. Samples were collected from 57 cattle with naturally acquired bovine fascioliasis and no other disease out of 659 cattle examined within Nsukka tropical ecosystem in southeast Nigeria. The selected slaughtered cattle were confirmed free from other possible diseases through visual inspection of the organs, intestine and tissues by qualified Veterinary officers at the Nsukka Ogige Central market abattoir.

Collection and inspection of liver tissue samples

Carefully selected liver tissue samples of 57 Fasciola infected and 20 non-infected groups were collected immediately after inspection by visualization and palpation of the entire organ. The liver samples were incised at the ventral sides, cutting the bile ducts open to check thoroughly for the presence of the parasite. They are thus certified free from any other possible disease after careful inspection by qualified Veterinary officers. The liver samples collected were subjected to proper histopathological procedures.

Histopathological studies

The liver tissue samples collected were fixed in formol saline solution for at least 24 h, and then washed with tap water for 12 h. Serials of alcohol (methyl, ethyl and absolute) were used in an ascending order (70 to 100%) for the dehydration of the tissue samples. Tissue specimens were cleared in xylene and embedded in paraffin. The paraffin blocks were sectioned at 3 micron thicknesses by slide microtome. The sections were floated on a water bath maintained at 2 to 3°C below the melting point of paraffin wax and later placed on a hot plate thematically maintained at 2 to 3°C above the paraffin wax melting point. After proper drying (15 to 30 min), the obtained tissue sections were mounted on glass slides and stained with haematoxylin and eosin avoiding air bubbles for histopathological examinations. The prepared permanent slides were mounted on light microscope one after the other and viewed at different magnifications. The photographs of the different slides were taken accordingly.

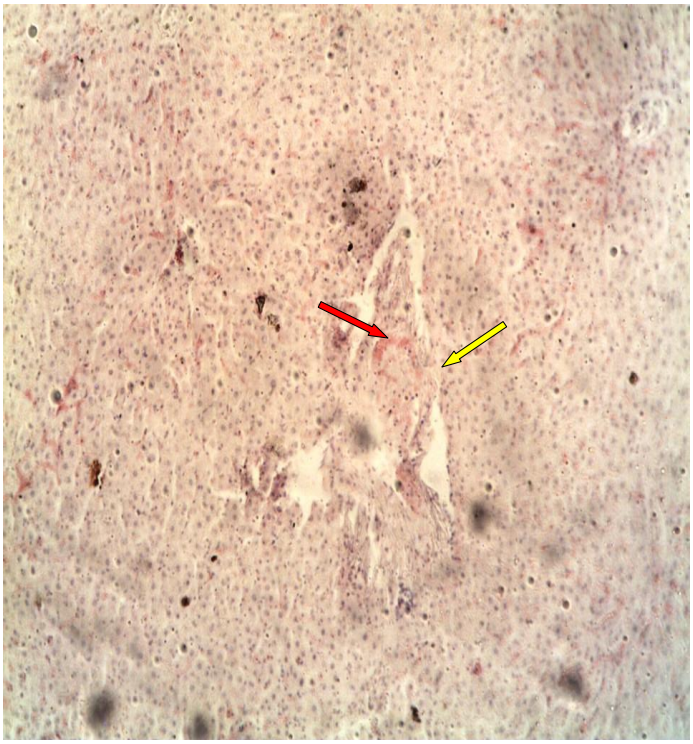

Figure 1. Normal liver tissue architecture showing the central vein (yellow arrow) and the hepatic triads (red arrow) (Magnification: x 100, Stain: haematoxylin and eosin).

RESULTS

Histopathology of the non-infected livers

The non-infected livers microscopically, consisted of normal liver tissue cells with normal sizes of sinusoids, bile ducts, portal tracts and hepatic triads as seen in Figures 1, 2 and 3. The nucleus and the cytoplasmic walls were still in their proper shapes and no recognizable change was observed in the liver tissues.

Histopathology of *Fasciola* infected livers

Macroscopically, some of the infected livers appeared to be slightly swollen with pale color at the round edges, while some appeared greatly swollen, with a few small irregular whitish areas indicating fibrosis over the parietal surface. In some cases, the capsule was thick and rough with whitish or reddish discoloration and parenchyma was hard due to fibrous tissue. Fibrosis of the bile ducts with numerous small and large patches scattered over the parietal surface and the pipe stem appearance of the liver were noticed. Microscopically, contrary to the normal structures seen in the non-infected livers, various changes were observed in the liver structures of *Fasciola* infected cattle, which occurred in varying degrees depending

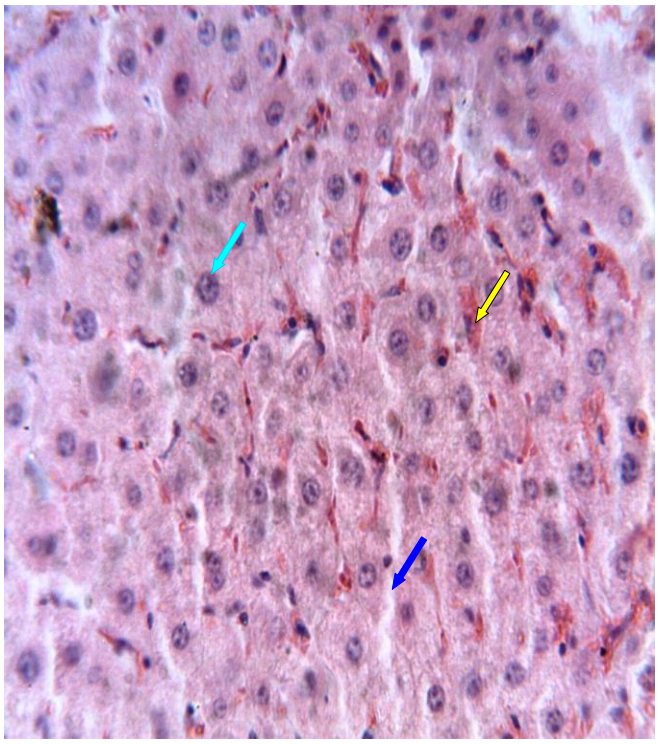

Figure 2. Normal liver tissue structure (enlarged), showing the normal hepatocytes (with their nuclei and cell walls- green arrow) and sinusoids- blue arrow (with glycogen materials within - yellow arrow), Magn: x 400, Stain: haematoxylin and eosin.

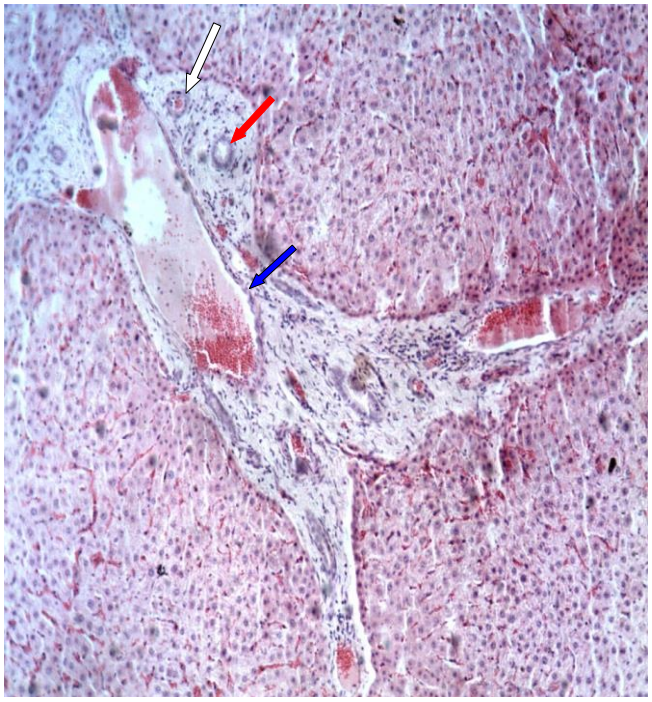

Figure 3. A normal hepathic triad showing normal sizes of the hepathic vein (blue arrow), hepathic artery (white arrow) and bile ducts (red arrow). Magn: x 100, Stain: haematoxylin and eosin.

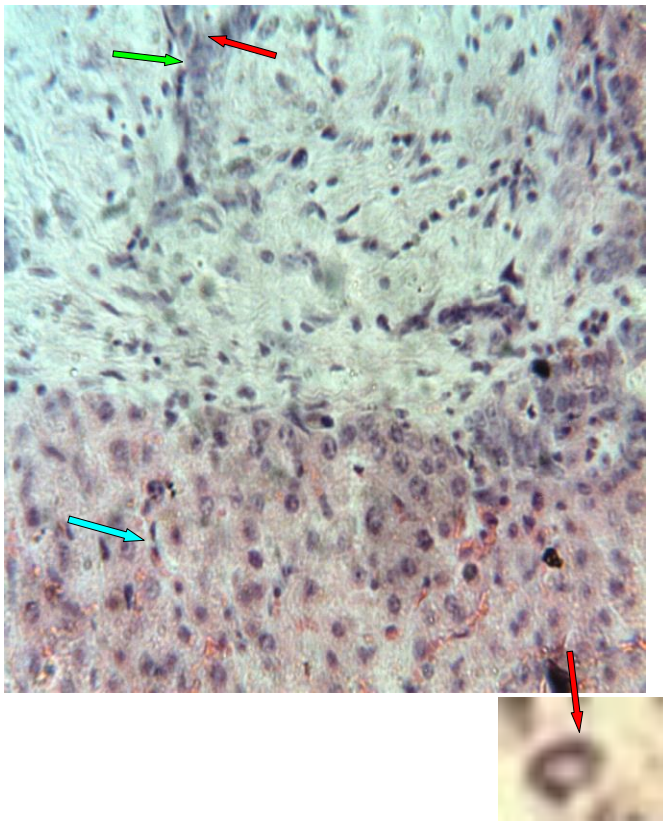

Figure 4. The parenchymal phase of the infecton (the acute phase) showing necrosis of the liver cells and accumulation of granulocytes (green arrrow) at the infection site attacking the antigenic substances (fluke eggs - Red arrow). A section of the liver was still unattacted by the disease (light green arrow). Magnification: x 400, Stain: haematoxylin and eosin.

on the duration and intensity of the infection. In Figure 4, remarkable necrosis and fibrosis of the hepatic parenchyma cells are observed. The migration of the young flukes within the liver tissues and parenchyma cells had caused serious damages to the hepatocytes. The cell walls have degenerated, the nuclei deformed and the cytoplasmic contents emptied into the sinusoids. Some macrophages and lymphocytes have infiltrated within the infection site and are seen aggregating around some antigenic substances (the fluke eggs). This indicates the acute phase or the parenchymal phase of the infection with its consequent pathological changes. The destruction of the tissues followed the migration of the flukes.

In Figures 5 and 6, it was observed that the dilation of the bile ducts with necrotic changes in the columnar cells surrounding the bile ducts. Also, mild fibrosis was noticed in the bile ducts together with the hepatic portal triads. The presence of the mature flukes in the bile ducts have initiated various cellular reactions and damaging effects on the bile duct walls. The alterations had lead to focal inflammatory cells infiltrations in the hepatic parenchyma and cellular infiltrations in the portal tracts (Figure 6). This

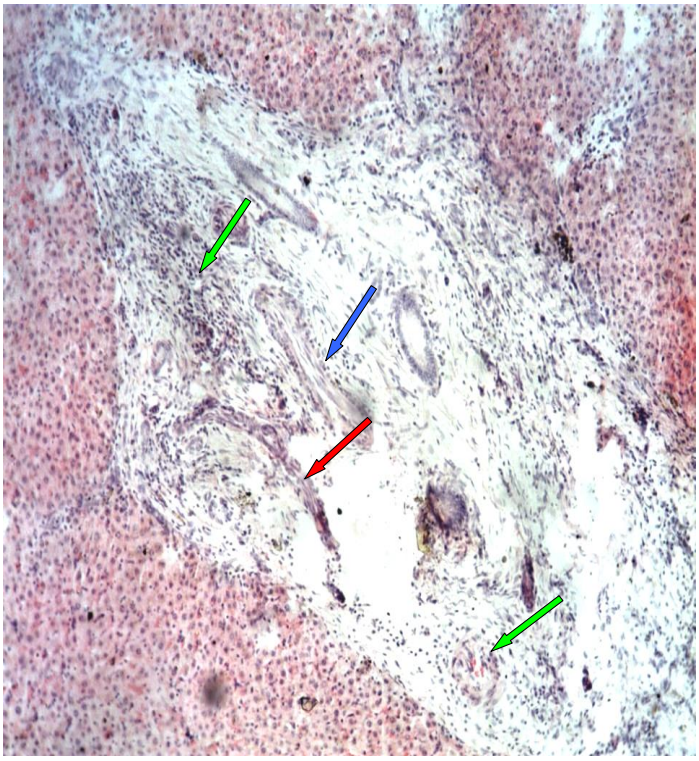

Figure 5. The chronic phase of the infection showing cellular infiltrations of the tracts (green arrows), necrosis of the hepatocytes, bile ducts (light blue arrow) and vascular walls (red arrow). Magn: x100, Stain: haematoxylin and eosin.

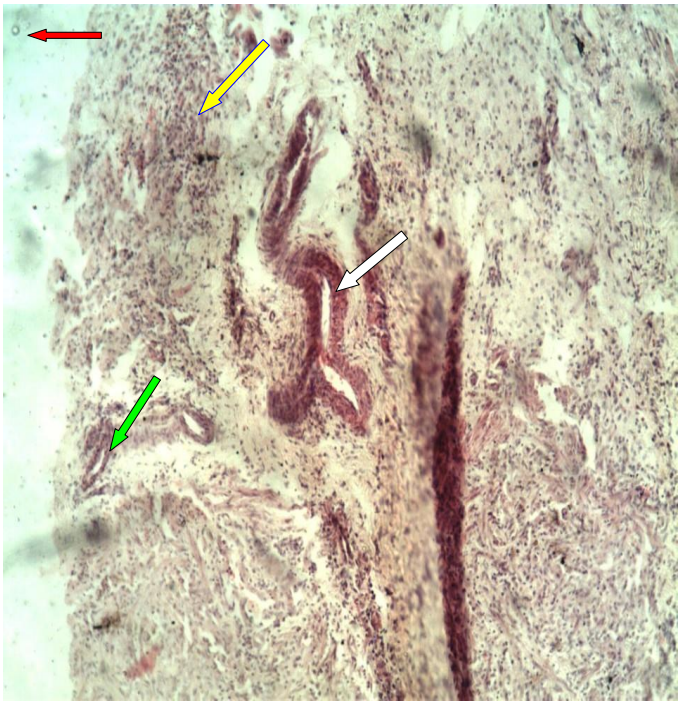

Figure 7. Showing gross necrosis and fibrosis, migratory tracts (green arrow) with secretions by the flukes (white arrow) coupled with biliary proliferations and cirrhosis (yellow arrow) with eosinophilic infiltrations in the large portal tracts (red arrow). Magnification: x 400, Stain: haematoxylin and eosin.

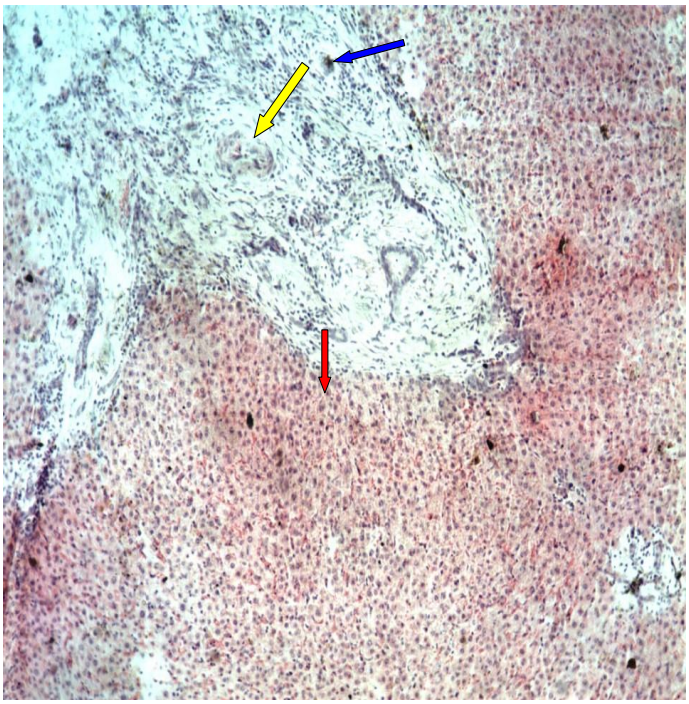

Figure 6. Showing adjoining tracts with cellular infiltration (blue arrow) and vacoulation of the endothelial cells (yellow arrow) within the hepatic triad and some normal zone (red arrow) Magnification: x 100, Stain: haematoxylin and eosin.

indicates the beginning of the chronic phase of the infection. Figure 7 reveals an advanced stage of the infection which involved severe necrosis and fibrosis of the hepatic parenchyma and tissues. The fine-grained reddish brown material in the peripherial areas of some tracks was similar to the residue of ingested substances in the caeca of immature flukes and apparently had been defaecated by them. Degenerated hepatocytes surrounding such tracks appeared more dark-stained compared to other areas.

Fresh migrational tracks of all sizes were observed, which were mainly composed of eosinophilic debris and disintegrated hepatocytes and also biliary proliferations and cirrhosis with eosinophilic infiltrations in the large portal tracts. Figure 8 indicates gross necrotic and fibrotic effects on the bile duct walls caused by the migrating flukes in the liver (Chronic phase). The flukes inflicted extensive mechanical and toxic damage to hepatocytes and other tissue components in the tracks and closely surrounding areas. The infection site also bears abundant eosinophilic cells and macrophages filled with cytoplasmic infiltrations. Often tissue elements surrounding the tracks were affected by a pronounced coagulative necrosis (Figure 8). The adjoining portal areas and the congested sinusoids were abundantly infiltrated by eosinophils, lymphocytes and macrophages. Some irregular fragments from mesenchymal tissue often occurred

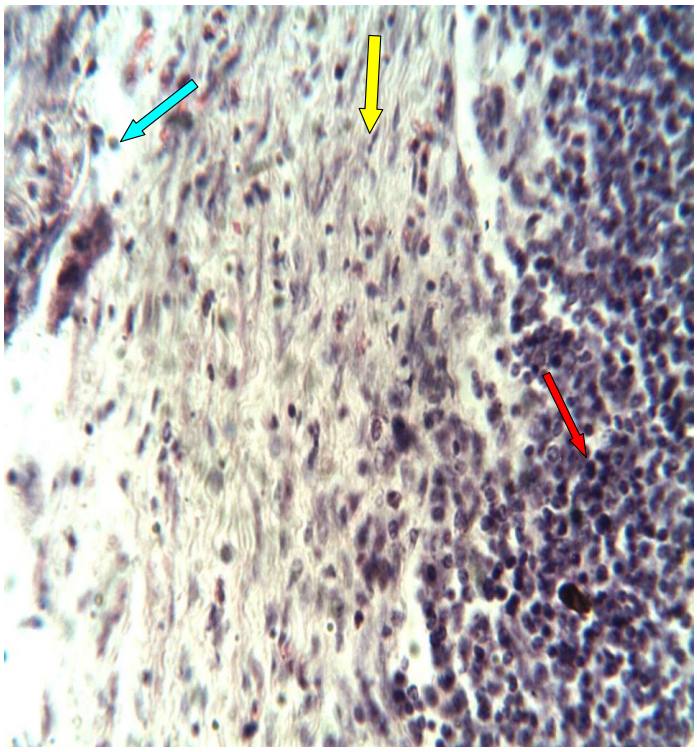

Figure 8. Showing the hyperplastic bile duct walls (yellow arrow), gross necrosis and fibrotic effects caused by the migrating immature flukes. The infection site also bears abundant eosinophilic cells within the duct (green arrow), mast cells (red arrow) and macrophages filled with cytoplasmic infiltrations. Magnification: x 400, Stain: haematoxylin and eosin.

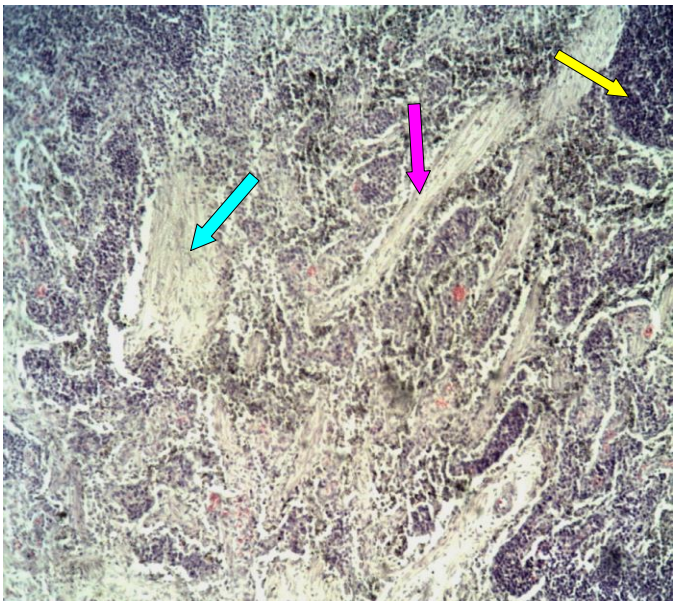

Figure 9. Showing the cirrhotic effects on the liver tissues (yellow arrow), healing of the migratory tracts (pink arrow) and monolobular fibrosis (green arrow). Magnification: x 400, Stain: haematoxylin and eosin.

in the larger tracks resulting from extensive damage. Liver cirrhosis was observed in some parts of the liver tissues (Figures 9 and 10), coupled with very severe necrosis and fibrosis of the connective tissues and some remarkable healing tracts. Some encapsulated and degenerating immature flukes embedded within the collagen materials of the connective tissues of the liver in addition with eosinphilic infiltrations and haemoharrgic effects on the portal tracts were observed (Figure 11). The necrosis of extravascular collagen occurred occasionally in association with migrational tracks in the immediate vicinity of broad collagenic bundles. Some areas of collagen were profusely surrounded by eosinophils (Figure 11) and Silver impregnation revealed the altered areas to be irregular fibrillary fragments.

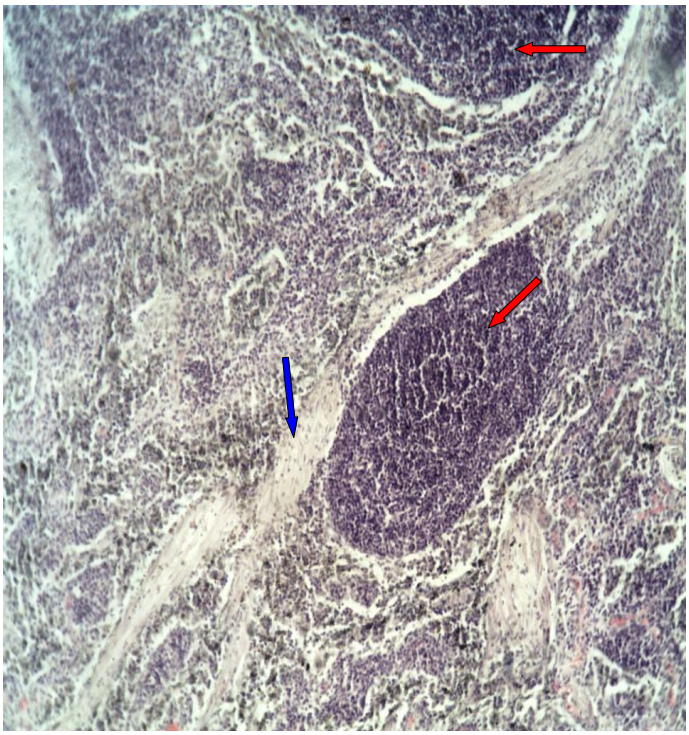

Figure 10. Showing liver parenchymal cirrhosis (red arrows) and healing effects in the migratory tracts (blue arrow).

DISCUSSION

This study dealt with the macroscopic liver lesions of fascioliasis in infected and non-infected cattle. In some cases, the affected liver was slightly swollen and appeared pale in color with round edge, the capsule was thick, rough with whitish or reddish discoloration and fibrosis of the bile ducts which indicated sub-acute form of infection. Similar observations were made by Ahmedullah et al. (2007). The numerous small and large

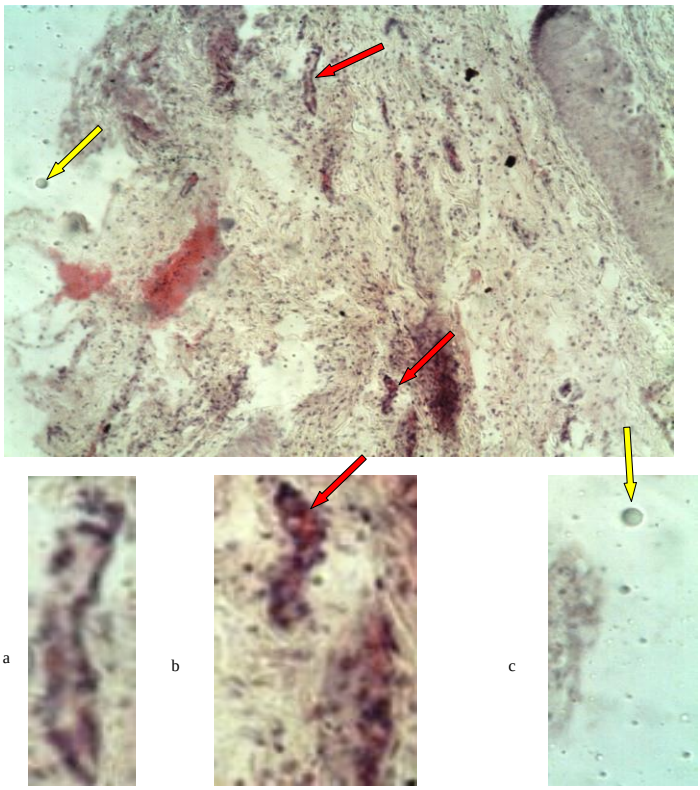

Figure 11. Showing very severe necrosis and fibrosis with some encapsulated and degenerating immature flukes embedded within the collagen materials of the connective tissues of the liver (the red arrows - a and b) in addition with eosinphilic infiltrations (yellow arrow - c) and haemoharrgic effects. Magn: x 400, Stain: haematoxylin and eosin.

patches scattered over the parietal surface could be the indication of transperitoneal route of migration of young flukes. The damage of hepatic cells near these tracts might have resulted from feeding habit of these premature parasites and is the most common cause of bovine cirrhosis (Njoku-Tony and Okoli, 2011). Some parts of bile ducts had cystic appearance due to dilation. In some other cases, the liver was greatly enlarged with presence of a few small irregular whitish areas indicating fibrosis over the parietal surface and parenchyma was hard due to fibrous tissue which was thought to be due to healing of migratory tracts of immature parasites. In cross section of some livers, also recorded was the pipe stem appearance of the liver caused by the migration of the parasites. Ansari-Lari and Moazzeni (2006) also reported same result on the prevalence of liver condemnations due to fascioliasis.

Microscopically, the histopathological changes of the liver were discussed in acute and chronic phases. During the acute phase of infection, the parenchymal damages were due to the migration of young flukes of *F. gigantica* and these were seen to be either moderate, severe or very severe and gross damages, showing markedly degenerative and necrotic changes in the hepatocytes and the surrounding liver tissues. Pigments and fibrosis with focal inflammatory cells infiltration in the hepatic parenchyma were detected. Considerable fibrous connective tissue proliferations were noted at the portal areas with associated haemorrhage.

Hepatic siderosis was also observed in this study. These observations were similar to those reported by Coppo et al. (2011) in Northeastern Argentina and by Usip et al. (2014) in South-south Nigeria. In this investigation, eosinophil infiltration coupled with the accumulation of the endothelial cells, macrophages and lymphocytes were part of the prominent features, particularly in the early stage and migratory phase of infection. The formation of granulomata around fluke eggs was also observed. The eosinophil granulocytes are generally assumed to be attracted by immune complexes which would be stimulated by histamine release causing the body to produce more endogenous histamine, which degranulate and dump histamine, along with other inflammatory molecules into the body. Thus, anti-histamines have the ability to inhibit the release of histamine from mast cells (Paulo et al., 2010). Flagstad and Nielsen (1972), in their experimental *F. hepatica* infection in calves, mentioned the accumulation of eosinophils in association with the cell damage caused by the migration of young flukes, but commented that eosinophils are few in the livers of calves with a hypoplastic thymus. They suggested that normal thymus lymphocytes are stimulated by necrotic material produced by damaged hepatocytes or collagen in liver, the thymus lymphocytes in turn stimulate the bone marrow to produce more eosinophils. Hsu et al. (1977) suggested that eosinophils seem to be closely associated with T. cells and that in the destruction of parasites eosinophils play an important role. In some livers, degenerating immature flukes embedded within the necrotic and fibrotic tissues were observed. These could be flukes trapped and destroyed by the granulocytes. Haroun et al. (1986) also observed degenerative and necrotic changes in hepatocytes associated with haemorrhage, fibrosis, increased lobulation of the liver, mononuclear cell infiltration with haemosiderin deposition in fluke tracks and portal areas and the formation of granulomata around fluke eggs and fluke remnants in sheep naturally infected with *F. gigantica*.

In chronic phase, there were areas of focal inflamematory cells infiltration in the hepatic parenchyma as well as in the portal areas; the infiltration with lymphocytes and mononuclear cells and proliferation of fibroblasts represented the haemorrhagic tracts. Heavy accumulation of lymphocytes and proliferation of fibrous connective tissues in the portal areas distorted lobular architectures. There were hyperplastic changes of the epithelial cells of the bile ducts with periductal connective tissue proliferation. In most advanced stages these hyperplastic bile ducts appeared like granular structures which produced

a thick and adenomatous picture as was recorded in the study of Ahmedullah et al. (2007). The nature of these changes has been related to many factors, particularly mechanical irritation caused by the motion of the parasites and chemical substances and toxins produced by flukes (Massoud and Vedadi, 1983). Biliary proliferation and formation of numerous simple bile ducts in the fibromatic tracts was rather a characteristic picture in cattle (Massoud and Vedadi, 1983). Frequent thrombosis, significant haemorrhages, and extensive damage were associated mainly with the largest tracks. There is a suggestion that, in the bile ducts of cattle, increased fibrosis and calcium deposition usually reduce the accommodation available to the parasite, so that the life-span of flukes may be reduced to as little as 9 to 10 months (Doaa et al., 2007). However, in *F. gigantica* in cattle, which produces much less calcification of ducts, the parasite certainly can live much longer. In the chronically infected livers, the mast cells are apparently increased, as is the case in cirrhotic livers. Lotfy et al. (2003) reported degenerative changes in the hepatocytes and biliary cirrhosis in the histopathological examination of liver of cattle infected with *Fasciola*. The present study indicates that the proliferation and continuous erosion of the mucosa of bile ducts and hepatic cell damages result in a considerable loss of various essential substances from the *Fasciola* infected livers.

Conclusion

It could be concluded that the histopathological changes in the livers of cattle infected with *F. gigantica* reflected tissue damage, which can amount to significant economic losses in animals and great health problems in man. Serious care and attention are required of both the veterinary workers and the public health planners to ensure that seriously damaged livers are not passed on for human consumption because of their deranged nutritional values and health risk problems. The grazing of cattle should be restricted to lesser snail infected sites to reduce the rate of animal infection and the consequent economic losses.

Conflict of interests

The authors did not declare any conflict of interest.

REFERENCES

Ansari-Lari M, Moazzeni M (2006). A retrospective survey of liver fluke disease in livestock based on abattoir data in Shiraz, south of Iran. Prev. Vet. Med. 73(1): 93 - 96.

Coppo JA, Mussart NB, Zeinsteger PA (2011). Hematological indicators of liver damage during the subclinical phase of fasciolosis in steers from Northeastern Argentina. Comp. Clin. Pathol. 20(4): 397-401.

Flagstad SD, Nielsen K (1972). The course of experimental *F. hepatica* infection in calves with a deficient cellular immunity. Res. Vet. Sci. 13: 468 - 475.

Haroun EM, Gadir AH, Gameel AA (1986). Studies on naturally-occurring ovine fascioliasis in the Sudan. J. Helminthol. 60(1):47 - 53.

Hillyer GV (2005). Fasciola antigens as vaccines against fascioliasis and schistosomiasis. J. Helminthol. 79(3): 241-247.

Hsu SY, Li FF, Isacson P (1977). The role of eosinophils in the mechanism of Schistosome immunity. Proc. 61st Federation of American Soc. Exp. Biol. 36: 1057.

Ibironke AA, Fasina FO (2010). Socio-economic implications of bovine liver rejection in a major abattoir in south-western Nigeria. Rev. de Ciências Agrárias 33:2.

Lotfy HS, Mahmoud SM, Abdel-Gawad MA (2003). Some studies on Fascioliasis in Mid-Egypt. Agric. Res. 81(2): 209 - 227.

Marcos LA, Tagle M, Terashima A, Bussalleu A, Ramirez C, Carrasco C, Valdez L, Huerta-Mercado J, Freedman DO Vinetz JM, Gotuzzo E (2008). Natural History, Clinicoradiologic Correlates, and Response to Triclabendazole in Acute Massive Fascioliasis. Am. J. Trop. Med. Hyg. 78(2):222-227.

Massoud J, Vedadi L (1983). Histopathology of Liver in Cattle Spontaneously Infected with *Fasciola hepatica* and *Fasciola gigantica* in Iran. Iran. J. Public Health 2 (1-2): 01 – 20.

Njoku-Tony RF, Okoli GC (2011). Prevalence of fascioliasis among slaughtered sheep in selected abattoirs in Imo State, Nigeria. J. Amer. Sci. 7(2): 361-366.

Paulo RC, Roberta FJC, Celina WM, Carlos d'AMF (2010). Histamine, histamine receptors and antihistamines: new concepts. An. Bras. Dermatol. 85:2.

Rana MAA, Roohi N, Khan MA (2014). Fascioliasis in cattle- a review. J. Anim. Plant Sci. 24(3): 668-675.

Usip LP, Ibanga ES, Edoho HJ, Amadi EC, Utah E (2014). Prevalence of fascioliasis and the economic loss of condemned liver due to Fasciola infection in cattle slaughtered at three abattoirs in Eket Urban, Akwa Ibom State of Nigeria. Glob. Adv. Res. J. Food Sci. Technol. 3(2):54-75.

African Journal of Biotechnology

Related Journals Published by Academic Journals

- *Biotechnology and Molecular Biology Reviews*
- *African Journal of Microbiology Research*
- *African Journal of Biochemistry Research*
- *African Journal of Environmental Science and Technology*
- *African Journal of Food Science*
- *African Journal of Plant Science*
- *Journal of Bioinformatics and Sequence Analysis*
- *International Journal of Biodiversity and Conservation*

academicJournals